2018

Centrifugal Microfluidics For Label-Free Isolation Of Leukocytes Subpopulations From Whole Blood

Yuxi Sun
University of Alabama at Birmingham

CENTRIFUGAL MICROFLUIDICS FOR LABEL-FREE ISOLATION OF LEUKOCYTES SUBPOPULATIONS FROM WHOLE BLOOD

by

YUXI SUN

PALANIAPPAN SETHU, COMMITTEE CHAIR
HO-WOOK JUN
RAMASWAMY KANNAPPAN
LUFANG ZHOU
GANESH HALADE

A DISSERTATION

Submitted to the graduate faculty of the University of Alabama at Birmingham,
in partial fulfilment of the requirements for the degree of
Doctor of Philosophy

BIRMINGHAM, ALABAMA

2018

MINIATURIZED LABEL-FREE LEUKOCYTES SUBPOPULATION ISOLATION FROM WHOLE BLOOD VIA CENTRIFUGAL FORCE

YUXI SUN

BIOMEDICAL ENGINEERING

ABSTRACT

Leukocytes carry critical information regarding the immediate immune and inflammation status of the patients. Analysis of leukocytes requires isolation from blood since the leukocytes only consist <1% of all blood cells. Commonly used isolation processes exploit physical or biochemical differences between different cell types to enable separations. Current isolation methods inevitably subject cells to physical or biochemical stress that can activate leukocytes and change their natural state. Thus, information contained within isolated leukocytes is a combination of the natural state of the cell and an artifact of the isolation process. Microfluidics which takes advantage of scaling effects within microscale structures can ensure rapid and gentle alternatives to conventional isolation methods and is ideal for sorting, and analysis of cells and particles. The precise control of flow/particles and scaling effects of microfluidics have been applied for blood cells sorting and isolation. However, the limited processing capability and throughput as well as complex fabrication and operations have hampered widespread adoption of these approaches for replacement of conventional methods. My goal was to develop a simple yet powerful microfluidic tool that enables rapid separation of leukocytes while ensuring sufficient throughput, and minimizing isolation process induced activation without the need any sample pre-processing. This project is divided into two specific aims: **i)** to miniaturize the conventional density gradient centrifugation using centrifugal microfluidics for PBMC isolation and evaluate separation efficiency

and activation status of isolated cells in comparison to conventional techniques; **ii)** develop new approach for PBMC sorting using microfluidic phase partitioning to enable separation of cells based on differences in cell surface energy. For specific aim 1, PBMCs were isolated based on differences in densities using microfluidic density gradient centrifugation. We show that PBMCs can be isolated from 100µl whole blood within 5 minutes. Evaluation of leukocyte activation via profiling of expression of surface integrins and chemokine receptors shows that our microfluidic approach significantly reduced PBMC activation in comparison to conventional isolation approaches. In specific aim 2, we sought to isolate cells based on differenced in surface energy using two-phase partitioning of dextran (DEX) and polyethylene glycol (PEG). Proof of concept demonstrations was accomplished using with polystyrene and silicon dioxide microbeads which represent a mixture of white blood cells and red blood cells. The DEX and PEG mixtures were introduced into a circular channel and phase separated under centrifugal force into unique DEX and PEG phases. The bead mixture was isolated via differences in their affinity to the two phases.

Keywords: PBMC, cell sorting, microfluidic, centrifugal force, density gradient

ACKNOWLEDGMENTS

I thank everyone who has mentored and supported me through this process. Special thanks to my advisor, Dr. Palaniappan Sethu for his mentorship, guidance, and support during my tenure as graduate student. I thank my committee members, Drs. Palaniappan Sethu, Ho-Wook Jun, Ganesh Halade, Lufang Zhou, and Ramaswamy Kannappan. I also thank my peers and collaborators who have helped me to learn and succeed.

TABLE OF CONTENTS

Page

LIST OF TABLES

LIST OF FIGURES

Figure *Page*

INTRODUCTION

MICROFLUIDIC ADAPTION OF DENSITY GRADIENT CENTRIFUGATION FOR ISOLATION OF PARTICLES AND CELLS

LOW-STRESS MICROFLUIDIC DENSITY-GRADIENT CENTRIFUGATION FOR BLOOD CELL SORTING

CENTRIFUGAL MICROFLUIDIC PLATFORM FOR FAST AQUEOUS TWO-PHASE PARTITIONING WITH BEADS DEMONSTRATION

LIST OF ABBREVIATIONS

ATPS	Aqueous Two-Phase System
PBMC	Peripheral Blood Mononuclear Cell
RBC	Red Blood Cell
WBC	White Blood Cell
CBC	Complete Blood Counts
CTC	Circulating Tumor Cells
DLD	Deterministic lateral displacement
Re	Reynold's Number
De	Dean's Number
DEPFFF	Dielectrophoretic Field-flow-fractionation
DFF	Dean Flow Fraction
DGC	Density Gradient Centrifugation
MOFF	Multi-orifice Flow Fractionation
LYSIS	Red Blood Cell lysis
DEX	Dextran
PEG	Polyethylene Glycol
PDMS	Polydimethylsiloxane
PS	Polystyrene Beads
SD	Silicon Oxide Beads

INTRODUCTION

Background

White Blood Cells in Blood

Blood is a bodily fluid that delivers necessary biomolecules like nutrients, oxygen and removes metabolic wastes through all parts of the body. Blood consists of plasma, red blood cells (RBCs), white blood cells (WBCs) and platelets which circulate throughout the entire body. Each of these components contains critical information related to overall health of the body and associated tissues or organs[1-3 4-6]. By volume, plasma constitutes roughly ~ 50% of blood, RBC constitute~ 45% of blood and WBC constitutes <1% of blood. WBCs cells can be extremely valuable for health monitoring, disease diagnosis and prognosis, and understanding the overall health of the human body. WBCs are a heterogeneous group of nucleated cells that are found in circulation. Leukocytes are commonly referred to as WBCs as following isolation, WBC appear as an enriched white buffy layer. There are 5 major subpopulations in WBC: lymphocytes, monocytes, neutrophils, eosinophils and basophils. In healthy adults, neutrophils consist roughly 60% of total WBC, lymphocytes consist roughly 30%, and Monocytes consists roughly 5%. Despite the fact that WBCs account for <1% of total cells in blood, they carryout both the innate and adaptive immune functions which protect the body in the event of injury, infection and disease. WBCs therefore play an important and indispensable role in inflammation and resolution of inflammation in the event of injury, infection or disease [7-13]. The role of WBC subpopulations in mediating the body's

response to various diseases such as diabetes, cancers, cardiovascular disease, autoimmune disorders, pulmonary disease and metabolic disorders has been studied extensively [14-18]. Various subpopulations of WBC like neutrophils and macrophages migrate to injured or diseased tissues like in the cases of cancer and atherosclerosis [15,19]. In other studies, the role of WBC in the initiation and progression of disease has been elucidated via the knockout of WBC specific surface antigens. The current method of validating the role of WBC in various disease pathologies relies on the study of WBC counts altered in diseased populations compared with healthy populations, and the expression of specific markers on WBCs as observed in disease. [20,21]

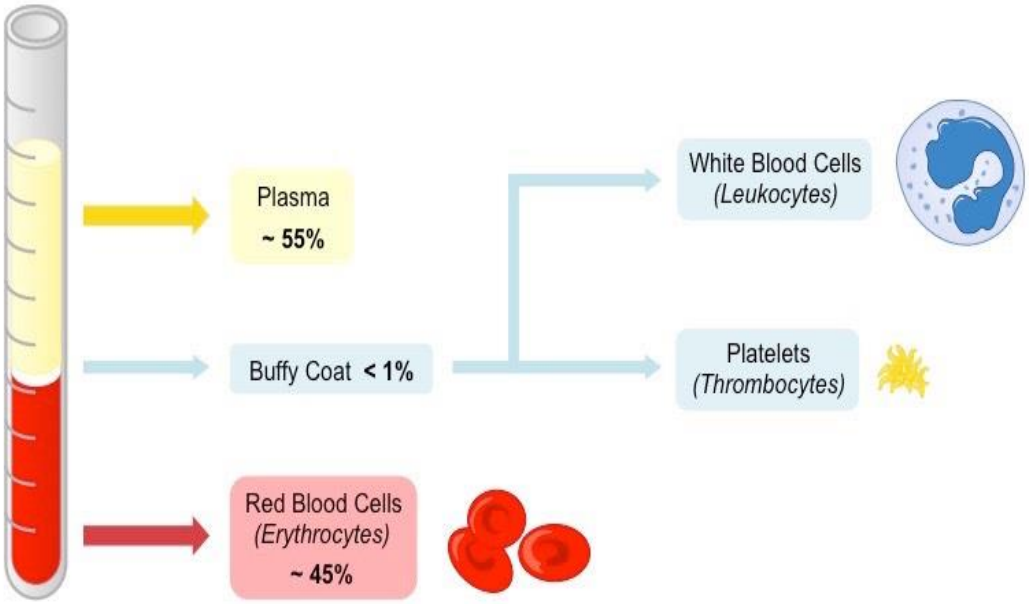

Figure 1. The Composition of Blood. Blood accounts for 7% of body weight in an average adult. In volume about 55% of blood is plasma. In plasma, 92% of the volume is water, 8% of represents blood plasma proteins, and trace amounts of other materials. One microliter blood contains 4-6 million RBCs, 4000-1000 WBCs, and 200,000-500,000

platelets. Reproduced from http://ib.bioninja.com.au/standard-level/topic-6-human-physiology/62-the-blood-system/blood-composition.html

WBC for Health Monitoring and Disease Diagnosis

Specific WBCs (neutrophils and monocytes) that facilitate innate immune responses are typically the first responder to any injury or infection and respond to local signaling cues from affected tissue to maintain homeostasis. Other WBCs (lymphocytes) are involved in adaptive immunity which is a late and programmed response where specific lymphocytes (T and B cells) respond in a highly specific fashion via changes in gene and protein expression resulting in rapid proliferation and production of antibodies or cytokines [22]. Evaluating these time-dependent changes provides a snapshot of the body's immediate status and has great potential for accurate early diagnosis of disease or injury to provide optimal treatment options.

The current most commonly used WBC based diagnostic test is the evaluation of the absolute number counts of subpopulations using Complete Blood Counters (CBC) [23,24]. These instruments distinguish differences in different cell types typically via measurement of electrical resistance, conductance or impedance as cells pass in between two electrodes in a single stream. Another instrument that is commonly used to evaluate leukocytes is the flow cytometer which relies on light scattering (forward and side scatter) to distinguish cells based on shape, size, and cytoplasmic complexity[25-27]. Flow cytometry is therefore simple yet powerful. The absolute numbers of WBC subpopulation could be predictive of the patient's immediate prognosis in various conditions including stroke and myocardial infarction [28 29]. Besides the absolute numbers, the changes to the

WBC cell surface and intracellular molecular expression can be of great value in research laboratories or in the clinical setting. The challenge associated with analysis of WBCs is that they are extremely sensitive to the environmental changes and can become easily activated due to different stimuli[30]. Moreover, isolation of blood from the body also induces continuous changes in blood cells once they leave the body. WBCs can become activated as a consequence of the isolation technique or prolonged maintenance outside the body may not be accurate or reliable predictors of the patient's condition[30].

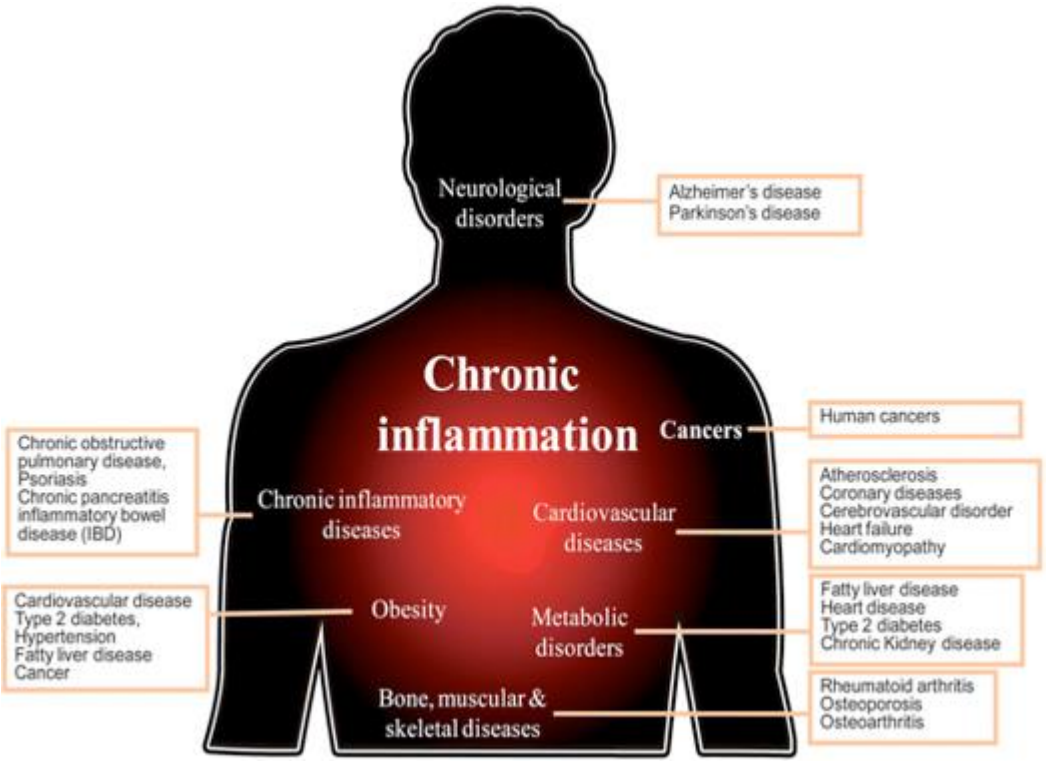

Figure 2. The Chronic Inflammation Disorders with Causal Origins in Inflammatory Processes. The chronic inflammation refers to long-term inflammation that could last from months to years. It can result from failure to eliminate cues of acute inflammation, autoimmune disorder or exposure to low dose of irritant for long period. Inflammatory abnormalities are a large group disorders that underline a vast variety of human disease

like cancer, atherosclerosis, obesity, diabetes and many others. Reproduced from https://healthvigo.blogspot.com/2018/01/chronic-inflammation-definition.html

Blood Cell Sorting

WBC isolation from blood is necessary since WBCs only consist less than 1% of blood cells in volume or numbers. The extremely large number of RBCs must be removed before WBC can be analyzed. Blood cell isolation is accomplished by exploiting differences in either physical or biochemical properties between different blood cell types. The enrichment of WBC from whole blood consists of mainly removing RBCs. The differences in density, shape, vulnerability to osmotic pressure, deformability, electrophoresis properties and surface tension have been studied extensively for the possible application of WBC isolation from whole blood [31-35]. Three methods of isolation are most commonly used for WBC isolation and are considered superior to others: affinity-based isolation [36], RBC lysis [37] and density gradient centrifugation [38]. Affinity-based isolation has been used for over 20 years whereas RBC lysis and density gradient centrifugation have been used for over 50 years. Despite development of several newer techniques, none have shown the capability to improve or replace these three techniques which are considered the gold standard. As we gain more knowledge with regards to blood cells and their role in health and disease, we better understand the sensitivity and responses of WBCs to various factors including isolation methods which can induce WBC activation and changes of WBCs in terms of surface marker expression, gene expression, and cytokine secretion [39-42].

Conventional WBC isolation

Methods for isolation of WBCs and depletion of RBCs have been around for over 50 years. Several methods have been developed to isolate WBC or WBC subpopulations for further studies or analysis. Amongst the various methods available for WBC separations, three methods have been found superior to others due to important factors that include isolation efficiency, ease of operation, ability to be performed using common lab equipment and sufficient processing capability. These three techniques are: immuno-affinity based separations [36], density-gradient centrifugation isolation [35], and RBC-lysis [43].

Immunoaffinity separations take advantage of the specific antigen-antibody interactions for highly specific capture of WBC subpopulations to immobilized antibodies. The strength of this method is the use of highly specific interactions to isolate high purity samples of specific leukocyte sub-populations. However, the highly specific interaction means the isolation is antibody biased and prior knowledge of the antibody-antigen interaction needs to be known. Further for efficient isolations, the sample has to be diluted and the throughput is extreme low due to time needed for interactions between the cell surface markers and the immobilized capture antibodies to occur [44]. Another drawback is that the interaction of antigen-antibody can also initiate signaling cascades within leukocytes causing them to become activated due to the antibody binding event [36]. RBC lysis methods are another popular method used for isolation of all major WBCs. Typically, an ammonium chloride based lysis buffer is used to lyse RBCs by exploiting the presence of the enzyme carbonic anhydrase which is present only within RBCs [43]. The mechanism of osmotic lysis is as follows: ammonium diffuses freely through the cell membrane and increases the concentration of intracellular hydroxide. Hydroxide reacts

with intracellular carbon dioxide to form bicarbonate. In red blood cells, the intracellular bicarbonate is exchanged with the extracellular chloride through the chloride/bicarbonate transmembrane anion exchanger of RBCs. The result is an influx of H_2O inside RBCs, which causes cellular swelling and eventually rupture of the cell membrane. Another commonly used lysis buffer is pure deionized water. Since RBCs do not contain a nucleus, they are more vulnerable to osmotic pressure [45]. By precisely control the time RBCs are exposed to DI water, WBCs can be preserved while RBCs are lysed. Although lysis techniques are simple and convenient to use, the collected samples contain total WBCs including neutrophils, lymphocytes and monocytes. The neutrophils make up ~ 70% of WBCs. Therefore, any analysis on lymphocytes or monocytes requires additional purification steps for evaluation. The hemoglobin (heme and hemin) released from lysed RBCs can also potentially activate WBCs [45].

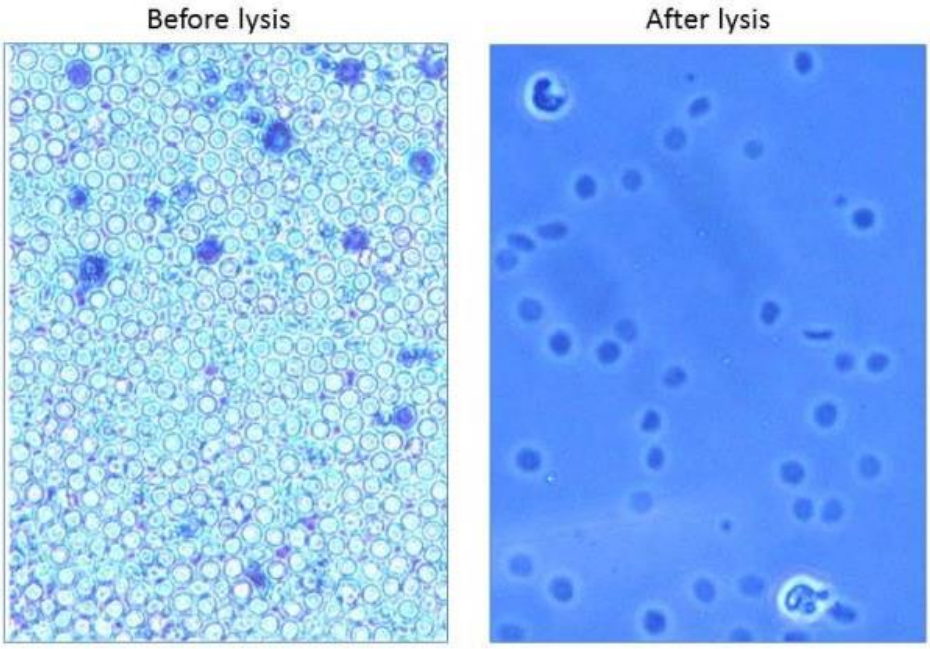

Figure 3. The RBC lysis for WBC isolation. RBCs are lysed by the immune chloride solution under room temperature for 5 minutes. All the RBCs are removed and leave all WBC subpopulations. Reproduced from https://www.novusbio.com/products/red-blood-cell-rbc-lysis-buffer_nbp2-29442

Another popular method used for isolation of peripheral blood mononuclear cells (PBMC) is the density-based centrifugation isolation. Density-based centrifugation exploits the density differences between PBMCs (lymphocytes and monocytes) and granulocytes or RBCs. The density of PBMCs is ~1.07g/ml, whereas the density of granulocytes and RBCs are higher at is ~ 1.09g/ml and ~ 2.1g/ml respectively. When whole blood is layered on top of a medium of intermediate density (Ficoll or Percoll,1.077g/ml) and subject to centrifugal force at 300-700g for 20-40 minutes. The PBMCs are concentrated on top of density gradient and granulocytes and RBCs pellet to the bottom of the tube. By careful pipetting, the PBMC layer can be extracted. This process is both time-consuming and labor-intensive. Isolation of the PBMC layer requires careful pipetting and typically results in ~ 50% of the total PBMCs. Ficoll or Percoll solutions used for this process could have a negative effect on PBMC activation [46]. The major issue with this approach is the high level of stress associated with the centrifugation process which has been known to cause activation of WBCs via changes in intracellular signaling and expression of cell surface markers [35,47,48].

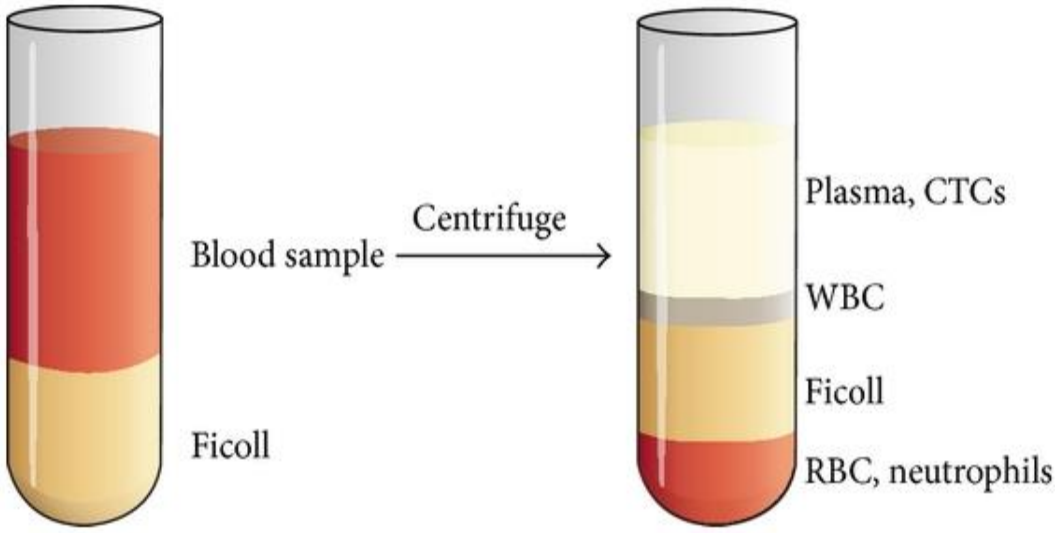

Figure 4. Conventional Density Gradient Centrifugation for WBC Isolation. By exploiting the density difference between PBMCs and RBC. Diluted blood was layered on top of the Ficoll and spun at 700g force for 20 minutes. Then the PBMCs are isolated when RBCs and neutrophils are forced into Ficoll layer pelleting to the bottom and PBMCs remain on top of Ficoll layer due to the density difference. Reproduced from https://openi.nlm.nih.gov/detailedresult.php?img=PMC4419234_BMRI2015-239362.001&req=4

Isolation of WBC Subpopulations with Minimal-activation

To be able analyze WBCs which accurately reflect the immediate status of the body, WBC activation needs to be minimized as much as possible prior to analysis. The most important factor is the time between WBC collection and analysis. Once WBCs are removed from circulation in the body, WBCs undergo continuous changes due to the influence of various environmental factors [30]. Therefore, the time between blood

collection and WBC analysis is the critical for accurate analysis of WBC to reflect the in-vivo status. Another important factor is the isolation process itself [49]. Each of the above three methods introduces unnecessary stress (physical or biochemical) which elicits a response from the WBCs. Immuno-affinity based approaches result in activation via antibody-antigen interactions and take extended duration of time for processing, lysis based techniques do not isolate WBCs into different subpopulations and cause activation via exposure to hemoglobin (heme and hemin) released from RBC lysis [50] and conventional density gradient centrifugation are time consuming and results in exposure of WBCs to high levels of physical centrifugal stress during processing and loss of cells during manual fractionation [50,51] [46].

Following blood draw, activation of WBCs is inevitable. However, if activation can be limited by minimizing time between blood collection and WBC analysis along with limiting various physical and biochemical stimuli that impact cells during the isolation process, then the isolated WBC sample will provide significantly higher quality information. To accomplish this, microfluidic lab-on-a-chip techniques are ideal as they provide the opportunity to process samples immediately following blood draw and enable analysis within a matter of minutes as opposed to hours as with conventional methods. Moreover, miniaturization also provides additional opportunities to significantly minimize physical and biochemical stress experienced by WBCs during the isolation process.

Microfluidic Cell Sorting

Microfluidic techniques have been used for cell sorting due to several advantages associated with miniaturization. First, the microfluidic channels have extremely high surface area-to-volume ratio that can be beneficial in terms of providing additional surface area for a given volume of blood as in the case of affinity-based approaches. Second, at these size scales unique flow phenomena including laminar flow, Deans flow etc. come into play providing new approaches to manipulate and sort cells. Microfluidics can also provide techniques where every single cell is evaluated/sorted under the exact same conditions [52,53] and this has led to widespread use of microfluidic approaches especially for isolation of rare cells that are present in extremely low numbers in the blood at a frequency of ~one cell per milliliter. Despite several microfluidic based approaches, the only FDA approved method for isolation of circulating tumor cells (CTCs) is the Veridex CELLSEARCH which employs a size filter to separate CTCs from other blood cells and achieves confirmation via imaging [54]. Microfluidic techniques for isolation of WBCs from blood employ various techniques including inertial focusing effects, microfluidic centrifugation, surface tension, pillar-like structures as filters, lateral displacement, deformability of cells and immuno-affinity based approaches. However, these microfluidic approaches have been limited to proof-of-concept demonstrations and have not found widespread use in laboratories or clinics due to low throughput, poor efficiency and the need to pre-process samples prior to use. Recent advances in microfluidic approaches for cell sorting are highlighted in Figures 5-7[55].

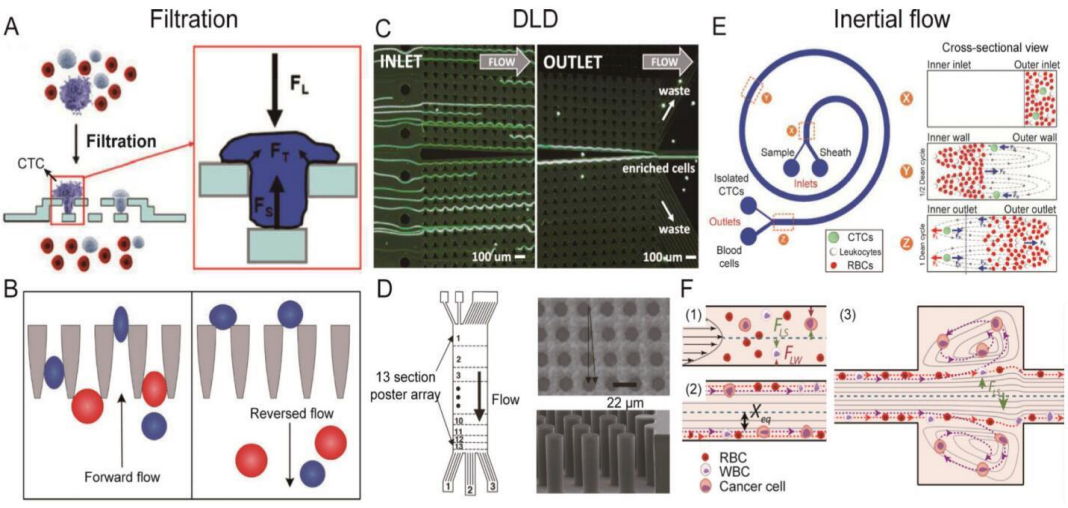

Figure 5. (A) Filtration using a 3D microfilter device and (inset) the applied forces on a trapped cell. FL: force caused by the fluidic flow pressure. FS: supporting force from the bottom membrane. FT: tensional stress force on the plasma membrane. (B) Microfluidic ratchet cell sorting mechanism. Smaller and more deformable cells can squeeze through the funnel constrictions during forward flow. However, they are unable to pass back through the funnels when the flow direction is reversed periodically to unclog the filter. (C) A Deterministic lateral displacement (DLD) device with one inlet and two outlets (collection and waste). Using a symmetrical design, large cells dispersed in the inlet are focused against the central channel wall, where they can be collected at the collection outlet, while smaller cells enter the waste outlet. (D) A DLD device designed to separate WBCs from RBCs and platelets. 13 sections of post arrays with different critical diameters and spacings were used to separate cells with a range of diameters. (E) Schematic illustration of the separation principle for high-throughput CTC isolation using Dean Flow Fractionation. Under the influence of Dean drag forces (blue arrows), the smaller hematologic cells migrate along the Dean vortices towards the inner wall, then back towards the outer wall again. The larger CTCs will experience additional strong

inertial lift forces (red arrows) and focus along the microchannel inner wall, thus achieving separation. (F) The principle of a vortex chip based on inertial forces. At the channel inlet, cells are randomly distributed and experience two opposing lift forces, the wall effect FLW and the shear-gradient lift force FLS. As a result, cells migrate to dynamic lateral equilibrium positions, Xeq. Upon entrance into the reservoir, the wall effect is reduced. Larger cells still experience a large FLS and are pushed away from the channel centerline into the vortices. Smaller cells do not experience enough FLS and remain in the main flow. Reproduced from Yan et. al. 2016.

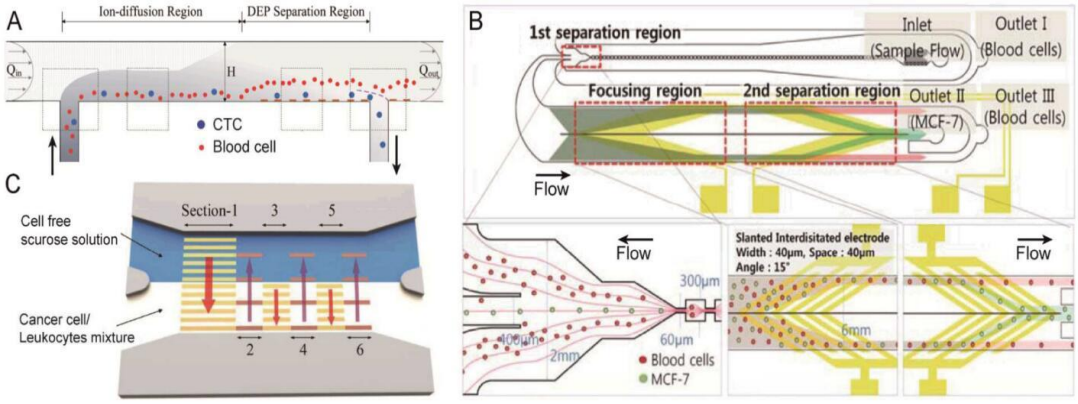

Figure 6. (A) A continuous-flow chamber based on dielectrophoretic field-flow-fractionation (DEPFFF) to isolate tumor cells from peripheral blood mononuclear cells (PBMNs). (B) Schematic diagram of a microfluidic device for cancer cell separation using multi-orifice flow fractionation (MOFF) and DEP. In the first separation region, the relatively larger MCF-7 cells and a few blood cells pass into the center channel and enter the DEP channel, while most blood cells exit at Outlet I. In the focusing region, all cells experience a positive DEP force and then align along both sides of the channel. Finally, the second separation region selectively isolates MCF-7 cells via DEP. (C) An illustration of a microfluidic device using an optically induced-dielectrophoretic (ODEP) force for

cancer cell isolation. Six sections of animated (moving in the direction of the red arrows) light-bar screens were digitally projected onto the CTC isolation zone. Reproduced from Yan et. al. 2016.

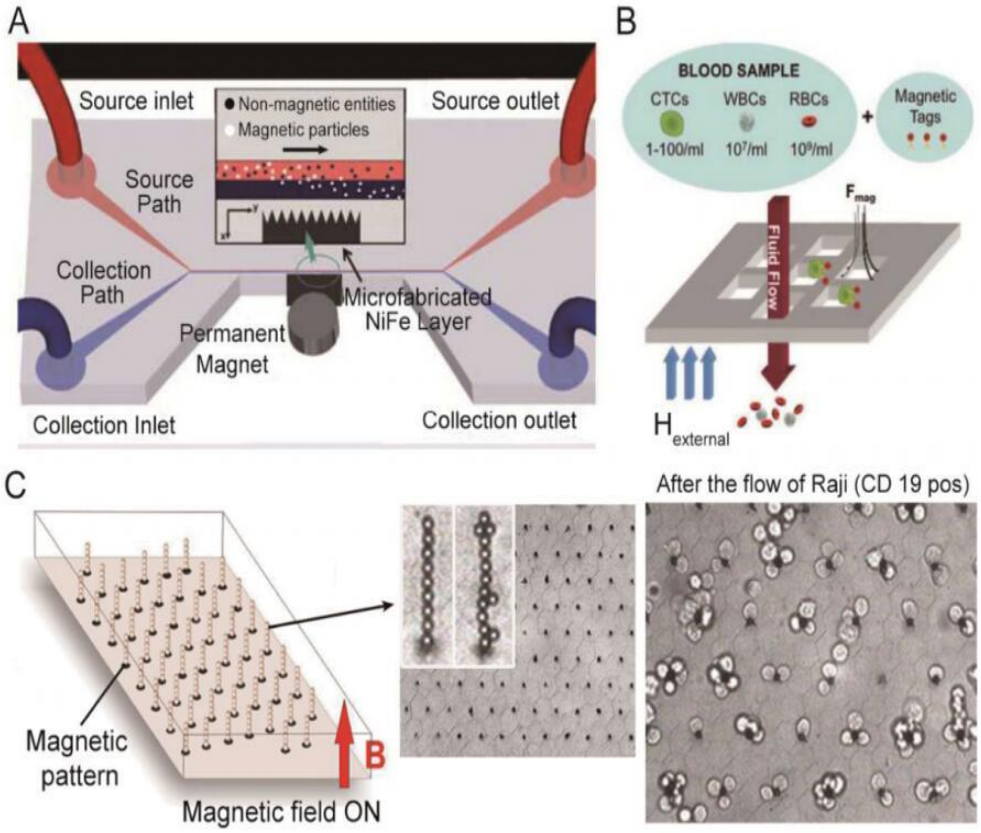

Figure 7. (A) Schematic of a magnetophoretic microdevice with two inlets and two outlets. Inset shows how magnetic beads flowing from the upper source path are pulled across the laminar streamline boundary into the lower collection path when subjected to a magnetic field gradient. (B) Capture principle of a magnetic sifter. A whole blood sample is labeled with magnetic tags and pumped through the pores by an applied external magnetic field. Magnetically labeled target cells are captured at the pore edges where

high magnetic field gradients exist. Unlabeled cells pass through the pores. (C) Operating principle and practical implementation of the Ephesia system. A hexagonal array of magnetic ink is patterned on the bottom of a microfluidic channel. The application of an external vertically-aligned magnetic field induces the formation of a regular array of magnetic bead columns localized on top of the ink dots. After the passage of 400 Raji cells, numerous cells are captured on the columns. Reproduced from Yan et. al. 2016.

Microfluidic approaches have been widely explored for cell sorting especially to address complex problems like rare cell sorting in complex blood samples. These approaches exploit scaling effects and confined volumes possible in the microscale and rely on flow phenomena in conjunction with unique geometries, immobilized antibodies or externally applied force field to enable separations as illustrated Figures 5, 6 and 7.

Microfluidic Density Gradient Centrifugation: Design Considerations

The major design challenge in miniaturizing conventional density gradient centrifugation is accounting for scaling effects that distinguish microscale fluid behavior from fluid behavior in the macroscale. Fluid flow in microfluidic channels is primarily laminar. However, in low aspect ratio channels, at higher Reynolds number flows, when cells and particles comparable to the size of the flow channels, the parabolic flow profile that develops within these channels results in a velocity gradient across the cross-section of the channel which generates inertial lift forces that force cells and particles to the outer walls[56,57]. The wall lift forces push back on the cells/particles and equilibrium is achieved, resulting in focusing close to the walls with larger particles closer to the wall and smaller particles further away. When rectangular channels arranged in a curved/spiral

fashion, secondary Deans forces also develop resulting in rotational effects on the flowing fluid. This results in a single focusing position close to the inner wall. To enable microfluidic density gradient centrifugation, it is essential to maintain laminar flow while minimizing inertial focusing effects and Deans flow.

To determine if microfluidic density gradient centrifugation is indeed possible, it is essential to understand the fluid flow within our design. Specifically, we need to evaluate both Reynolds number (Re) and Deans number (De). Reynold's number (Re) is a parameter that is used to describe flow regime: laminar or turbulent. Turbulent flow is the most common flow profile in conventional systems and is chaotic and unpredictable.

$$\mathrm{Re} = \frac{\rho u D}{\mu}$$

where ρ is the density, u is the velocity, D is the hydraulic diameter and μ is the flow viscosity. The hydraulic diameter is a computed value that depends on the cross-sectional geometry. When Re>2300, flow tends to be chaotic and become turbulent. When Re<2300, flow tends to be stable where flow streams are side by side but not mixing except diffusion and become laminar.

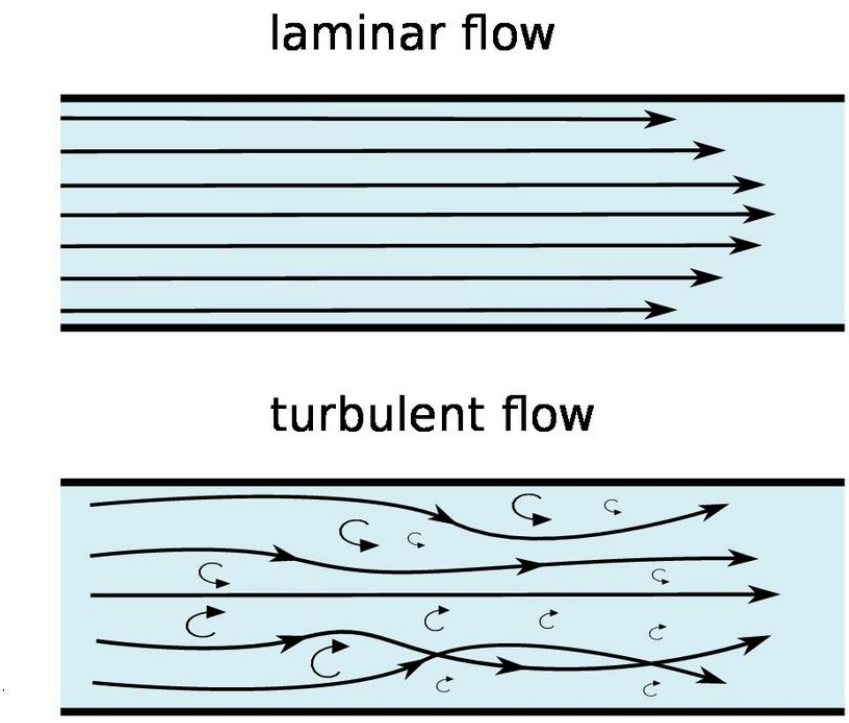

Figure 8. The Flow Streamlines in Laminar and Turbulent flow. Reproduced from https://www.simscale.com/forum/t/what-is-laminar-flow/70247

De is a parameter that is used to predict the secondary flow profile in curvature channels. With circular or spiral geometry, Deans flow could lead to two counter-rotating vortices shown in figure 9. The current physics behind Dean flow dynamics in spiral microchannel is based on the assumption of two counter-rotating vortices that develop due to the longer path that the fluid on the outer part of the channel takes in comparison to the fluid closer to the inner wall. De number could be calculated as:

$$De = \sqrt{\frac{d}{2r}\frac{\rho v d}{\mu}}$$

Where r the radium of the curvature, ρ is the density, u is the velocity, d is the hydraulic diameter and μ is the flow viscosity. Deans flow along with inertial focusing effects has been exploited for rare cell sorting shown in Figure 9.

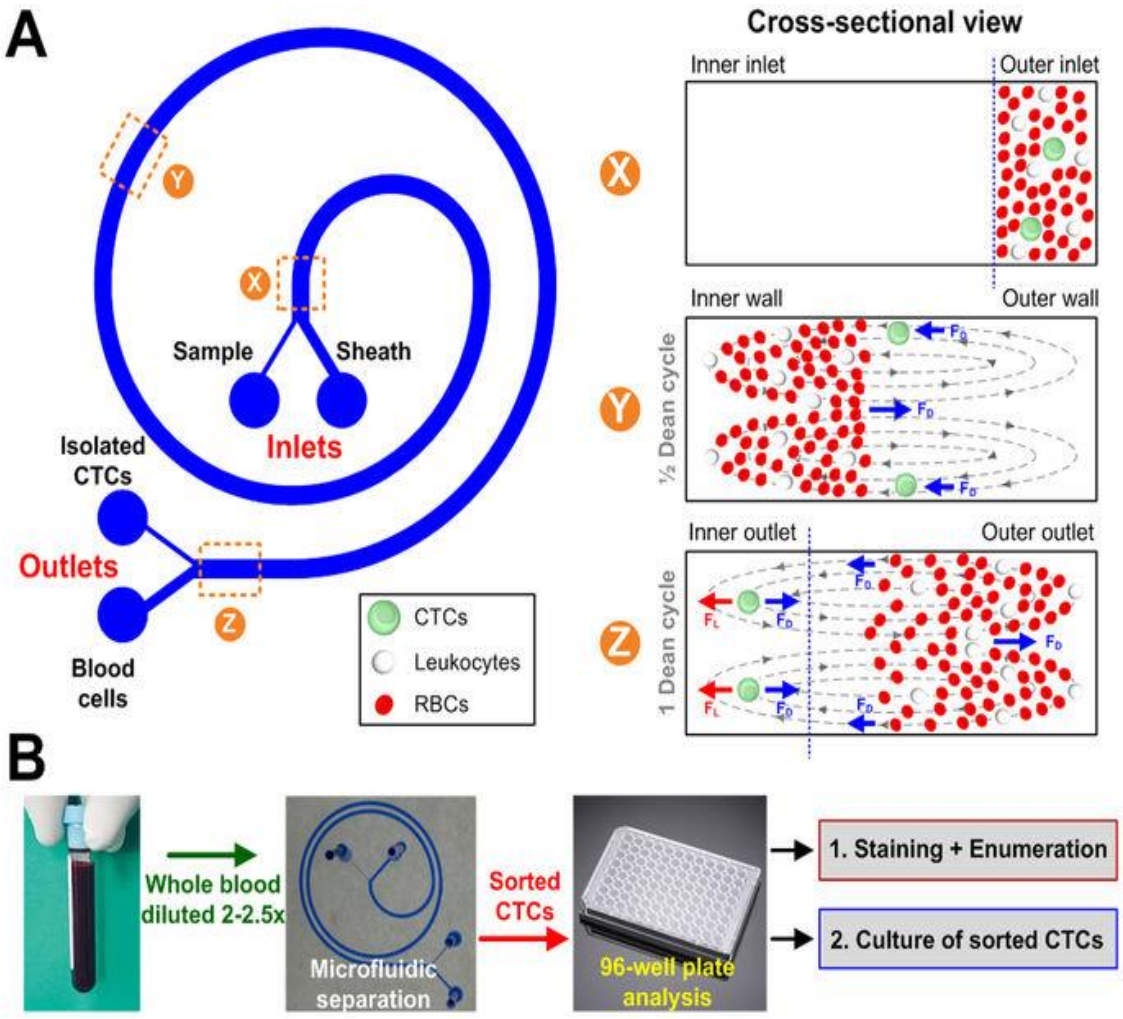

Figure 9. Schematic illustration of the separation principle for high-throughput CTCs isolation using *Dean Flow Fractionation (DFF)*. Blood sample and sheath fluid are pumped through the outer and inner inlets of the spiral device respectively. Under the influence of Dean drag forces (F_D (*blue arrows*)), the smaller hematologic cells (RBCs and leukocytes) migrate along the Dean vortices towards the inner wall, then back to outer wall again (Dean cycle 1), while the larger CTCs experience additional strong

inertial lift forces (F_L (*red arrows*)) and focus along the microchannel inner wall, thus achieving separation. (B) Overall workflow of device operation and coupling with 96-well plate for various downstream applications such as CTCs enumeration and culture of sorted CTCs. Image reproduced from Hou et. al. 2013.

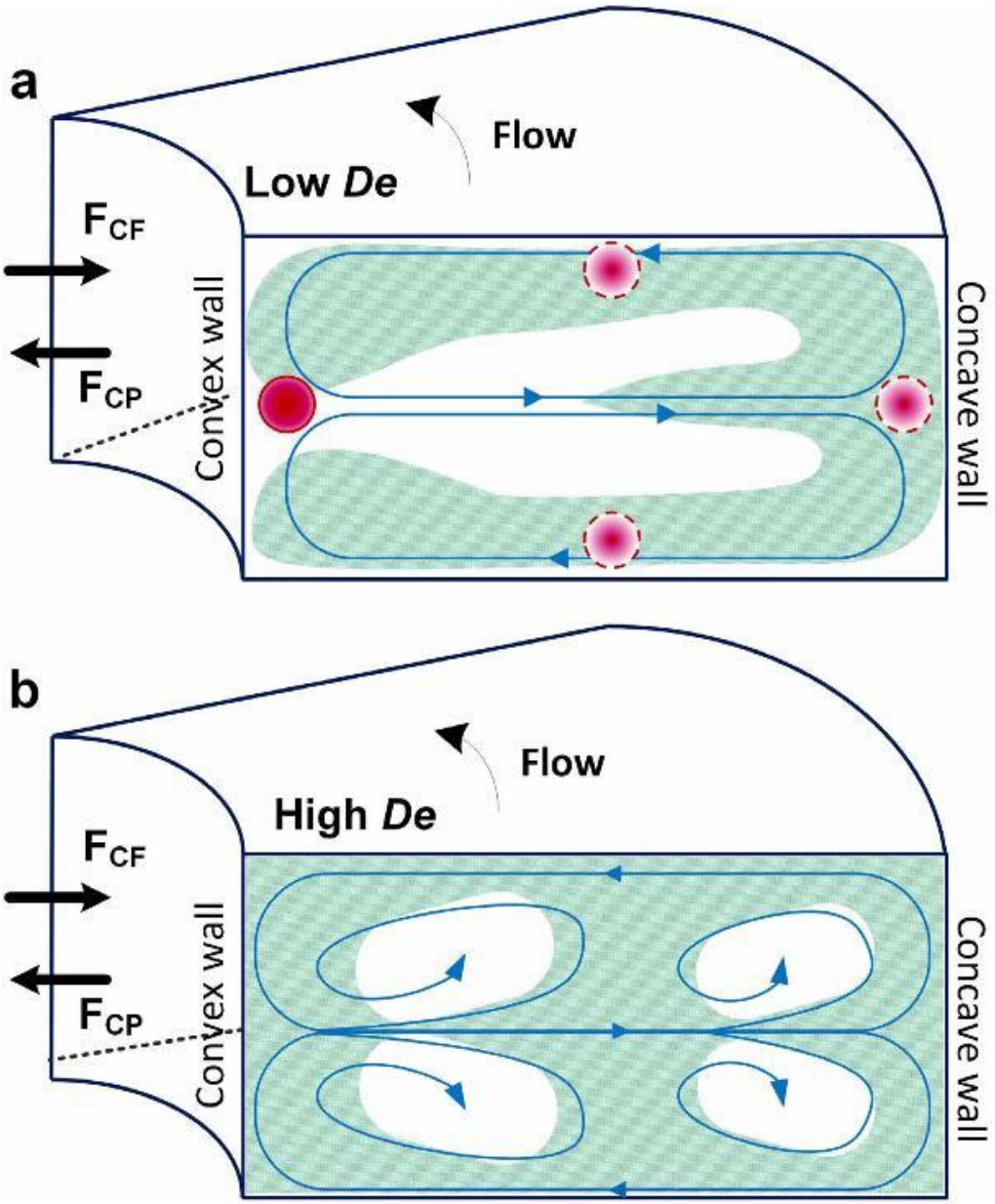

Figure 10. Schematic illustrating two counter rotating vortices in a curved rectangular channel. Image reproduced from Nivedita. et. al.2017

Inertial focusing of particles and cells in straight microchannel has been extensively studied for cell sorting. The focusing occurs due to parabolic flow profile-induced inertial lift force and wall-induced lift force. The focusing position is dependent on the size of the particles or cells.

Conceptually, for our setup to work, first, we require the centrifugal forces to be much greater than the inertial lift forces rendering the focusing effects due to fluid flow in the channels irrelevant and second, we also require the viscous forces to be significantly stronger than the secondary Deans forces to avoid mixing to the two phases and allow the two phases to flow in laminar streams side by side. This is achieved by achieving specific geometries for a given spinning speed to ensure that the Reynolds number which dictates the magnitude of the inertial lift forces and Deans number which dictates the magnitude of forces that cause fluid rotation within the channels to be small enough to not affect the flow and separation within the microfluidic channels.

Microfluidic Centrifugation Platform for Blood Cell Separations

Microfluidic centrifugation platform has many advantages over other microfluidic systems which require pumps for transport of fluid. The centrifugation platform is relatively small and consists of a flat disc to immobilize the microfluidic device and enable spinning at predetermined speeds. A microfluidic device with samples loaded in the reservoirs can be operated via spinning the flat disc on the rotary platform. The rotary motion provides both the centrifugal forces necessary of the cell separations and to

induce transport of the cell sample and Ficoll into the microfluidic channels. This simple setup can easily be translated into a portable platform compatible with operation at bedside in a clinical setting for rapid sample processing. The rotational motion generates significant centrifugal force to cause migration of cells/particles as well as liquid of interest based on differences in densities for cell/particle separations. There have been prior studies that have miniaturized conventional density gradient centrifugation with Ficoll and Blood[57-59]. However, this platform utilizes a small sample of blood preloaded into the device rather than reproducing this process in a continuous flow format. The disadvantages with this approach include the small sample volume, complexities associated with fractionation and operation of the device. This approach is shown in the Figure 11 below.

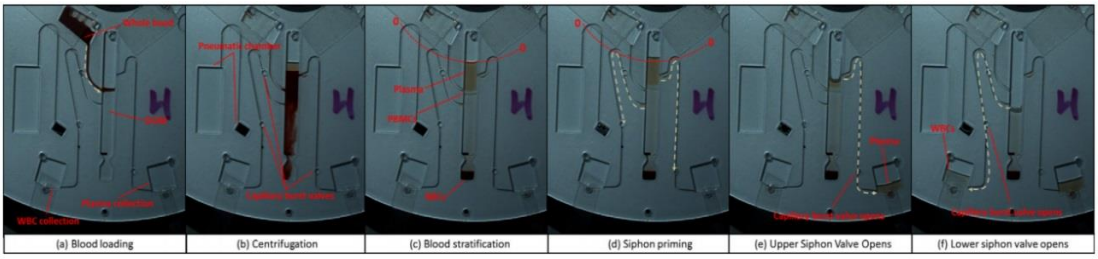

Figure 11. WBC isolation using a dual siphon, split pneumatic chamber. (a) The disc is loaded with DGM as the whole blood is introduced during disc acceleration. (b) RBCs sediment. Note that the siphons have a number of capillary burst valves. The upper capillary valve on the lower siphon prevents the DGM pre-priming siphon while the disc is stopped for blood loading. (c) Stratified blood in the chamber. Note that the plasma remains below the siphon crest points. (d) The disc is decelerated and the bulk liquid is displaced radially inwards and the siphon prime. The siphon priming is halted by the capillary burst valves. The siphons must be primed at a lower frequency (~2.5 Hz) than the nominal frequency (~15 Hz) to prevent the capillary valves from bursting early or out

of sequence. However, due to the low hydrostatic priming pressure at this spin rate, the crest of the lower siphon required treatment using a surfactant to achieve reliable priming. The upper siphon was not treated. (e) The spin rate is increased and the burst valve of the upper siphon capillary is opened, thus removing the plasma to the collection chamber. (f) The spin rate is increased further and the lower siphon valve opens for removing the WBCs (with some plasma and DGM) to the WBC collection chamber This study has validated the possibility of isolating WBC from whole blood with miniaturized density gradient. However, due to the intrinsic drawback of the microchannel, the blood sample loading (10µl) and throughput has prevented this platform to be practical for subsequent analysis. Image reproduced from Kinahan. et. al. 2016

Activation of Leukocytes

Lymphocytes are responsible for both adaptive and innate immunity and travel from the blood to inflamed sites through a multi-step process involving recognition of a chemokine gradient and activated vascular endothelial cells via a process extravasation. Chemoattractant cytokines (chemokines) regulate this trafficking by forming a concentration gradient that directs migration of leukocytes[60-62]. The endothelium proximal to the injury site also becomes inflamed and caused activated monocytes and granulocytes to initially roll, attach and transmigrate across the endothelium thereby extravasating into the injured tissue. The production of chemokines in inflammation triggers the overexpression of the chemokine receptors on the surface of WBCs and is considered an early marker of leukocyte activation. Further, expression of integrins is

also important for leukocyte rolling and attachment to the inflamed endothelium and an increase in the expression on the surface of leukocytes can also be considered a marker of early leukocyte activation. Both chemokine receptors and integrins can be impacted by the isolation process and evaluation of both these markers can serve as an indication of impact of the isolation process on artefactual activation of leukocytes [63,64].

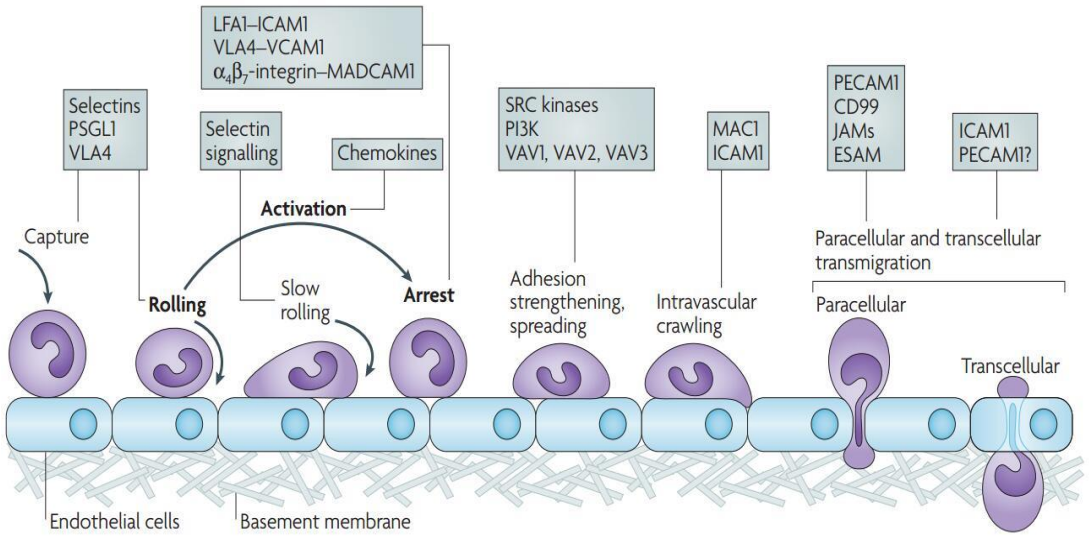

Figure 12. The Updated Leukocytes Adhesion Cascade. The original three steps are shown in bold: rolling, which is mediated by selectins, activation, which is mediated by chemokines, and arrest, which is mediated by integrins. Progress has been made in defining additional steps: capture (or tethering), slow rolling, adhesion strengthening and spreading, intravascular crawling, and paracellular and transcellular transmigration. Image reproduced by Ley. et. al. 2007.

Aqueous Two-phase Partitioning

Phase partitioning has been used for extraction and purification of biomolecules and cells. Aqueous two-phase systems (ATPSs) is most common phase partitioning approach which takes advantage of two immiscible polymer solutions under certain temperature, ionic strength, and polymer concentration. Even though the mechanism is not fully understood, they have been applied for numerous extractions of biomolecules like nucleic acids and proteins for its simple yet efficient approach [65-68]. The selection and purification relies on surface tension, ion charge based on certain parameters like the choice of polymer types, buffer ions and use of specific ligands. When two immiscible phases like polyethylene glycol (PEG) and Dextran (DEX) are dissolved in a salt solution like phosphate buffered saline and allowed to separate, PEG and DEX separate with the heavier DEX at the bottom and the lighter PEG at the top. While the saline partitions equally, various salts do not partition equally resulting in each of the solutions acquiring a net charge. When a mixture of cells or biomolecules are introduced within this environment, they migrate to energetically favorable locations either in the PEG phase, DEX phase or at the interface [65]. Conventional phase partitioning is performed in a 15 or 50 mL tubes and requires ~ 24 hours for complete partitioning. By miniaturizing phase partitioning we aim to exploit both centrifugal forces and microscale channels to enable rapid phase partitioning within a few minutes with automated fractionation of phase separated cells. By using a microfluidic device on a rotary platform we aimed to accomplish phase partitioning. The microchannel consists of segments for mixing featuring serpent shape channel and phase partition straight shape channel. At the end of the microchannel, each phase can be extracted to the designated outlet via resistance manipulation. Previous miniaturized WBC isolation uses charged dextran and PEG after

phase partitioning for selective cell sorting [65,69,70]. Our goal is to integrate dextran/PEG mixing, phase partitioning along with cell sorting, and extraction into a single device. Compared with conventional cell sorting principles, phase partitioning introduces less stress in biofriendly environment that is ideal to preserve WBCs in their natural state.

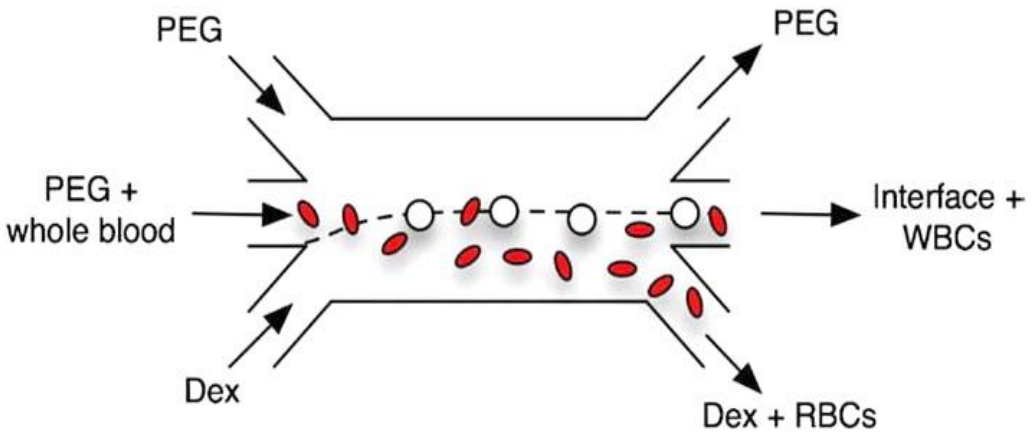

Figure 13. Schematic illustration of leukocyte separation based on microfluidic aqueous two-phase system (ATPS). In this exmaple, whole blood diluted in PEG is exposed to a PEG-Dex interface, represented by the dashed line. Due to differences in surface energies, the leukocytes prefer the interface while RBCs migrate into the Dex region. From SooHoo et. al. 2009.

Thesis Goals

My goal is to apply microfluidic approaches particularly in the context of techniques that exploit centrifugal forces to either significantly improve on conventional separation techniques or to develop completely new techniques not possible in the macroscale. There are two parts to my thesis project: (1) miniaturize conventional density gradient

centrifugation for isolation of PBMCs from whole blood and (2) develop new phase partitioning technique for WBC subpopulation isolation.

Hypothesis and Specific Aims

Microfluidic provides a powerful platform to achieve sorting of leukocyte sub-populations from whole blood with great potential to be translated into point-of-care technologies for rapid isolation thereby minimizing the time between blood draw and attainment of target cells. . Microfluidics also provides unique opportunities to minimize both physical and biochemical stress. Therefore, I hypothesized that *"Centrifugal microfluidic adaptation of conventional density gradient centrifugation will result in a rapid and gentle technique capable of isolation of PBMCs from whole blood where all PBMC subpopulations are preserved with minimal isolation process induced activation"*. Moreover, this process does not require the use of pumps or complex manipulation and is compatible with point-of-care adoption in the clinical setting. I also hypothesized that *"Microfluidic phase partitioning represents a new technique for separation of cells based on differences in surface energy and microfluidic adaptation will result in rapid and efficient partitioning of phases and separation of cell enabling a completely new approach for blood cell sorting"*.

To test my hypothesis, I formulated three specific aims:

Specific Aim1: *To demonstrate feasibility that density gradient centrifugation can be accomplished within a microfluidic platform where the sample stream and the Ficol stream can be layered side-by-side with sufficient centrifugal forces to enable separation of particles of different densities while at the same time minimizing Deans forces that cause fluidic rotation and mixing.*

Specific Aim2: *To accomplish separation of PBMCs from whole blood using microfluidic density gradient centrifugation and demonstrate that various PBMC sub-populations can be preserved while minimizing isolation process induced activation of different sub-populations.*

Specific Aim3: *To demonstrate preliminary proof-of-concept demonstrations that rapid and efficient phase partitioning can be accomplished using centrifugal microfluidics and this partitioning can be used to separate beads with different surface energy.*

My thesis project therefore will test my two hypotheses via completion of these three specific aims.

MICROFLUIDIC ADAPTION OF DENSITY GRADIENT CENTRIFUGATION FOR ISOLATION OF PARTICLES AND CELLS

by

YUXI SUN, PALANIAPPAN SETHU

MDPI Bioengineering 2017,4(3)

Format adapted for dissertation

Abstract:

Density gradient centrifugation is a label-free approach that has been extensively used for cell separations. Though elegant, this process is time consuming (>30 mins), subjects cells to high levels of stress (> 350 g) and relies on user skill to enable fractionation of cells that layer as a narrow band between the density gradient medium and platelet-rich plasma. We hypothesized that microfluidic adaptation of this technique could transform this process into a rapid fractionation approach where samples are separated in a continuous fashion while being exposed to lower levels of stress (< 100 g) for shorter durations of time (< 3 mins). To demonstrate proof-of-concept, we designed a microfluidic density gradient centrifugation device and constructed a setup to introduce samples and medium like Ficoll in a continuous, pump-less fashion where cells and particles can be exposed to centrifugal force and separated via different outlets. Proof-of-concept studies using binary mixtures of low density polystyrene beads (1.02 g/cm^3) and high-density silicon dioxide beads (2.2 g/cm^3) with Ficoll-Paque (1.06 g/cm^3) show that separation is indeed feasible with > 99% separation efficiency suggesting that this approach can be further adapted for separation of cells.

Keywords: Cell Separations; Label-free cell separation; Microfluidics; Density gradient centrifugation

Introduction

Cells in the body are either organized as complex multi-cellular tissue or as heterogeneous mixtures in fluids such as blood. Separation of cells into different sub-populations is an essential step for various applications such as immune-phenotyping, tissue engineering and evaluation of systemic inflammation [2,71-77]. The focus of the majority of cell separations approaches is the isolation of cells in blood as they provide important prognostic and diagnostic information [44,72,76]. Blood consists of plasma, erythrocytes, leukocytes and platelets.

Leukocytes or white blood cells are responsible for maintenance of immune homeostasis and for protecting the body from injury and infections. Therefore, sampling leukocytes from a patient provides valuable information regarding the immediate immune and inflammatory status of the patient [44,73,78]. Cell separation approaches exploit differences in either physical properties or biochemical specificities of different cell types to accomplish separation of cells into different sub-populations. Commonly used techniques include erythrocyte or red blood cell lysis which relies on selective susceptibility of erythrocytes to lysis when suspended in an ammonium chloride buffer [43], density gradient centrifugation which takes advantage of differences in mass density between mononuclear leukocytes and erythrocytes and granulocytes [79] and immuno-affinity separations which rely of antibody-cell surface antigen interactions to enable capture [36]. Leukocyte sub-populations provide superior diagnostic and prognostic information in comparison to total leukocytes. However, isolation of leukocytes into sub-populations requires the use of antibodies or methods like density gradient centrifugation which can both lead to activation of leukocytes due to the leukocyte binding event [80] or

due to high levels of stress [40] during the isolation process. Considering the fact that leukocytes are highly sensitive to isolation process induced stress which can result in artificial leukocyte activation [40], it is important to develop antibody-free approaches which minimally stress cells during the isolation process.

Density gradient centrifugation is one of the most commonly used separation methods for fractionation of leukocyte subpopulations from the perspective of efficiency, purity and cost. By exploiting density difference among leukocyte subpopulations and erythrocytes, less dense peripheral blood mononuclear cells (PBMCs) are enriched in a suspended buffy layer after following >350g centrifugation for 30 minutes. User skills are critical for extraction to ensure efficient fractionation via removal of the thin band of PBMCs layered in between the Ficoll-Paque layer and platelet-rich plasma. However, this approach imposes stress cells leading to activation of leukocytes [40].

Microfluidics provides a powerful platform for analysis of small biological samples via precise manipulation of the fluids. Several microfluidics based approaches have been developed to isolate and analyze leukocyte populations. The most common microfluidic approaches for isolation of mononuclear leukocytes or peripheral blood mononuclear cells (PBMCs) have exploited size difference to achieve separation of target cells via either filtration or inertial focusing based platforms[81-83]. However, these approaches have not found use in the clinical setting due to inherent limitations with these techniques to distinguish cells with small size difference. Microfluidic filtration approaches also have to deal with issues such as cell deformability and the tradeoffs between throughput and clogging of microfluidic filters [84]. Inertial focusing also relies on cell size differences to accomplish cell sorting but size difference among blood cells is not sufficient enough to isolate PBMC and may require significant sample dilution to work effectively [85].

Microfluidic magnetophoretic, dielectrophoretic and acoustophoretic devices have been developed and used either with or without antibodies but their throughput and separation efficiency have prevented widespread adoption in the clinic or research setting [83,86-89]. Therefore, while microfluidics provides new opportunities for cell separation with potential to minimize isolation process induced activation of cells by minimizing stress and processing times, we have yet to see clinical adaptation of these techniques.

There have been several prior efforts that have utilized centrifugal force to drive fluids or achieve cellular separations using microfluidic approaches. However, there approaches do not accomplish high fidelity miniaturization of conventional density gradient centrifugation where red blood cells and PNMs are isolated from PBMCs in unique fractions. Al-Faqheri et al present an excellent review summarizing centrifugal force based microfluidic efforts for cell separations[90]. Other works of importance to the method discussed in this paper include a manuscript by Balter et al used centrifugal microfluidics to label and count leukocyte populations[91], a manuscript by Yu et al where they use centrifugal forces to drive fluid flow and accomplish leukocyte capture on immuno-modified surfaces[92], Ramachandraiah et al [93] developed a lab-on-a-chip DVD for labeling and counting of $CD4^+$ cells, a centrifugally driven immunoassay where antibody coated beads are transported via centrifugal forces and an ELISA like readout is used to facilitate accurate dosing of VEGF[94], Schaff et al [95]developed an immunoassay using centrifugal microfluidics for evaluation of biomarkers in blood, and another manuscript by Zhang et al [96]where a centrifugal microfluidic platform was used to separate plasma from the blood cells and used to separate plasma and determine hematocrit. There are also few examples of density gradient centrifugation using miniaturized platforms. Kinahan et al [97] developed a spira mirabilis inspired geometry for

blood processing using density gradient media. Later they developed a similar platform to fractionate mononuclear blood cells[98]. Rather than operate in a continuous mode, they developed a valving system to contain samples within a chamber during application of centrifugal force. Another paper by Moen et al[99] describes a density gradient process where total leukocytes are separated from red blood cells at high efficiency. Finally, Ukita et al [100] developed a percoll gradient based density gradient centrifugation to separate beads of different densities. The technique presented in this paper is unique as it faithfully mimics conventional density gradient centrifugation using Ficol Paque.

The major design challenge in miniaturizing conventional density gradient centrifugation is to account for scaling effects that distinguish microscale fluid behavior from conventional macroscale effects. Fluid flow in microfluidic channels is primarily laminar. However, in low aspect ratio channels, at higher Reynolds number flows, when cells and particles comparable to the size of the channel flow via these channels, the parabolic flow profile that develops in these channels results in a velocity gradient across the cross-section of the channel which generates lift forces that force cells and particles to the outer walls. The wall lift forces push back on the cells/particles and equilibrium is achieved, resulting in focusing close to the walls with larger particles closer to the wall and smaller particles further away. When rectangular channels arranged in a curved/spiral fashion, secondary Deans forces also develop resulting in rotational effects on the flowing fluid. This results in a single focusing position close to the inner wall.

For our setup to work conceptually, we require the centrifugal forces to be much greater than the inertial lift forces rendering the focusing effects due to fluid flow in the channels irrelevant and for minimal generation of secondary Deans forces which can

cause mixing to the two phases flowing side by side. This is achieved by achieving specific geometries for a given spinning speed to ensure that the Reynolds number which dictates the magnitude of the inertial lift forces and Deans number which dictates the magnitude of forces that cause fluid rotation within the channels to be small enough to not affect the flow and separation within the microfluidic channels.

$$\text{Re} = \frac{\rho u L}{\mu}$$

$$\text{De} = \sqrt{\frac{d}{2r}\frac{\rho v d}{\mu}}$$

This paper details an approach that has great potential to be adapted for separation of PBMCs in the clinical setting. Conventional density gradient centrifugation with Ficoll-Paque was miniaturized as a pump-free, continuous, label-free microfluidic system that when mounted onto a custom built rotary platform can enable separation of cells based on differences in density. While conceptually simple and straightforward, the significance of inertial effects in microfluidic channels and Deans forces associated with microfluidic channels that have curvature associated with them, it is important to minimize both these effects to ensure laminar flow of blood and Ficoll streams side by side as they transit the entire microfluidic device. This was accomplished via careful manipulation of channel dimensions, fluidic resistances, orientation of inlets and outlets and direction of rotation. To demonstrate successful proof of concept of this technique to separate cells/particles of different densities, we utilized low density polystyrene beads (PS) (1.02 g/cm^3) and high density silicon dioxide (SD) beads (2.2 g/cm^3) with Ficoll-Paque (1.06 g/cm^3).

2. Materials and Methods

2.1. Materials Microfluidic Device Fabrication

Microfluidic devices were fabricated using methods previously established in our laboratory [101]. Briefly, a 2D layout of the channel architecture was created using AutoCAD layout software (Autodesk, Inc., San Rafael, CA) and printed using a high-resolution printer on a mylar sheet (Fineline Imaging, Colorado Springs, CO). This photolithography mask was then used to define channel structures using a negative photoresist (SU-8 50, Microchem Corp, Westborough, MA) on a silicon wafer. Using standard soft-lithography, the microfluidic devices were molded using (poly)dimethylsiloxane (PDMS) (Dow Corning, Midland, MI) and bonded to either a silicon or glass wafer. Access holes for the 2 inlets and 2 outlets were punched using a 22-gauge blunt syringe needle and tubing was press fitted to introduce and remove fluids. Two holes were also punched close to the center of the device to hold 2ml Nalgene Cryogenic Vials (Thermo Scientific, Waltham, MA) reservoirs. The caps of reservoirs were punched holes by 22-gauge needle for delivering samples contained within the reservoirs into the main channel via the connecting tubing.

2.2. Centrifugation System

A system was designed and fabricated to enable microfluidic density gradient centrifugation. The system consists of a variable speed DC motor (AO Smith, Pitt City, OH) and a custom designed rotary platform that can be mounted on the motor to hold the microfluidic device (Fig. 1). The rotary platform has a machined slot to hold the silicon

wafer in place during spinning and two slots at diametrically opposite locations to collect the samples from the two outlets. The system spins clockwise with maximum speed of 1725 rpm.

2.3. Particles and Fluids

To demonstrate proof-of-concept, we used 2 different particles with different densities and a Ficoll-Paque solution with an intermediate density. Specifically, we used low density fluorescently labeled polystyrene beads (1.02 g/cm3) (Thermo Fisher Scientific, Waltham, MA) and high density silicon dioxide beads (2.2 g/cm3) (Thermo Fisher Scientific, Waltham, MA) with Ficoll-Paque (1.06 g/cm3) (GE Healthcare, Uppsala, Sweden). The particles were suspended as a 2% solution in 1X phosphate buffered saline (PBS) with either a detergent or 1% bovine serum albumin (BSA) to prevent aggregation. The solutions were vigorously shaken prior to use, loaded in beads reservoir along with Ficoll-Paque and accelerated rapidly to 50% of maximum speed for 5 minutes and then gradually decelerated until the system came to rest.

2.2. Flow Characterization

1X (PBS) (Thermo Fisher Scientific, Waltham, WA) and Ficoll-Paque Plus (GE Healthcare, Uppsala, Sweden) were loaded in each reservoirs and the centrifugation system was operated at 20%,30%, 40%, 50%, 70% and 90% of maximum spinning speed for 5 minutes (n = 3). After spinning stops, the inlet reservoirs and outlet collection tubes

were removed and the quantity of liquids in each was measured to estimate the collective and relative flow rates.

2.5. Evaluation of Samples

Evaluation was of samples within the channels and collected in the reservoirs were evaluated using bright field and fluorescence microscopy (Nikon TE 2000, Nikon Instruments, Melville, NY). For evaluation of beads within the channels, PDMS devices bonded to glass were directly imaged at different locations. Samples collected in the reservoirs were analyzed using a hemocytometer. Fluorescently labeled polystyrene beads were distinguished from silicon dioxide beads via fluorescence imaging.

3. Results

3.1. Device Dimensions for Optimal Laminar Flow and Layering

Various designs were evaluated for establishment of optimal laminar flow and layering of the sample stream over the Ficoll-Paque stream. The design that produced the optimal results without inducing mixing due to inertial forces and Deans forces was a 3 mm wide with a pitch of 45 mm **(Fig 1)**. The total channel length was 20 cm and the channel ran along the circumference of the silicon/glass wafer with room provided for the inlets and outlets. The width of the channels was 3 mm and the height was 50 μm resulting in an aspect ratio of 60:1 (w:h). To avoid secondary forces that typically develop in microfluidic channels, we found that channel heights greater than 100 μm result in inertial forces that cause particle migration towards the side walls and Deans flow resulting fluid rotation within the channels which disrupts the laminar flow within

the channels. Therefore, a channel height of 50 µm and a channel width of 3 mm were selected to avoid fluid rotation and inertial particle migration within the channels.

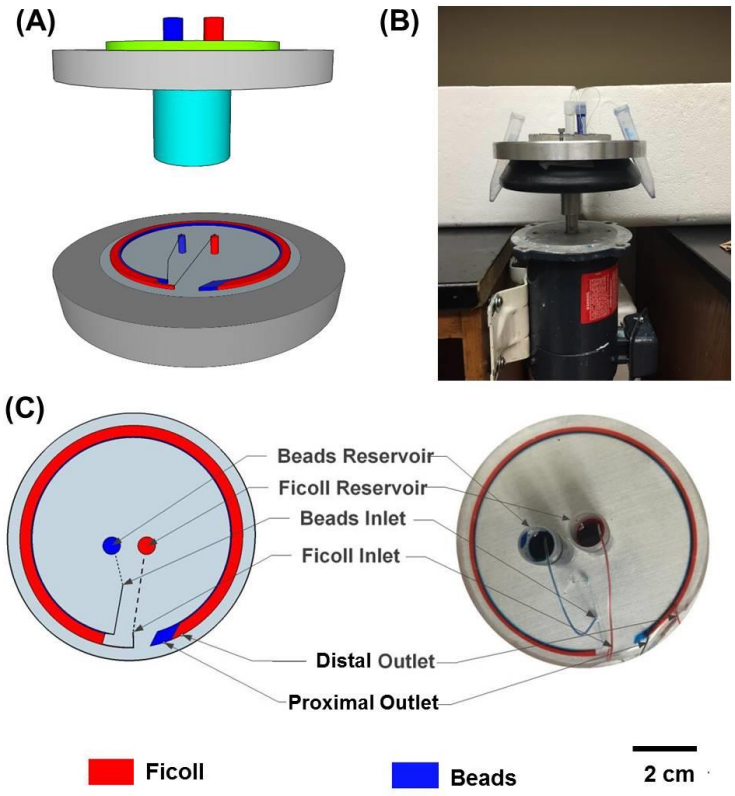

Figure 1. Setup for microfluidic density gradient centrifugation. (A) Simplified schematic of the device (B) Picture of the centrifugation system consisting of the custom designed rotary platform mounted onto the motor to hold the microfluidic device. (C) Schematic and actual image of layering of colored 1X PBS streams within the device.

3.2. Characterization of Total and Relative Flow Rates

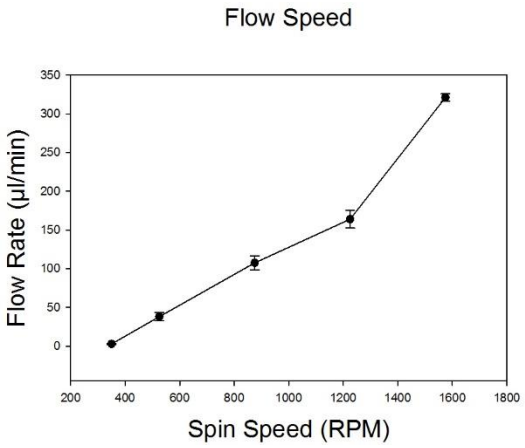

Figure 2: Characterization of fluid flow rates (1X PBS and Ficoll-Paque) at 20%. 30%,50%,70% and 90% of the motor's maxmum speed (1750rpm) (n = 3). The ratio of PBS to Ficoll was maintained constant at 1:3 by adjusting the resistances of the tubing.

To estimate the total and relative flow rates of particle samples and Ficoll-Paque, we measure the quantity of liquid in the inlet reservoirs and in the outlet collection tubes following spinning at different speeds ranging from 400 to 1600 rpm **(Fig. 2)**. The ratio of particle sample to Ficoll-Paque was maintained at 1:4 via adjustment of fluidic resistances leading into the main flow channel. This ratio remained relatively constant regardless of the spin speed and was ideal for particle separations. The total flow rate ranged from 50 mL/min at 550 rpm to a maximum flow rate of 330 mL/min at 1600 rpm. These results were consistent (n = 3) and the standard deviations negligible.

3.3. PS Bead Separation

To demonstrate initial proof-of-concept, a 2% solution of PS beads (1.02 g/cm^3) suspended in a 1X PBS solution were flowed into the system and layered over either 1X PBS (1.00 g/cm^3) or Ficoll-Paque (1.06 g/cm^3) when the device was spun at a speed of

875 rpm which generates centrifugal force of ~ 40g. As expected when layered over 1X PBS, the centrifugal force pushes the PS beads through the lower density 1X PBS resulting in > 99% of PS beads being collected via the distal outlet **(Fig. 3, top)**. However, when the PS beads were layered over the higher density Ficoll-Paque, the PS beads remain at the interface of the Ficoll-Paque layer unable to transit through the higher density medium resulting in > 98% of PS beads fractionated via the proximal outlet **(Fig. 3, middle)**. Results are represented as means ± SD (n = 5).

3.4 SD Bead Separation

SD beads with a density of 2.2 g/cm^3 are heavier than Ficoll-Paque and we sought to determine if we could isolate SD beads via the distal outlet when the device was spun at a speed of 875 rpm which generates centrifugal force of ~ 40g. Results confirm that the heavier SD particles do indeed transit through the Ficoll-Paque and > 99% of the beads can be fractionated via the distal outlet **(Fig. 3 bottom)**. Results are represented as means ± SD (n = 5).

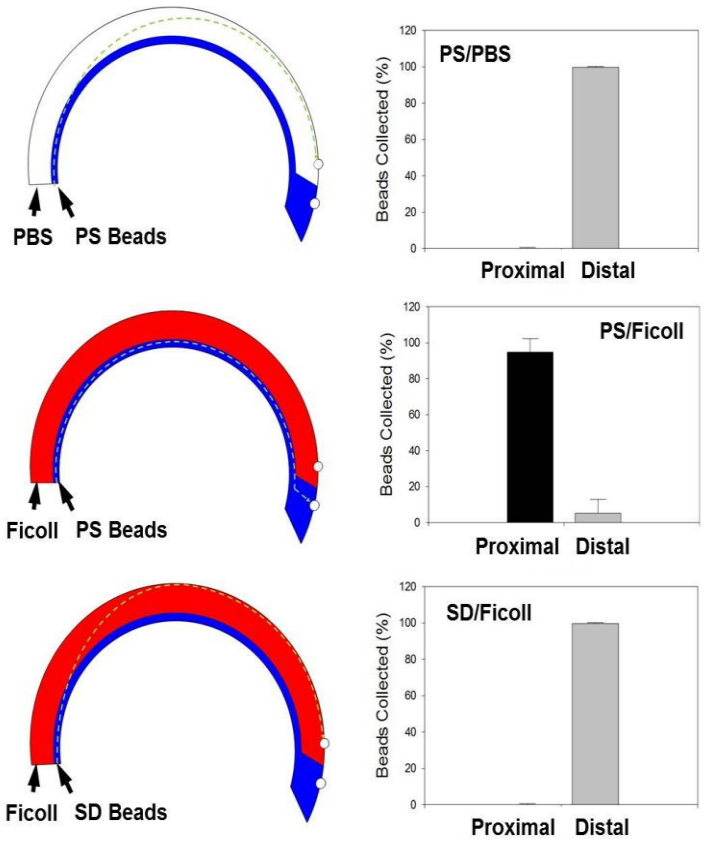

Figure 3: Proof-of-Concept Studies were established by flowing either PS or SD beads solutions with either 1X PBS or Ficoll to determine migration behavior and isolation via either the proximal or distal outlets. On the left is the schematic with hypothesized path of travel through the microfluidic channel at a speed of 875 rpm (40g) and on the right is a plot with % of beads collected at each outlet for the following conditions: (A) PS Beads and 1X PBS, (B) PS Beads and Ficoll and (C) SD Beads and Ficoll (n = 5).

3.5 Separation of PS-SD Bead Mixture

Finally to the ability of this device to achieve separation of particles of low and high density particles with a medium of intermediate density was accomplished. A 1X PBS

solution containing a 4% solution of equal amounts of PS and SD beads was layered over Ficoll-Paque and the device was spun at 875 rpm (40g). Bright field and fluorescence images of PS and SD beads at different locations (inlet, intermediate location within the channel and outlet) during this process are shown in **Figure 5**. Results confirm that high efficiency separation of PS and SD beads can indeed be accomplished using this approach with > 99% PS beads collected via the proximal outlet and > 99% of SD beads fractionated via the distal outlet **(Fig. 4)**. Results are represented as means ± SD (n = 5).

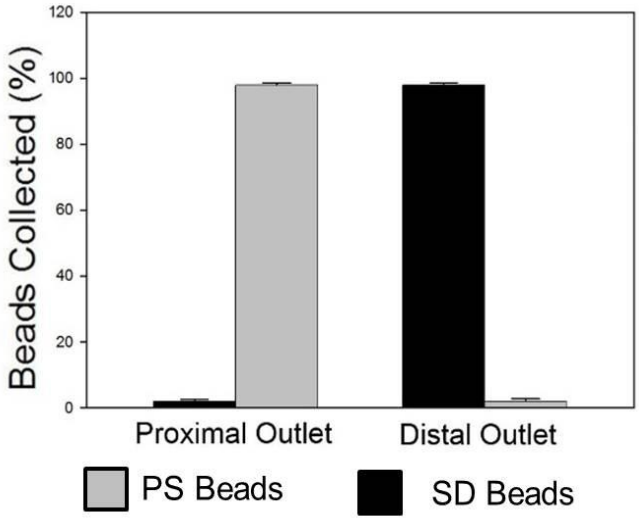

Figure 4: Quantitative assessment of beads collected via the proximal and distal outlets using a hemocytometer under bright field imaging and fluorescence microscopy. Results show that > 99% of PS beads were obtained via the proximal outlet whereas > 99% of SD beads were obtained via the distal outlet (n = 5).

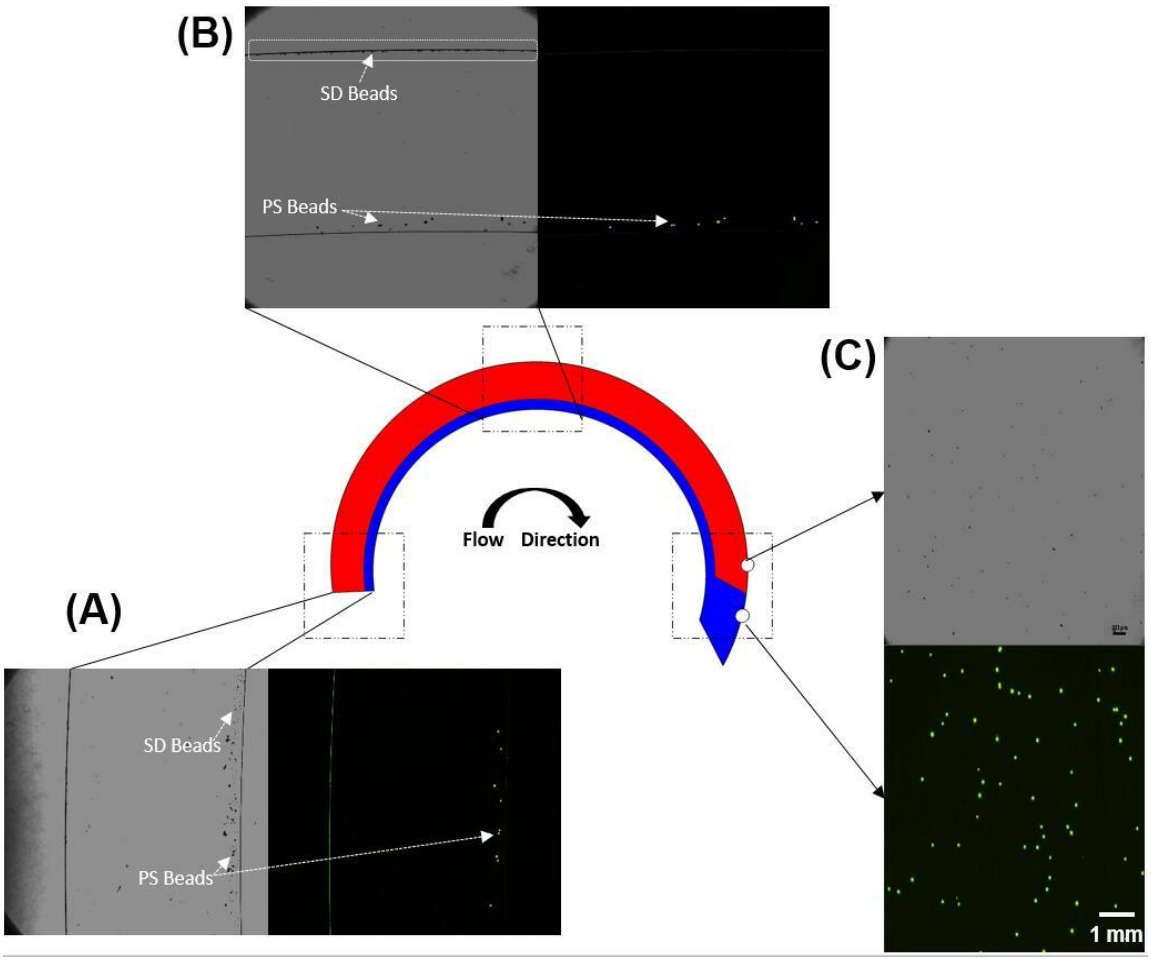

Figure 5: Images of PS (fluorescently labeled) and SD (unlabeled) beads at different locations during the microfluidic density gradient centrifugation process. PS beads are visible in both the brightfield and fluorescence images whereas the SD beads are only visible in the fluorescence images. (A) At the inlet, both PS and SD beads are closer to the inner wall, (B) as the beads transit through the device, centrifugal force moves the heavier SD beads through the Ficoll and the SD beads can be seen close to the outer wall (highlighted region) whereas the PS beads are unable to migrate into the Ficoll and (C) Collected samples at the proximal and distal outlets confirm separation of PS and SD beads via the proximal and distal outlets respectively.

4. Discussion

Density gradient centrifugation is an elegant technique that exploits differences in cell mass densities to achieve separation of PBMCs from erythrocytes and polymorphonuclear cells (PNMs). While this technique has been extensively used for over 50 years, shortcomings associated with high levels of stress imposed on cells, extended processing times and need for skilled technicians to cleanly isolate the fractionated samples have not been addressed. Microfluidics systems have great potential to miniaturize conventional macroscale separation approaches where samples confined in micrometer sized channels can be manipulated to enable faster, more precise and highly effective separations. To overcome the high levels of stress on cellular samples and minimize separation time, we sought to develop a microfluidic adaptation of conventional density gradient separation process focused on minimizing duration and magnitude of centrifugation induced stress on cells.

To accomplish this, we designed a system that could house a microfluidic device that was bonded to a 4" silicon wafer and subject it to rotary motion to induce centrifugal force for cell and particle separation. The microfluidic device itself consists of channel where cell/particle samples can be layered as a laminar stream over medium like Ficoll-Paque. Within microfluidic devices, low Reynolds number flows ensure that viscous forces are dominant and laminar flow is achieved. In order to minimize inertial effects and potential Deans forces that can induce rotational mixing of the sample stream with the Ficoll-Paque, the width of the channel (3 mm) was significantly larger than the height of the channels (50 μm) resulting in an aspect ratio of 60:1 (w:h) and ensuring large interfacial contact area between the fluids and the device. This ensured that introduction

of two streams of fluids with different viscosity and density can be maintained as laminar streams and the layering is maintained during rotational motion of the device. It is also critical that the samples flow direction is in the same direction of the rotary motion to avoid disruption of the layering process. Further it is important to position and orient the inlet reservoirs and inlets correctly to ensure proper flow of samples and Ficoll-Paque into the device. In our pump-less system, centrifugal force was used to induce fluid flow by ensuring that the outlets were placed further from the center of the wafer than the inlets. The ratio of fluids was adjusted by controlling the fluidic resistances (tubing and inlet channel length and diameter). To achieve proper fractionation, the fluidic resistance of the two outlets was adjusted to ensure proper fractionation of low and high density particles. Finally, to avoid trapping and retention of the high density particles within the channels, the spin speed (magnitude of centrifugal force) needs to be controlled to ensure that the high density particles travel into the Ficoll-Paque layer but do not travel all the way to the outer wall.

Prior to optimizing this system for separation of cells, we sought to demonstrate proof-of-concept using particles. Polystyrene (PS) particles have a lower mass density than Ficoll-Paque whereas silicon dioxide (SD) particles have a higher mass density and provide ideal particles for feasibility demonstrations. Initially, to confirm that beads introduced within the system experienced centrifugal force and moved across the channel we tested PS beads in solution with PBS. Our results confirm that higher density PS particles move through the lower density PBS and are collected via the proximal outlet. When the same PS beads were layered over Ficoll-Paque the higher density Ficoll-Paque retarded the motion of the PS beads and the PS beads were collected via the distal outlet. When SD beads were layered over Ficoll-Paque, the higher density SD beads easily

transited through the Ficoll-Paque and were collected via the proximal outlet. Finally, when a binary mixture of PS and SD beads were layered over Ficoll-Paque, the low density PS beads remained at the interface of the Ficoll-Paque layer and were collected via the distal outlet whereas the high density SD beads transited through the Ficoll-Paque and were collected at the proximal outlet. The separation efficiencies for all separations were > 99% confirming that the conventional Density Gradient Centrifugation can be effectively miniaturized.

We believe that this technique is directly translatable to separation of blood cells. We utilized a maximum spinning speed of 875 rpm which translates to a residence time of 16 seconds within the device. This speed was sufficient to generate enough centrifugal force to move SD beads (2.2g/cm^3) which have a significantly higher density than Ficoll-paque (1.07g/cm^3) close to the outer wall. Increased spinning speeds resulted in pinching of SD beads against the walls due to higher centrifugal force which prevents collection of SD beads out of the channels. For blood cells we anticipate that based on the insignificant density difference between red blood cells (1.08 g/cm^3) as well as granulocytes (1.077 g/cm^3) and Ficol-Paque, that a higher spin speed (~ 2500 rpm) and longer residence time (42 Seconds) was necessary for red blood cells and granulocytes depletion. These calculations were made using a modified stokes settling velocity equation.

5. Conclusions

In summary, we demonstrate successful microfluidic adaptation of conventional density gradient centrifugation. Proof-of-concept studies demonstrate high efficiency separation of low density PS beads from high density SD beads when separated using a

medium like Ficoll-Paque. These results suggest that this approach can potentially be adapted for separation of PBMCs from whole blood.

Acknowledgments: YS was supported by an Alabama EPSCoR Graduate Research Scholars Program. This work was supported by the NSF CAREER Award # 1149059 to PS and the Comprehensive Cardiovascular Center and the Division of Cardiovascular Disease at the University of Alabama at Birmingham.

Author Contributions: Y.S. designed and performed all the experiment. P.S. as the principal investigator, provided conceptual and technical guidance for all aspects of the project.

Conflicts of Interest: The authors declare no conflict of interest.

References

1. Byeon, Y., C.S. Ki, and K.H. Han, *Isolation of nucleated red blood cells in maternal blood for Non-invasive prenatal diagnosis.* Biomed Microdevices, 2015. **17**(6): p. 118.
2. Aghazarian, A., et al., *Evaluation of Leukocyte Threshold Values in Semen to Detect Inflammation Involving Seminal Interleukin-6 and Interleukin-8.* Urology, 2015. **86**(1): p. 52-6.
3. Schafer, D., et al., *Prostaglandin D2-supplemented "functional eicosanoid testing and typing" assay with peripheral blood leukocytes as a new tool in the diagnosis of systemic mast cell activation disease: an explorative diagnostic study.* J Transl Med, 2014. **12**: p. 213.
4. Wojcik, M., et al., *Increased expression of immune-related genes in leukocytes of patients with diagnosed gestational diabetes mellitus (GDM).* Exp Biol Med (Maywood), 2016. **241**(5): p. 457-65.
5. Hashemian, A.M., et al., *Diagnostic Value of Leukocyte Esterase Test Strip Reagents for Rapid Clinical Diagnosis of Spontaneous Bacterial Peritonitis in Patients Admitted to Hospital Emergency Departments in Iran.* Iran Red Crescent Med J, 2015. **17**(10): p. e21341.
6. Wang, H., L. Xu, and L. Lu, *Detection of cyprinid herpesvirus 2 in peripheral blood cells of silver crucian carp, Carassius auratus gibelio (Bloch), suggests its potential in viral diagnosis.* J Fish Dis, 2016. **39**(2): p. 155-62.
7. Mariucci, S., et al., *Lymphocyte subpopulation and dendritic cell phenotyping during antineoplastic therapy in human solid tumors.* Clin Exp Med, 2011. **11**(4): p. 199-210.

8. Cheng, X., et al., *Enhancing the performance of a point-of-care CD4+ T-cell counting microchip through monocyte depletion for HIV/AIDS diagnostics.* Lab Chip, 2009. **9**(10): p. 1357-64.

9. Mitroulis, I., et al., *Leukocyte integrins: role in leukocyte recruitment and as therapeutic targets in inflammatory disease.* Pharmacol Ther, 2015. **147**: p. 123-35.

10. Chernyshev, A.V., et al., *Erythrocyte lysis in isotonic solution of ammonium chloride: theoretical modeling and experimental verification.* J Theor Biol, 2008. **251**(1): p. 93-107.

11. Brosseron, F., K. Marcus, and C. May, *Isolating peripheral lymphocytes by density gradient centrifugation and magnetic cell sorting.* Methods Mol Biol, 2015. **1295**: p. 33-42.

12. Pelak, O., et al., *Lymphocyte enrichment using CD81-targeted immunoaffinity matrix.* Cytometry A, 2016.

13. Newton, R.A., M. Thiel, and N. Hogg, *Signaling mechanisms and the activation of leukocyte integrins.* J Leukoc Biol, 1997. **61**(4): p. 422-6.

14. Zhou, L., et al., *Impact of human granulocyte and monocyte isolation procedures on functional studies.* Clin Vaccine Immunol, 2012. **19**(7): p. 1065-74.

15. Bhuvanendran Nair Gourikutty, S., C.P. Chang, and P.D. Puiu, *Microfluidic immunomagnetic cell separation from whole blood.* J Chromatogr B Analyt Technol Biomed Life Sci, 2016. **1011**: p. 77-88.

16. Chen, G.D., et al., *Nanoporous micro-element arrays for particle interception in microfluidic cell separation.* Lab Chip, 2012. **12**(17): p. 3159-67.

17. Chen, W., et al., *Surface-micromachined microfiltration membranes for efficient isolation and functional immunophenotyping of subpopulations of immune cells.* Adv Healthc Mater, 2013. **2**(7): p. 965-75.

18. Li, X., et al., *Continuous-flow microfluidic blood cell sorting for unprocessed whole blood using surface-micromachined microfiltration membranes.* Lab Chip, 2014. **14**(14): p. 2565-75.

19. Xiang, N. and Z. Ni, *High-throughput blood cell focusing and plasma isolation using spiral inertial microfluidic devices.* Biomed Microdevices, 2015. **17**(6): p. 110.

20. Darabi, J. and C. Guo, *Continuous isolation of monocytes using a magnetophoretic-based microfluidic Chip.* Biomed Microdevices, 2016. **18**(5): p. 77.

21. Ding, X., et al., *Cell separation using tilted-angle standing surface acoustic waves.* Proc Natl Acad Sci U S A, 2014. **111**(36): p. 12992-7.

22. Grenvall, C., et al., *Concurrent isolation of lymphocytes and granulocytes using prefocused free flow acoustophoresis.* Anal Chem, 2015. **87**(11): p. 5596-604.

23. Zhu, H., et al., *Screen-printed microfluidic dielectrophoresis chip for cell separation.* Biosens Bioelectron, 2015. **63**: p. 371-8.

24. Al-Faqheri, W., et al., *Particle/cell separation on microfluidic platforms based on centrifugation effect: a review.* Microfluidics and Nanofluidics, 2017. **21**(6): p. 102.

25. Balter, M.L., et al., *Differential Leukocyte Counting via Fluorescent Detection and Image Processing on a Centrifugal Microfluidic Platform.* Anal Methods, 2016. **8**(47): p. 8272-8279.

26. Yu, Z.T.F., et al., *Centrifugal microfluidics for sorting immune cells from whole blood.* Sensors and Actuators B: Chemical, 2017. **245**: p. 1050-1061.

27. Ramachandraiah, H., et al., *Lab-on-DVD: standard DVD drives as a novel laser scanning microscope for image based point of care diagnostics.* Lab Chip, 2013. **13**(8): p. 1578-85.

28. Walsh III, D.I., et al., *A centrifugal fluidic immunoassay for ocular diagnostics with an enzymatically hydrolyzed fluorogenic substrate.* Lab on a Chip, 2014. **14**(15): p. 2673-2680.

29. Schaff, U.Y. and G.J. Sommer, *Whole blood immunoassay based on centrifugal bead sedimentation.* Clinical chemistry, 2011. **57**(5): p. 753-761.

30. Zhang, J., et al., *A lab-on-CD prototype for high-speed blood separation.* Journal of micromechanics and microengineering, 2008. **18**(12): p. 125025.

31. Kinahan, D.J., et al., *Spira mirabilis enhanced whole blood processing in a lab-on-a-disk.* Sensors and Actuators A: Physical, 2014. **215**: p. 71-76.

32. Kinahan, D.J., et al., *Density-gradient mediated band extraction of leukocytes from whole blood using centrifugo-pneumatic siphon valving on centrifugal microfluidic discs.* PloS one, 2016. **11**(5): p. e0155545.

33. Moen, S.T., C.L. Hatcher, and A.K. Singh, *A centrifugal microfluidic platform that separates whole blood samples into multiple removable fractions due to several discrete but continuous density gradient sections.* PloS one, 2016. **11**(4): p. e0153137.

34. Ukita, Y., T. Oguro, and Y. Takamura, *Density-gradient-assisted centrifugal microfluidics: an approach to continuous-mode particle separation.* Biomed Microdevices, 2017. **19**(2): p. 24.

35. Patibandla, P.K., et al., *Hyperglycemic arterial disturbed flow niche as an in vitro model of atherosclerosis.* Anal Chem, 2014. **86**(21): p. 10948-54.

LOW-STRESS MICROFLUIDIC DENSITY GRADIENT CENTRIFUGATION FOR CELL SORTING

by

YUXI SUN, PALANIAPPAN SETHU

In preparation for *Biomedical Microdevice*

Format adapted for dissertation

ABSTRACT

Density gradient centrifugation exploits density differences between different blood cells to accomplish separation of peripheral blood mononuclear cells (PBMCs) from polymorphonuclear (PNM) cells, and erythrocytes or red blood cells (RBCs). While density gradient centrifugation offers a label-free alternative avoiding the use of harsh lysis buffers for blood cell isolation, it is a time-consuming and labor-intensive process during which blood cells are subject to high-levels of centrifugal force that can artifactually activate cells. To provide a low-stress alternative to this elegant method, we miniaturized and automated this process using microfluidics to ensure continuous PBMCs isolation from whole blood while avoiding the exposure to high-levels of centrifugal stress in a simple flow-through format. Within this device, a density gradient is established by exploiting laminar flow within microfluidic channels to layer a thin stream of blood over a larger stream of Ficoll. Using this approach we demonstrate successful isolation of PBMCs from whole blood with preservation of monocytes and different lymphocyte subpopulations similar to that seen with conventional density gradient centrifugation. Evaluation of activation status of PBMCs isolated with this technique shows that our approach achieves minimal isolation process induced activation of cells in comparison to conventional lysis or density gradient centrifugation. This simple, automated microfluidic density gradient centrifugation technique can potentially serve as tool for rapid and activation-free technique for isolation of PBMCs from whole blood for point-of-care applications.

INTRODUCTION

Blood cells contain vital information as changes in immune and inflammatory status of the body are almost immediately reflected in changes in the numbers and activation status of leukocyte sub-populations.[1,3,102-104] There has been significant interest in trying to use this information for advanced diagnosis, to predict patient clinical trajectories, and for determination of patient-specific treatment alternatives. The presence of large numbers of erythrocytes or red blood cells (RBCs) presents a significant challenge as unique signatures indicative of injury or disease in specific leukocyte sub-populations are often not distinguishable when dealing with complex heterogeneous mixtures of cells.[105] Therefore, at a minimum, depletion of RBCs and isolation of leukocytes or leukocyte sub-populations is necessary to obtain highly specific information that can be used for evaluation of patients. Leukocytes are extremely sensitive to changes in environment and stress [106,107]. Isolation of blood and prolonged maintenance ex-vivo after isolation impacts both viability and activation status of leukocytes in a time dependent manner.[108,109] Even the method of collection can alter gene expression profiles of isolated leukocytes.[108,109] Physical or chemical stress during isolation represents additional stimuli that can activate also leukocytes.[39,46] Therefore it is critical that leukocyte isolation be accomplished rapidly following blood draw with minimal stress during the isolation process.

Immuno-affinity techniques provide an elegant method to achieve highly selective isolation of leukocytes and leukocyte sub-populations but the antibody binding event itself can be a source of activation.[110,111] Further, it is essential to have prior understanding of cell surface markers to enable isolation of target cell populations.[112] Therefore, label-free approaches are highly desirable to minimize activation and bias

during the isolation process. Two commonly used techniques for label-free isolation of leukocytes from whole blood are **(A)** Density gradient centrifugation (DGC) and **(B)** Erythrocyte or red blood cell (RBC) lysis (LYSIS). DGC is an elegant process that relies on differences in mass densities of different cell types to enable separation in a label-free fashion. DGC is typically accomplished with a density gradient medium like ficoll, percoll, sucrose or dextran which has intermediate mass density between peripheral blood mononuclear cells (PBMCs) and polymorphonuclear cells (PNMs) and RBCs [79,113]. LYSIS utilizes different osmotic lytic agents like deionized water, NaCl buffer, NH_4Cl-$KHCO_3$ buffer to accomplish isolation of total leukocytes by selective lysis of RBCs [114]. While both DCG and LYSIS methods are label-free and do not require the use of antibodies which can be an additional source of activation, DCG is associated with exposure of leukocytes to high levels of stress (~800g) for extended periods of time (~ 20 mins)[115] whereas LYSIS exposes leukocytes to osmotic solutions and contact with free hemoglobin (heme and hemin) form lysed RBCs which both cause leukocyte activation.[116]

Leukocytes express various surface markers that can be qualitatively and quantitatively evaluated to determine activation status.[80] Transcriptionally regulated markers of activation require a certain amount of time (i.e. transcription of mRNA and translation of proteins) to be useful in evaluating activation. Therefore we focused on activation markers that do not require transcriptional regulation but are already either expressed on the cell surface and become damaged following activation or are contained in vesicles within the cell and translocate to the cell surface following activation. Monocytes in circulation do not express high levels of integrins on the cell surface.

However, immediately following activation the expression of integrins (CD11b/CD18) is transiently upregulated to enable monocytes to roll and attach to the endothelium and transmigrate into the underlying tissue.[117] Therefore evaluation of CD11b/CD18 can be utilized as a highly sensitive marker of monocyte activation and has been previously been used as a highly sensitive marker to evaluate isolation process induced monocyte and granulocyte activation following RBC lysis.[118] There have also been several reports that chemokine (C-C and C-X-C motif) receptors in particular are highly sensitive to stress from isolation processes like DGC. In reviewing literature, we found that expression of CCR2 and CCR4 receptors on lymphocytes and CCR2 on monocytes was significantly reduced following DGC. This reduction in expression was found to be a long-term effect and could not be recovered even with treatment with pro-inflammatory stimuli.[118]

Microfluidics deals with manipulation of fluids within devices in the sub-millimeter scale and can significantly enhance efficiency in comparison to conventional macroscale processes. Scaling effects can also be enhanced to exploit phenomena like low Reynolds Number (Re) laminar flow to enable processes not possible in the macroscale. Previously, our group miniaturized RBC lysis process within a microfluidic platform and demonstrated high efficiency isolation of leukocytes with minimal isolation process induced activation.[49] However, RBC lysis results in isolation of total leukocytes and evaluation of heterogeneous populations is associated with loss in quality of information in comparison to isolated sub-populations.[46] Several groups including ours have previously sought to miniaturize conventional DGC but most demonstrations have been limited to proof-of-concept studies using beads which have significant differences in density.[99,119] One group achieved microfluidic separations of blood cells but the platform

used requires step-by-step layering of blood over Ficoll and processing of small (< 20 μL) of blood and requires complex operation of valves to be able to fractionate separated layers.[120]

In this study we sought to develop a continuous and automated microfluidic device to accomplish isolation of PBMCs (monocytes and lymphocytes) from RBCs and PNMs (granulocytes, basophils, eosinophils, mast cells) by miniaturizing conventional density gradient centrifugation to transform this technique from a high-stress and lengthy isolation process into a rapid and low-stress alternative. Specifically, we hypothesized that establishment of laminar flow and reducing the separation distances by over an order of magnitude will drastically reduce the time and forces necessary to achieve high efficiency density gradient centrifugation. We ultimately envision this device to be adopted for point-of-care processing of blood from patients for isolation of PBMCs. Our design allows for evaluation of blood without any pre-processing, automated metering and delivery of blood and Ficoll into the device, and seamless collection of different cellular fractions via different outlets. Further, this device will require only a simple rotary platform and both fluid transport and centrifugal force are generated via rotary motion of this platform.

MATERIALS AND METHODS

Device Operation

The device design for microfluidic density gradient centrifugation (MICRO) and images of the actual device with blood and Ficoll layers is detailed in **Fig. 1A-C**. The device is initially primed with Ficoll and rid of any air bubbles. Then blood and Ficoll

were loaded into the reservoirs with tubing connections as shown in **Fig. 1A** and the device is subject to rotary motion. Centrifugal forces generated as a consequence of the rotary motion cause flow of both blood and Ficoll into the microchannels arranged in a spiral fashion. The centrifugal force also acts on the blood and Ficoll streams to establish a continuous density gradient across the width of the channel. Force balance on cells within the microchannels shows that cells experience drag forces in the direction of the fluid flow along with centrifugal and buoyancy forces that act in opposite directions across the width of the channel **(Fig.1D)**. For heavier cells (RBCs and PNMs) the centrifugal force is >> than the buoyancy forces and the net result is movement of cells towards the outer wall and collection in the bottom outlet that fractionates fluid in the lower half of the channel. For lighter cells (PBMCs) the buoyancy force > centrifugal force and the net result is maintenance of cells at the blood/Ficoll interface and collection via the top outlet which fractionates fluid in the upper half of the channel.

Device Design and Fabrication

Devices were fabricated using previously established techniques for soft-lithography in our laboratory.[121-123] Briefly, channel architectures were laid out using AutoCAD (Autodesk, San Rafael, CA) and printed as a 2D dark-field mask onto a transparency using a high-resolution printer (Fineline Imaging, Boulder, CO). The mask was then used to define a mold using negative photoresist SU-8 (Microchem, Westborough, MA) that was spun onto a 4" silicon wafer at a thickness of 25 μm and developed using SU-8 developer (Microchem, Westborough, MA). Following creation of mold, the devices were cast using polydimethylsiloxane (PDMS) (Sylgard 184, Dow Corning, Midland, MI), holes for placement of reservoirs and for inlet and outlet tubing were punched and

irreversibly bonded to either a 4” glass or silicon wafer following treatment with oxygen plasma. The spiral microchannels have the following overall dimensions: H=25μm, W=3mm and L~60cm).

Device Characterization

Based on estimations of centrifugal forces necessary and upper limits for both Reynolds Number (Re) and Deans Number (De), we evaluated multiple designs and shortlisted 3-4 promising configurations. These configurations were then extensively tested and the locations of the blood and Ficoll reservoirs, lengths and diameters of the inlet and outlet tubing and the spin speed of the rotary platform were all optimized to ensure delivery of a narrow (~ 100 μm) stream of blood over a thick stream (~ 3 mm) of Ficoll, sufficient residence time and force to cause movement of all RBCs to the outer wall and flow rates sufficient to process ~ 30μL/min of blood.

Microfluidic density gradient centrifugation (MICRO)

Devices were primed with Ficoll and fresh blood purchased from a commercial vendor and Ficoll was loaded in reservoirs and collection tubes were placed at the outlets. The device was mounted on a rotary platform and spun at 3000 rpm for 3 minutes. The samples from each outlet were collected separately and the PBMCs from the inner outlet was washed and resuspended in 1X PBS prior to staining, fixation and evaluation using flow cytometry.

Conventional Density Gradient Centrifugation (DGC)

For DGC, blood was diluted with PBS at 1:1 ratio and 1 ml of diluted blood was carefully layered on top of 4ml Ficoll-Paque in a 15 mL tube and spun at 700g for 20 minutes in a refrigerated centrifuge. Then the plasma layer was removed and buffy coat layer containing the PBMCs was carefully fractionated. The collected sample was washed and resuspended in 1X PBS prior to staining, fixation and evaluation using flow cytometry.

RBC Lysis (LYSIS)

Isolation of total leukocytes using LYSIS was performed by mixing 1ml of whole blood with 14ml of RBC lysis buffer (NH_4Cl buffer) for 5 minutes. The mixture was then spun at 200g for 4minutes, the supernatant was discarded and pellet was resuspended in 1X PBS prior to staining, fixation and evaluation using flow cytometry.

Stain, Fixation, Isolation Protocol (SFI)

To preserve native expression levels of various surface markers, 1 mL of whole blood was first stained with fluorescently labelled antibodies associated with phenotypic and activation markers for ~ 40 minutes at room temperature and immediately fixed using 1% paraformaldehyde solution. This sample was then depleted of RBCs using standard RBC lysis protocol and resuspended in PBS for subsequent analysis.

Immunolabeling and Flow Cytometry Analysis

Isolated cell populations were stained with antibodies specific to phenotypic markers (Lymphocytes: CD3, CD4 and Monocytes: CD14) and activation markers (Lymphocytes: CCR2, CCR4 and Monocytes CCR2 and CD11b) for ~ 40 minutes at room temperature,

immediately fixed using 1% paraformaldehyde and resuspended in flow cytometry buffer for analysis using flow cytometry (FACSCalibur, Becton Dickinson, Franklin Lakes, NJ). Flow cytometry was used to obtain both forward and side scatter information from cells along with expression levels of various phenotype and activation markers. Cell activation was scored using unpaired *t*-tests with two-tailed significance $p<0.05$ for sample sizes of $n>3$.

RESULTS

Establishment of Laminar Flow and Layering of Blood over Ficoll

In order to facilitate MICRO separation, it is essential that laminar flow is established to ensure layering of blood and Ficoll layers. To accomplish this we ensured that 'Re' < 100 and 'De' was < 40 to ensure laminar flow and minimal impact of rotational secondary flows. Our design with a channel height of 25 μm and width of 3mm at the spin speed of 3000 rpm resulted in laminar flow as evidenced by visualization of distinct streams of water layered over Ficoll (colored to enable visualization) within the device at these conditions **(Fig. 1A-D)**. Our experiments suggest that maintaining high channel aspect ratios (w:h) is critical to ensuring generation minimal levels of rotational forces. We were able to achieve layering for aspect ratios > 1:60 (w:h). Another critical factor for efficient separation is the relative width of the blood and Ficoll streams. We experimentally determined that ratio of widths of blood stream to Ficoll needs to be at least 1:5 to achieve efficient separation **(Fig. 2)**.

Isolation of PBMCs and Depletion of RBCs and PNMs

To ensure that the MICRO protocol can efficiently isolate PBMCs while ensuring depletion of more dense RBCs and PNMs we compared cell populations isolated using MICRO with both DGC and LYSIS protocols. DGC should result in isolation of PBMCs with efficient depletion of RBCs and PNMs whereas LYSIS protocol should isolate all leukocytes free of RBCs. A total of 1 mL blood was processed using LYSIS and DGC whereas 100 µL was processed using MICRO. Flow Cytometric evaluation of various cell populations **(Fig. 3)** using light scatting suggests that all three techniques result in efficient depletion of RBCs as evidenced by clear identification of leukocyte sub-populations on the forward scatter (FSC) vs. side scatter (SSC) plot with both DGC and MICRO showing depletion of PNMs in addition to the RBCs. Even though a majority of PNMs (> 99%) were depleted using both DGC and MICRO, a small number of PNM contamination is visible from both scatter plots.

Effect on Lymphocyte Sub-Populations and Monocytes

Following confirmation that the MICRO protocol can indeed be used to isolate PBMCs and deplete RBCs and PNMs we sought to confirm if the relative ratios of different PBMC sub-populations isolated using MICRO was comparable to that seen with LYSIS and DGC. To phenotype lymphocyte sub-populations we gated for the lymphocyte region on the FSC vs. SSC plot and evaluated expression of phenotype markers CD3 vs. CD4. To evaluate monocytes we gated the monocyte region on the FSC vs. SSC plot and evaluated expression of monocyte phenotype marker CD14. There are multiple populations of lymphocytes and can be characterized as T-helper cells ($CD3^+CD4^+$), Cytolytic T cells ($CD3^+CD4^-$) and other lymphocytes including B-cells and NK cells ($CD3^-CD4^-$). Following LYSIS we see that ~ 33% of lymphocytes are

$CD3^+CD4^+$, ~ 23% of lymphocytes are $CD3^+CD4^-$ and 40% of lymphocytes are $CD3^-CD4^-$ **(Fig. 4A)**. With DGC the ratios were different with ~ 26% of lymphocytes are $CD3^+CD4^+$, ~ 20% of lymphocytes are $CD3^+CD4^-$ and 50% of lymphocytes are $CD3^-CD4^-$ **(Fig. 4B)**. MICRO appears to be closer to the ratios obtained with LYSIS with ~ 39% of lymphocytes are $CD3^+CD4^+$, ~ 23% of lymphocytes are $CD3^+CD4^-$ and 34% of lymphocytes are $CD3^-CD4^-$ **(Fig. 4C)**. There was no statistical significance between LYSIS and MICRO for all lymphocyte sub-populations but differences were significant when DGC was compared to both techniques for the $CD3^+CD4^+$ and $CD3^-CD4^-$ populations. Monocyte purity was evaluated by determining the number of cells expressing CD14, a monocyte phenotype marker in the monocyte region on the FSC vs. SSC plot. LYSIS resulted in ~ 70% of $CD14^+$ cells in the monocyte gate whereas this number was > 90% with DGC and > 95% with MICRO **(Fig. 5)**.

Lymphocyte Activation

To determine if the isolation process resulted in activation of lymphocytes, we evaluated expression of chemokine receptors CCR2 and CCR4 which are known to be lost following high stress DGC. To establish a control we developed a stain-fix-isolation (SFI) protocol which provides accomplishes staining and fixation immediately after the blood draw thereby labeling and preserving expression of cell surface markers prior to RBC depletion via lysis. Expression of CCR2 and CCR4 was evaluated on all lymphocytes isolated using LYSIS, DGC and MICRO and compared to expression on lymphocytes isolated via SFI **(Fig. 6)**. All lymphocytes in the lymphocyte gate on the FSC vs. SSC plot were considered. Our results confirm that in comparison to SFI, lymphocytes isolated using MICRO and LYSIS appear to have similar number of cells

with high and low expression of CCR2 and CCR4 receptors. However, DGC resulted in significant reduction in number of cells with high expression of CCR2 receptor. DGC also resulted in lower level of CCR4 expression on lymphocytes but this change was not statistically significant.

Monocyte Activation

To evaluate isolation process induced activation of monocytes, two activation markers that are highly sensitive to stress during the isolation process (CCR2 and CD11b) were selected. $CD14^+$ monocytes isolated using each of the four techniques present in the monocyte gate in the FSC vs. SSC plot were evaluated for expression levels of CD11b and CCR2 **(Fig. 7)**. Our results suggest that even though the mean fluorescence intensity levels were lower following LYSIS, the number of $CD11b^+$ was significantly lower suggesting that there may be selective loss of monocytes expressing CD11b. There was no significant difference in levels of expression CD11b or relative numbers of $CD14^+$ cells using SFI, MICRO and DGC. Evaluation of CCR2 expression on monocytes suggests that LYSIS resulted in significant loss of CCR2 expression on monocytes whereas the relative expression levels on CCR2 on $CD14^+$ monocytes isolated using MICRO and DGC were very similar to that seen with SFI.

DISCUSSION

Inflammation is the primary response the body to injury, infection and disease and involves activation of the body's immune response to provide protective function. The primary mediators of the inflammation are leukocytes and different sub-populations of leukocytes mediate innate and adaptive immunity. After the threat or insult is sufficiently

addressed, inflammation is gradually resolved via anti-inflammatory activities of different subsets of leukocytes signaling a return to normal function. Inflammation is a key player in our body's defense and satisfactory resolution is critical as chronic sustained inflammation can cause the body significantly more harm. Leukocytes are an integral part of the body's inflammatory response and the numbers and presence of different sub-populations of leukocytes correlate to the body's immediate immune and inflammatory status. Profiling of leukocyte subpopulations therefore provides unique opportunities to monitor and individual's immediate status and provides important information that can be used to diagnose profile, monitor, treat and evaluate effectiveness of treatment. Blood is commonly sampled in the clinical setting and used for rather simplistic evaluation of cell counts and presence of inflammatory secretome in serum. More complex evaluation of leukocytes for expression of markers of activation using techniques like flow cytometry or molecular expression techniques have not been commonly pursued due to complexities associated with ensuring that isolated cells are an accurate representation of the status of the patient.

Given the number of RBCs in whole blood, it is not surprising that evaluation of whole blood samples for molecular expression studies provides significantly lower quality information when compared to isolated leukocytes.[105] Therefore, at a minimum, RBC depletion is necessary for analysis of leukocytes and/or leukocyte sub-populations to ensure that samples can provide vital information regarding the state of the body. However, with increased processing involved in separation of leukocytes into different sub-populations, the information contained in the cells has greater potential to be compromised due to time and stress associated with these additional processing steps.

Antibody-based approaches that rely on affinity to specific antigens on the surface of the cell to enable isolation provide highly specific alternatives for cell sorting. Concerns relate to the fact that the antibody binding event and steps involved in ensuring binding and subsequent isolation can be a significant source of unnecessary activation.[110] Further, antibody based approaches rely on known antibody-cell interactions and require prior knowledge of molecular expression patterns on the cell surface. Therefore, label-free approaches like RBC lysis and DGC are more commonly used to ensure unbiased separation of leukocytes and leukocyte sub-populations.

Microfluidics provides unique opportunities to miniaturize conventional separation processes and minimize critical factors like time, stress and sample processing volumes. The RBC lysis has been previously miniaturized and results confirm that isolation high quality total leukocytes with minimal cell loss or activation can be accomplished using this approach.[49] This technique is highly suitable for isolation of total leukocytes but subsequent processing is necessary if isolation of leukocyte sub-populations is desired. To enable isolation of leukocyte sub-populations, several groups have attempted to miniaturize conventional DCG using microfluidics.[99,120,124,125] While there have been some successful attempts to miniaturize DGC, most approaches have demonstrated feasibility using bead solutions but have been unable to translate their approaches for continuous blood sorting. One group used pre-loaded samples to achieve separation of PBMCs from RBCs and PNMs but the capability to process sufficient sample volume was limited due to the small volume of the microfluidic chamber (< 20 µL of blood).[120] In this manuscript we report a new approach focused on taking microfluidic DGC beyond simple proof-of-concept studies using beads and demonstrating that this effort can be

used to isolate PBMCs from whole blood samples without any sample pre-processing. This is not a trivial process as several variables need to be optimized to ensure both laminar flow of Blood and Ficoll streams and sufficient centrifugal force to ensure clean separation of RBCs and PNMs. To accomplish this, we optimized the design including reservoirs, flow control elements (resistances at inlets and outlets), microfluidic channel dimensions and outlets to ensure that the device does not require any external manipulation and the rotary platform can provide both the centrifugal force necessary for separation and the driving force necessary for fluid flow. Following separation, the collection tubes can also be centrifuged to remove the supernatant and resuspend cells in physiological buffers for whole/live cell analysis or with lysis buffers for gene and protein expression analysis. The use of a single rotary platform to perform all necessary functions involved with cell separations ensures that this process can be automated and adapted for point-of-care deployment.

Our results validate our initial hypothesis that microfluidic adaptation of DCG will result in a faster and gentler process for isolation of PBMCs which ensures recovery of cells with minimal loss and minimal isolation process induced activation. Comparison of MICRO with LYSIS and DGC confirms that both lymphocytes and monocytes can be isolated without contamination with RBCs or granulocytes. Further evaluation of lymphocytes using phenotypic markers CD3 and CD4 suggests that the relative ratios of T-helper cells ($CD3^+CD4^+$), Cytolytic T cells ($CD3^+CD4^-$) and other lymphocytes including B-cells and NK cells ($CD3^-CD4^-$) is consistent with both LYSIS and MICRO but DGC produced higher number of $CD3^-CD4^-$ cells and lower numbers of $CD3^+CD4^+$ cells suggesting either selective enrichment of $CD3^-CD4^-$ cells or selective depletion of

$CD3^+CD4^+$ cells. Evaluation of cells within the monocyte gate for CD14, a monocyte phenotype marker shows that the number of $CD14^+$ monocytes was high with both DGC and MICRO but significantly lower with LYSIS. This suggests either preservation of cells that are not monocytes within the monocyte gate or damage to monocytes that causes changes to the expression of CD14 on these monocytes.

Our activation studies focused on highly sensitive markers of PBMC activation and rely on expression of chemokine receptors CCR2 and CCR4 on lymphocytes and CCR2 on monocytes which are known to be extremely sensitive to stress along with profiling of expression of CD11b on monocytes which is an integrin that is upregulated following activation in monocytes. To obtain a standard for comparison, we developed a new stain-fix-isolate technique which ensured staining of leukocytes in whole blood immediately following blood draw, fixation and then removal of RBCs via lysis. This accurately preserves the molecular expression signatures prior to the isolation and ensures that the isolation process itself does not change expression of cell surface markers as the cells are fixed during the RBC lysis process. Evaluation of lymphocytes isolated with different techniques suggests that in comparison to the SFI technique, CCR2 and CCR4 expression on lymphocytes was impacted following isolation with DGC but not with MICRO or LYSIS but only loss of CCR2 on lymphocytes isolated with DGC was statistically significant. This is consistent with prior studies that suggest that CCR2 receptors are lost on lymphocytes following high stress DGC and cannot be recovered even with stimulation[46]. Evaluation of monocyte populations for expression of CCR2 and CD11b shows that in comparison to SFI, LYSIS results in loss of expression of both CCR2 and CD11b which could either be damage of these surface markers or loss of cells expressing these markers. In comparison, both MICRO and DGC were similar to SFI. These results

collectively suggest that MICRO is the only technique that preserves cellular populations and expression patterns seen in whole blood as evidenced by the close similarity between MICRO and SFI in these activation studies.

In summary, we developed a microfluidic protocol for isolation of PBMCs from whole blood using density gradient centrifugation within microfluidic channels. This required significant design and validation to ensure laminar flow, layering and generation of sufficient centrifugal forces to facilitate separation of PBMCs from contaminating RBCs and PNMs. Evaluation of numbers and activation status of isolated cells suggests that this approach can potentially preserve monocytes and different lymphocyte sub-populations with minimal isolation process induced activation. Finally, the use of a simple rotary platform to deliver samples, facilitate separation and sample collection is ideal for transformation of this approach into a point-of-care device for isolation of PBMCs for rapid evaluation of patient blood samples.

ACKNOWLEDGEMENTS

YS was supported by an Alabama EPSCoR Graduate Research Scholars Program. This work was supported by the NSF CAREER Award # 1149059 to PS and the Comprehensive Cardiovascular Center and the Division of Cardiovascular Disease at the University of Alabama at Birmingham.

REFERENCES

(1) Arras, M.; Ito, W. D.; Scholz, D.; Winkler, B.; Schaper, J.; Schaper, W. *J Clin Invest* **1998**, *101*, 40-50.

(2) Fritsche, A.; Haring, H.; Stumvoll, M. *Dtsch Med Wochenschr* **2004**, *129*, 244-248.

(3) He, J.; Le, D. S.; Xu, X.; Scalise, M.; Ferrante, A. W.; Krakoff, J. *Eur J Endocrinol* **2010**, *162*, 275-280.

(4) Hersh, E. M.; Butler, W. T.; Rossen, R. D.; Morgan, R. O.; Suki, W. *J Immunol* **1971**, *107*, 571-578.

(5) Mellembakken, J. R.; Aukrust, P.; Olafsen, M. K.; Ueland, T.; Hestdal, K.; Videm, V. *Hypertension* **2002**, *39*, 155-160.

(6) Feezor, R. J.; Baker, H. V.; Mindrinos, M.; Hayden, D.; Tannahill, C. L.; Brownstein, B. H.; Fay, A.; MacMillan, S.; Laramie, J.; Xiao, W.; Moldawer, L. L.; Cobb, J. P.; Laudanski, K.; Miller-Graziano, C. L.; Maier, R. V.; Schoenfeld, D.; Davis, R. W.; Tompkins, R. G.; Inflammation; Host Response to Injury, L.-S. C. R. P. *Physiol Genomics* **2004**, *19*, 247-254.

(7) Fukuda, S.; Yasu, T.; Predescu, D. N.; Schmid-Schonbein, G. W. *Circ Res* **2000**, *86*, E13-18.

(8) Gibson, G. *Nat Rev Genet* **2008**, *9*, 575-581.

(9) Frank, R. S. *Blood* **1990**, *76*, 2606-2612.

(10) Jude, B.; Agraou, B.; McFadden, E. P.; Susen, S.; Bauters, C.; Lepelley, P.; Vanhaesbroucke, C.; Devos, P.; Cosson, A.; Asseman, P. *Circulation* **1994**, *90*, 1662-1668.

(11) Naranbhai, V.; Bartman, P.; Ndlovu, D.; Ramkalawon, P.; Ndung'u, T.; Wilson, D.; Altfeld, M.; Carr, W. H. *J Immunol Methods* **2011**, *366*, 28-35.

(12) Nieto, J. C.; Canto, E.; Zamora, C.; Ortiz, M. A.; Juarez, C.; Vidal, S. *PLoS One* **2012**, *7*, e31297.

(13) Krutmann, J.; Kirnbauer, R.; Kock, A.; Schwarz, T.; Schopf, E.; May, L. T.; Sehgal, P. B.; Luger, T. A. *J Immunol* **1990**, *145*, 1337-1342.

(14) von Bonin, A.; Huhn, J.; Fleischer, B. *Immunol Rev* **1998**, *161*, 43-53.

(15) Dubois, N. C.; Craft, A. M.; Sharma, P.; Elliott, D. A.; Stanley, E. G.; Elefanty, A. G.; Gramolini, A.; Keller, G. *Nat Biotechnol* **2011**, *29*, 1011-1018.

(16) Brosseron, F.; Marcus, K.; May, C. *Methods Mol Biol* **2015**, *1295*, 33-42.

(17) Hofland, L. J.; van Koetsveld, P. M.; Verleun, T. M.; Lamberts, S. W. *Acta Endocrinol (Copenh)* **1989**, *121*, 270-278.

(18) Li, S. H.; Liao, X.; Zhou, T. E.; Xiao, L. L.; Chen, Y. W.; Wu, F.; Wang, J. R.; Cheng, B.; Song, J. X.; Liu, H. W. *Ann Plast Surg* **2017**, *78*, 83-90.

(19) English, D.; Andersen, B. R. *J Immunol Methods* **1974**, *5*, 249-252.

(20) Helms, C. C.; Marvel, M.; Zhao, W.; Stahle, M.; Vest, R.; Kato, G. J.; Lee, J. S.; Christ, G.; Gladwin, M. T.; Hantgan, R. R.; Kim-Shapiro, D. B. *J Thromb Haemost* **2013**, *11*, 2148-2154.

(21) Newton, R. A.; Thiel, M.; Hogg, N. *J Leukoc Biol* **1997**, *61*, 422-426.

(22) Weber, C.; Erl, W.; Weber, P. C. *Biochem Biophys Res Commun* **1995**, *206*, 621-628.

(23) Sethu, P.; Moldawer, L. L.; Mindrinos, M. N.; Scumpia, P. O.; Tannahill, C. L.; Wilhelmy, J.; Efron, P. A.; Brownstein, B. H.; Tompkins, R. G.; Toner, M. *Anal Chem* **2006**, *78*, 5453-5461.

(24) Sethu, P.; Anahtar, M.; Moldawer, L. L.; Tompkins, R. G.; Toner, M. *Anal Chem* **2004**, *76*, 6247-6253.

(25) Moen, S. T.; Hatcher, C. L.; Singh, A. K. *PLoS One* **2016**, *11*, e0153137.

(26) Sun, Y.; Sethu, P. *Bioengineering (Basel)* **2017**, *4*.

(27) Kinahan, D. J.; Kearney, S. M.; Kilcawley, N. A.; Early, P. L.; Glynn, M. T.; Ducree, J. *PLoS One* **2016**, *11*, e0155545.

(28) Parichehreh, V.; Estrada, R.; Kumar, S. S.; Bhavanam, K. K.; Raj, V.; Raj, A.; Sethu, P. *Biomed Microdevices* **2011**, *13*, 453-462.

(29) Parichehreh, V.; Medepallai, K.; Babbarwal, K.; Sethu, P. *Lab Chip* **2013**, *13*, 892-900.

(30) Parichehreh, V.; Sethu, P. *Lab Chip* **2012**, *12*, 1296-1301.

(31) Amasia, M.; Madou, M. *Bioanalysis* **2010**, *2*, 1701-1710.

(32) Burger, R.; Ducree, J. *Expert Rev Mol Diagn* **2012**, *12*, 407-421.

FIGURE LEGENDS

Figure 1: (A) Actual setup with reservoirs mounted in the center of the device containing the spiral microfluidic channel, **(B)** Demonstration of layering and establishment of laminar flow using saline solution and colored Ficoll solution, **(C)** Proof-of-concept showing movement of RBCs introduced at the top of the channel across a colored stream of Ficoll solution and **(D)** Force balance on cells or particles introduced into the microchannel. For lighter particles Buoyancy Forces > Centrifugal forces which ensures that particles are confined to the top stream whereas for heavier particles the Centrifugal Forces > Buoyancy Forces causing movement towards the outer wall.

Figure 2. Flow rate of Blood and Ficoll streams as a function of spin speed of the rotary platform. Experiments were performed at a spin speed of 3000 rpm where the ratio of the widths of the Blood and Ficoll streams were ~ 1:5 resulting in a Blood flow rate of 30-35 µL/min.

Figure 3. PBMC Recovery: Flow cytometry scatter plots to distinguish leukocyte sub-populations based on forward scatter (FSC) and side scatter (SSC) on samples isolated using **(A)** RBC Lysis (LYSIS), **(B)** Density Gradient Centrifugation (DCG), and **(C)** Microfluidic Density Gradient Centrifugation (MICRO).

Figure 4. Lymphocyte Recovery: Flow cytometric evaluation of expression of CD3 vs. CD4 on cells that fall within the lymphocyte gate on the FSC vs. SSC plot for samples isolated using **(A)** RBC Lysis (LYSIS), **(B)** Density Gradient Centrifugation (DCG), and **(C)** Microfluidic Density Gradient Centrifugation (MICRO).

Figure 5. Monocytes Recovery: Evaluation of expression of CD14 on cells that fall within the monocyte gate on the FSC vs. SSC plot for samples isolated using **(A)** RBC Lysis (LYSIS), **(B)** Density Gradient Centrifugation (DCG), and **(C)** Microfluidic Density Gradient Centrifugation (MICRO).

Figure 6. Lymphocyte Activation: Determination of activation status of Lymphocytes evaluated using expression of chemokine receptors CCR2 **(top)** and CCR4 **(bottom)** for samples isolated using **(A)** Stain-Fix-Lyse protocol (SFI) **(B)** RBC Lysis (LYSIS), **(C)** Density Gradient Centrifugation (DCG), and **(D)** Microfluidic Density Gradient Centrifugation (MICRO).

Figure 7. Monocyte Activation: Determination of activation status of Monocytes evaluated using expression of integrin CD11b **(top)** and chemokine receptor CCR2 **(bottom)** for samples isolated using **(A)** Stain-Fix-Lyse protocol (SFI) **(B)** RBC Lysis (LYSIS), **(C)** Density Gradient Centrifugation (DCG), and **(D)** Microfluidic Density Gradient Centrifugation (MICRO).

Figure 1:

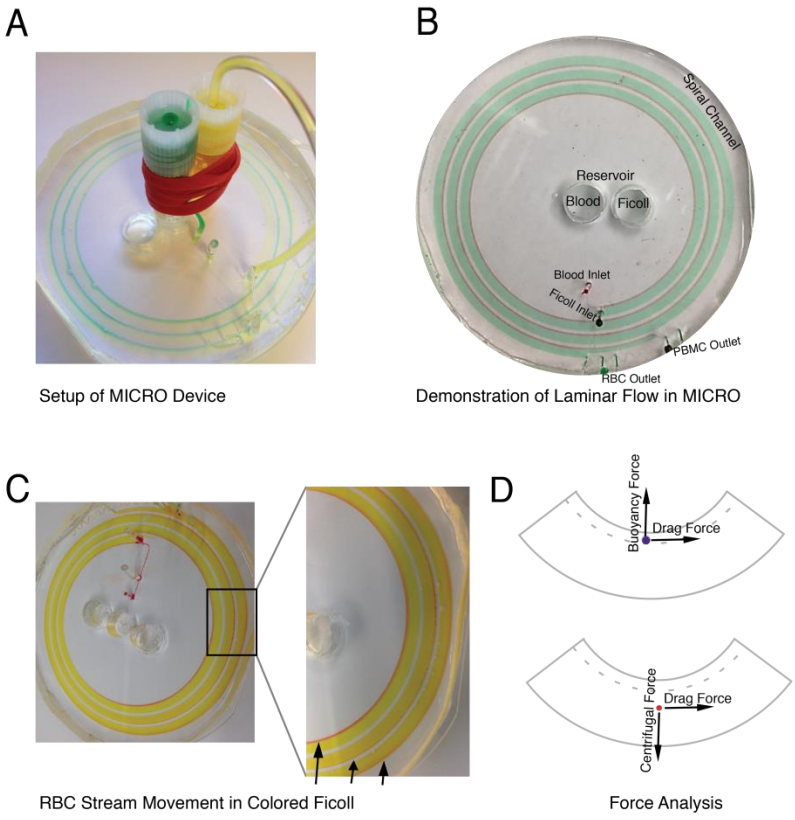

Setup of MICRO Device

Demonstration of Laminar Flow in MICRO

RBC Stream Movement in Colored Ficoll

Force Analysis

Figure 2:

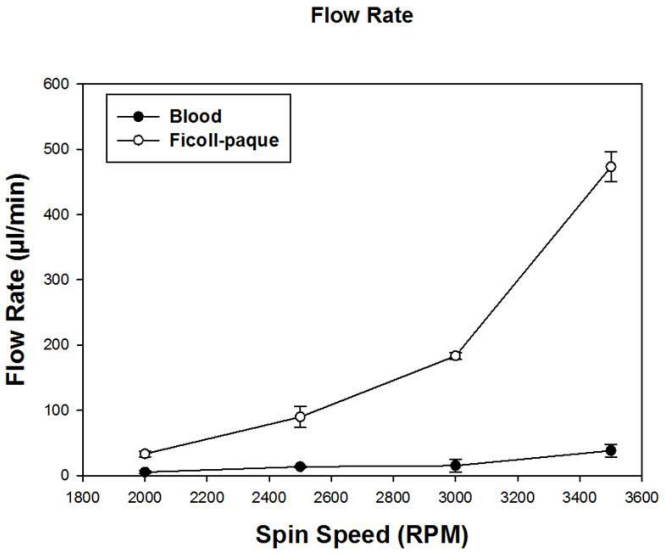
Flow Rate
Blood
Ficoll-paque
Flow Rate (µl/min)
600
500
400
300
200
100
0
1800
2000
2200
2400
2600
2800
3000
3200
3400
3600
Spin Speed (RPM)

Figure 3:

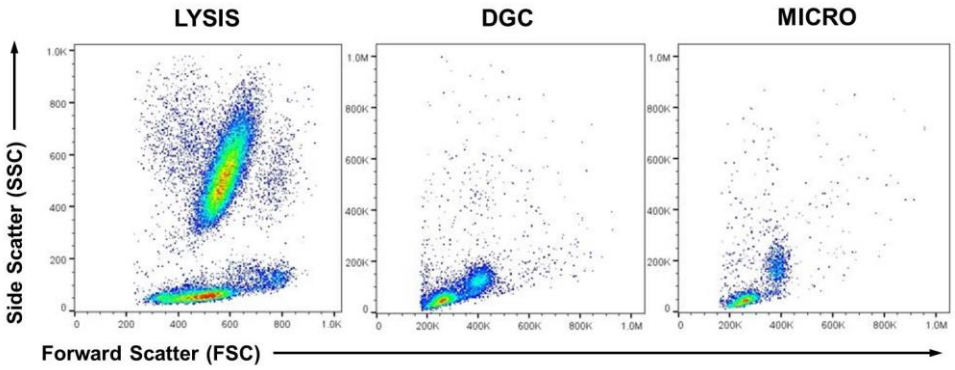

Figure 4:

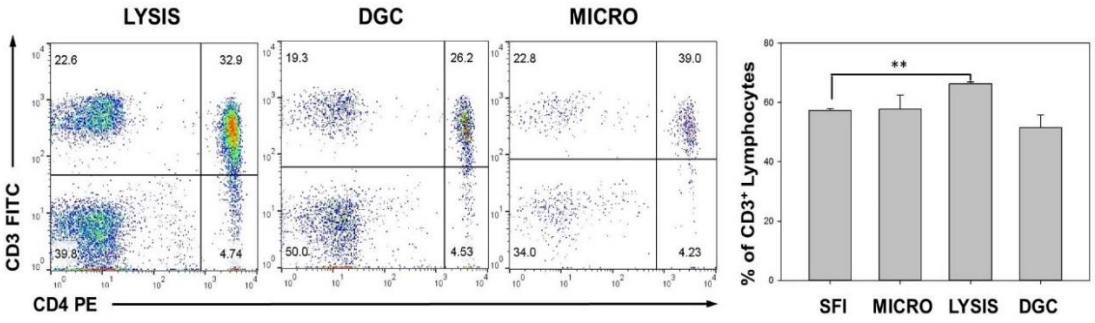
LYSIS
DGC
MICRO
22.6
32.9
39.8
4.74
19.3
26.2
50.0
4.53
22.8
39.0
34.0
4.23
CD3 FITC
CD4 PE
**
% of CD3+ Lymphocytes
SFI
MICRO
LYSIS
DGC

Figure 5:

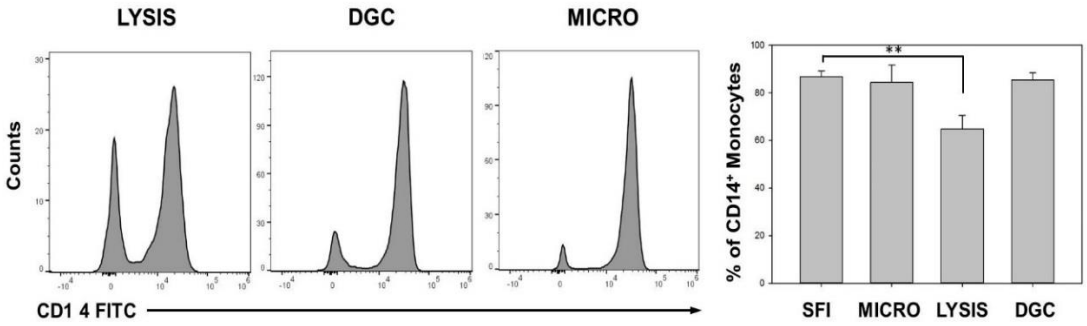
LYSIS
DGC
MICRO
Counts
CD1 4 FITC
% of CD14+ Monocytes
**
SFI
MICRO
LYSIS
DGC

Figure 6:

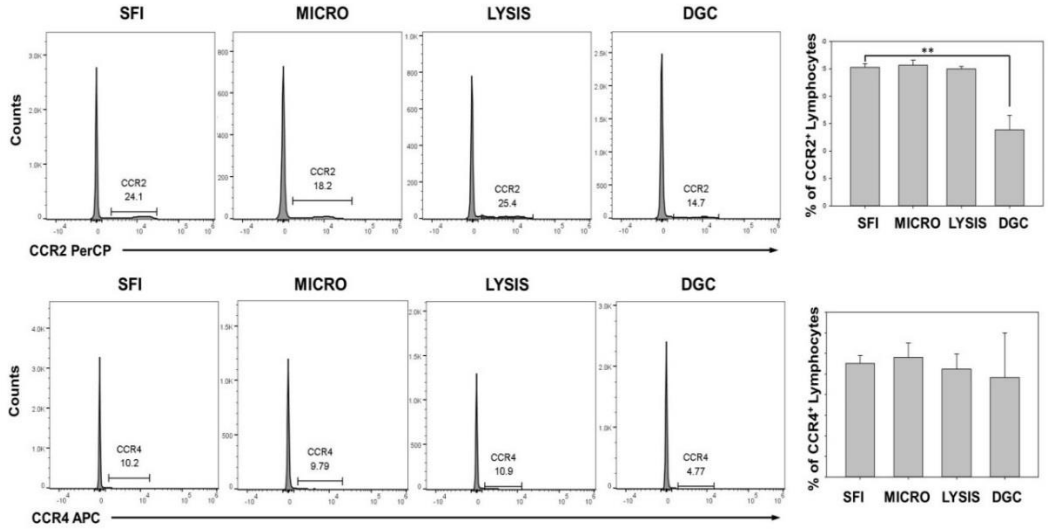
SFI
MICRO
LYSIS
DGC
Counts
CCR2
24.1
CCR2
18.2
CCR2
25.4
CCR2
14.7
CCR2 PerCP
% of CCR2+ Lymphocytes
**
SFI MICRO LYSIS DGC
SFI
MICRO
LYSIS
DGC
Counts
CCR4
10.2
CCR4
9.79
CCR4
10.9
CCR4
4.77
CCR4 APC
% of CCR4+ Lymphocytes
SFI MICRO LYSIS DGC

Figure 7:

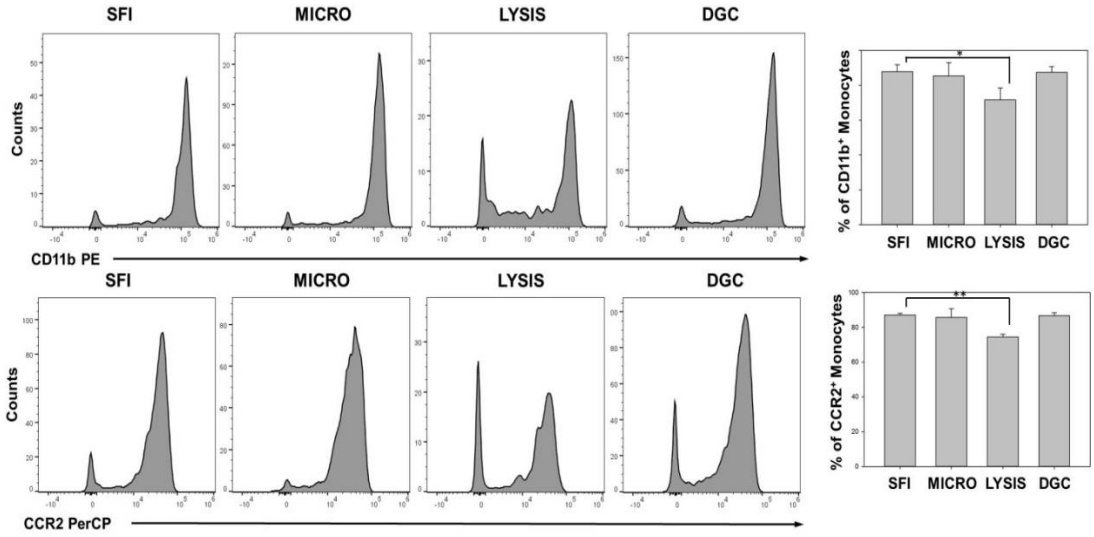
SFI
MICRO
LYSIS
DGC
Counts
CD11b PE
% of CD11b+ Monocytes
SFI
MICRO
LYSIS
DGC
Counts
CCR2 PerCP
% of CCR2+ Monocytes
SFI
MICRO
LYSIS
DGC

CENTRIFUGAL MICROFLUIDIC PLATFORM FOR FAST AQUEOUS TWO-PHASE PARTITIONING WITH BEADS DEMONSTRATION

by

YUXI SUN, PALANIAPPAN SETHU

In preparation for *BMES Annual Meeting*

Format adapted for dissertation

Centrifugal Microfluidic Platform for Fast Aqueous Two-Phase Partitioning with Beads Demonstration

Yuxi Sun[1], Palaniappan Sethu[1,2,]
Department of Biomedical Engineering[1], Department of Medicine[2]
University of Alabama at Birmingham, Birmingham, Alabama

Introduction: Aqueous two-phase partitioning system (APTS) is a simple yet powerful technique that has been used for isolation of proteins and other biomolecules. Conventional ATPS occurs when a mixture of two immiscible aqueous polymers in physiological buffer separates into two distinct phases under gravity or under influence of centrifugal force. During this phase partitioning, salts within the buffer do not partition equally resulting in a net charge in the partitioned phases. It is known that different cells like white blood cells and red blood cells preferentially partition to different phases based on differences in cell surface energy. Microfluidic APTS separations have been attempted previously for cell separations but required phases to be partitioned prior to cell sorting. We have developed a new approach where partitioning and cell separations are integrated and the cells/particles separate with the phases for more efficient and unique cell sorting.

Hypothesis: We hypothesize that miniaturization of phase partitioning using centrifugal microfluidics will enable a new technique for label-free and rapid separation of unique WBC sub-populations.

Methods: A microfluidic device was fabricated using soft lithographic techniques with a curved channel for APTS. Two reservoirs, one for polyethylene glycol (PEG) and one for dextran (DEX) were used to introduce the two solutions into the main channel. The main

channel consists of mixing and phase partitioning segments prior to the two outlets. Following entry into the main channel, microstructures were used to enable efficient mixing and remaining part of the channel was used to separate the phases using centrifugal force to expedite phase partitioning. The dimensions of the channel and flow rate were optimized to ensure laminar flow and prevent secondary Deans flow. Polystyrene (PS) beads and silicon dioxide (SD) beads introduced with the PEG solution were used to demonstrate proof-of-concept.

Results: An image of the mixing and phase partitioning segments is shown in Fig. 1. We show that we can enable mixing and phase partitioning using centrifugal force via spinning the device on a rotary platform. Polystyrene beads (fluorescent) and silicon oxide beads were separated into unique locations within the two separate phases under the centrifugal force as shown in Fig. 2 demonstrating preliminary feasibility of this approach.

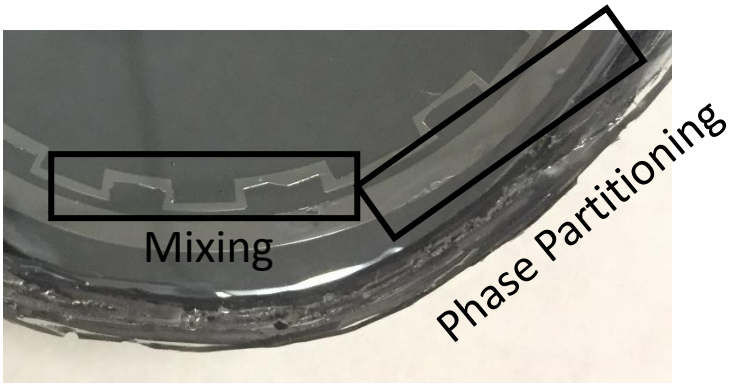

Figure 1. The Mixing and Phase Partitioning Segments of the Device.

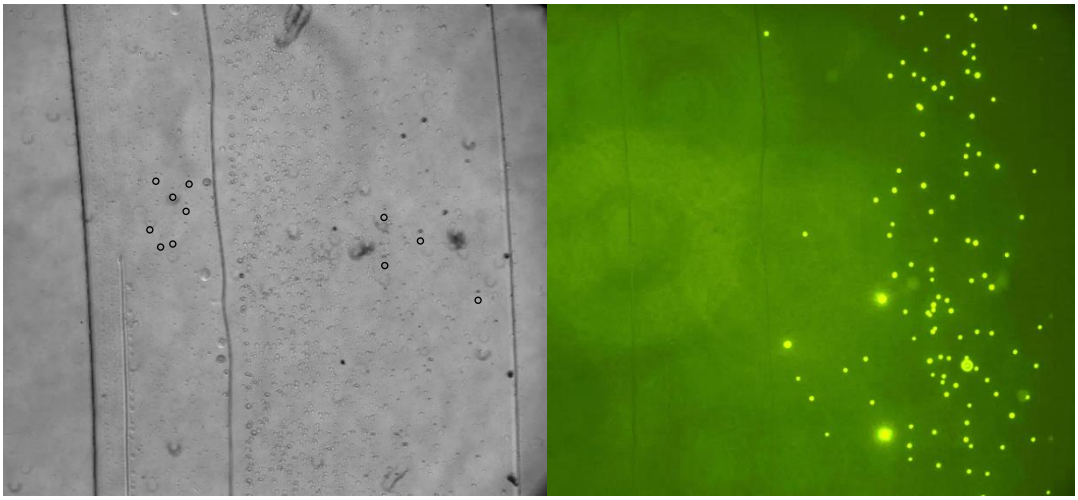

Figure 2. Separation of PS and SD Beads from Beads Mixture.

Conclusions: We performed proof-of-concept demonstration of phase partitioning in a centrifugal microfluidic device by enabling sample input, mixing, phase partitioning and sorting of beads. This approach has great potential to be applied for sorting of cells.

MICROFLUIDIC TECHNOLOGICES FOR BLOOD-BASED CANCER LIQUID BIOPSIES

by

YUXI SUN, THOMAS HUGLAND, AARON ROGERS, ASEN GHANIM, PALANIAAPAN SETHU

Analytica Chimica Acta 2018, 1012

Abstract

Blood-based liquid biopsies provide a minimally invasive alternative to identify cellular and molecular signatures that can be used as biomarkers to detect early-stage cancer, predict disease progression, longitudinally monitor response to chemotherapeutic drugs, and provide personalized treatment options. Specific targets in blood that can be used for detailed molecular analysis to develop highly specific and sensitive biomarkers include circulating tumor cells (CTCs), exosomes shed from tumor cells, cell-free circulating tumor DNA (cfDNA), and circulating RNA. Given the low abundance of CTCs and other tumor-derived products in blood, clinical evaluation of liquid biopsies is extremely challenging. Microfluidics technologies for cellular and molecular separations have great potential to either outperform conventional methods or enable completely new approaches for efficient separation of targets from complex samples like blood. In this article, we provide a comprehensive overview of blood-based targets that can be used for analysis of cancer, review microfluidic technologies that are currently used for isolation of CTCs, tumor derived exosomes, cfDNA, and circulating RNA, and provide a detailed discussion regarding potential opportunities for microfluidics-based approaches in cancer diagnostics.

Keywords: Microfluidics, cancer diagnostics, circulating tumor cells, exosomes, tumor cell DNA.

1. Overview

Cancer remains one of the leading causes of death worldwide. In the United States alone, there were ~ 1.6 million new cases and nearly 500,000 cancer related deaths in 2016 [126,127]. According to the American Cancer Society, solid tumors of the breast, lung, bronchus, prostate, colon, rectum and bladder remain the most common causes of cancer [127]. It is estimated that in the United States, > 15 million people are currently living beyond a cancer diagnosis with this number expected to rise to almost 19 million by 2024 representing an enormous cost burden (> $ 130 billion/year) [126,127]. New technologies have made detection of solid tumors routine process; but to improve prognosis, enhance quality of life, drive down treatment costs, and enable positive outcomes for cancer patients, better technologies are necessary to enable detection of cancers before symptoms appear, monitor disease progression and evaluate patient response to treatment.

Advances in genomics and molecular technologies have created great interest in the use of liquid biopsies as a non-invasive alternative to surgical biopsies to evaluate the wealth of information contained in cancer-associated cells and biomolecules found in bodily fluids [128-132]. Apart from being relatively low-risk to patients, these measurements can be made dynamically, enabling correlation of disease burden and progression to quantifiable biomarkers [130,131,133]. Liquid biopsies are not limited to blood [129,134] and can be performed using other bodily fluids including urine [135-137], stool [138,139], saliva [140-142], and cerebrospinal fluid [143-145]. However, urine or stool samples only provide insights into specific types of cancers (bladder or colon) whereas blood is more universal and can potentially be used to detect all cancers. The disadvantage of blood samples is the

presence of vast amounts of other cellular and molecular content that can greatly complicate detection and evaluation of biomarker targets. This review focuses on blood-based liquid biopsies, the challenges of isolating CTCs and other tumor-related products that are present at an extremely low frequency in blood and the use of microfluidics based technologies to sort through complex samples to identify specific targets. **Fig. 1** highlights locations of the primary tumor, metastasis of circulating tumor cells from the primary tumor location to secondary sites, and extravasation and establishment of the secondary tumor. During this process of metastasis, several cells (CTCs) and cell derived products (exosomes, cell-free DNA and RNA) are released and transit via circulating blood and can be sampled to provide valuable screening, prognostic and diagnostic information that can benefit patients via personalized therapeutics and to evaluate response to treatment.

Solid tumors originate in the epithelium of organs like the breasts, lungs, and colon and are the primary cause of malignancies [146,147]. Metastasis from solid tumors accounts for > 90% of cancer-related deaths and each stage of this process can result in release of specific cells or cell-derived products into the bloodstream [147,148]. The formation of a primary tumor requires the acquisition of resistance to apoptosis or programmed cell death [149-151]. Metastasis begins with tumor cells from the primary site invading adjacent tissues, migrating into blood circulation, travelling through the circulatory system, extravasation following arrest at a distal organ or tissue and expansion at the new location [132,152]. The primary stages of metastasis involve the detachment of epithelial cells from the extracellular matrix (ECM) and disruption of the actin cytoskeleton resulting in a rounded and unattached phenotype which typically is a trigger for apoptotic cell death via

anoikis and amorphosis (due to loss of contact of adherent cells with the ECM) [153-155]. This is followed by some cells migrating and entering circulation [154,156]. Once metastatic cells enter circulation, only a fraction of cells successfully evade the body's immune surveillance and establish metastatic foci at secondary locations [157,158]. After establishment at a secondary locations, tumors expand by recruiting new blood vessels and impacting normal function of tissues and organs [157,158]. Metastasis and tumor growth are intrinsically linked to the host circulation and blood is used to transport of cells (CTCs), tumor-derived exosomes, and cell-free ctDNA and RNA. Therefore, liquid biopsies of blood have great potential to identify and evaluate biomarkers to aid in early detection of cancer, monitoring disease progression and evaluating the response to treatment [132,133,159].

Microfluidic devices allow for manipulation of fluids within architectures on the size scale of 10s of micrometers (comparable to the size of a single cell) [160,161]. Miniaturization offers benefits both in terms of speed and costs using small amounts of reagents and buffers at significant faster sample processing rates[162,163]. Devices can be designed to ensure levels of precision not possible with conventional macroscale approaches while ensuring that every cell or biomolecule is evaluated in a homogeneous fashion which is extremely important when probing low abundance cells and biomolecules [164]. Microfluidics can also enable design of entirely new separation techniques where scaling effects can be exploited to ensure laminar flow, amplify secondary forces, and define unique geometries to selectively direct/confine/capture cells and cell-derived products [52,165]. Thus far, there is significant interest in microfluidic technologies for cancer diagnostics to isolate cancer cells and cell-derived products. The

vast majority of microfluidics-based approaches have focused on CTC isolation [166,167]. This can be attributed to various factors including the rapidly growing interest in CTCs in cancer diagnostics, the complexity of the problem of isolating CTCs which occur at extremely low frequency in circulating blood, and the inability of conventional macroscale approaches to satisfactorily address this issue. Other cancer cell-derived products like exosomes and circulating cell-free genetic materials have not been pursued with the same level of interest as CTCs possibly due to the fact that they can be isolated with a fair degree of reliability using conventional approaches. Therefore, microfluidic adaptation of these approaches has been relatively slow despite potential advantages that could transform these laboratory scale processes into point-of-care devices with enhancements in speed, purity and efficiency.

Currently, the only FDA approved test for evaluation of CTCs is the ELLSEARCH® Circulating Tumor Cell Kit. CELLSEARCH® is not intended for early diagnosis but is routinely used to monitor and predict cancer progression in metastatic cancer and evaluate response to chemotherapy [168]. CTCs counts using CELLSEARCH® have been shown to be a reliable independent predictor of progression-free survival (PFS) and overall survival (OS) in a percentage of patients with metastatic breast [169,170], colorectal [169], and prostate cancer [169]. While this test is not accepted as a substitute for solid tumor imaging, it is used to supplement imaging in the assessment of disease progression in patients. CELLSEARCH® uses a combination of immuno-magnetic capture along with live-cell imaging to identify CTCs and discriminate them from leukocytes using conventional macroscale approaches. Several companies including Inivata [44], Epic Sciences [78], Guardant [43], Janssen Diagnostics [79], Cellsee [36], Rarecells [80] , Biofluidica [40]

and SRI International [81]offer tests for CTCs and cfDNA. Some of these approaches utilize microfluidic interfaces to enhance capture efficiency or to provide confined geometries for sorting and isolation. In the research community, there is ongoing interest in microfluidic adaptation of CTC capture using both immuno-affinity based approaches and via exploitation of unique physical properties of these cells. There is also high interest in microfluidics-based approaches for capture of exosomes. However, thus far, these approaches are still in the pre-clinical or early clinical testing phases and will require more time before FDA approval is obtained and offered to patients.

In this review, we provide an extensive overview of different microfluidics approaches for isolation of different targets from blood-based liquid biopsies that can provide prognostic or diagnostic value. We also discuss the origins of each of these targets, their frequency of occurrence in blood, their physical and biochemical properties that can be exploited to enable separations, and the type of predictive information contained within these targets. This review is intended to provide researchers and commercial entities seeking to implement new technologies for cancer monitoring with the background necessary to understand the biological significance and complexities associated cancer biomarkers, identify potential biomarkers, and establish design parameters to successfully translate microfluidics-based technologies into the clinical setting.

2. Circulating Tumor Cells

2.1. Origins and frequency of occurrence

CTCs in blood were identified in 1869 from blood samples of a patient suffering from extensive breast cancer [171]. Since then, there have been efforts to identify the origin and

gain a broader understanding of the process of CTC migration into blood and extravasation into secondary sites [152]. CTCs originate either from the primary tumor or from a secondary metastatic site and enter blood circulation [172]. The exact mechanisms underlying the migration of CTCs into the blood stream is still not fully understood but various events including the hypoxic tumor environment [173], ECM remodeling [174], active proliferation [174] and epithelial to mesenchymal transition (EMT) [175] are all recognized as possible mediators of increased migratory potential of CTCs. Following entry into the blood stream, the CTCs are present in circulating blood transiently, possibly resulting from immune clearance, apoptosis, or secondary localization which translates to an extremely small number in circulation [176]. CTCs have been found in blood of a small percentage of patients well before clinically detectable metastasis [177,178]. However, consistent identification of CTCs is difficult due to variability in how cancer progresses in different individuals and in part due to the low sensitivity of methods to enumerate them [179]. Relatively, numbers of CTCs in circulation can increase as a function of expansion of the primary tumor or tumor cell proliferation at metastatic sites [180]. Recent work has also shown that the numbers of CTCs in circulation can decrease in response to reduction in tumor burden with effective therapy [180]. In developed metastatic cancer, CTCs are found at a rate of 1-10 CTCs per 10 mL of blood or 1 CTC per billion nucleated cells [172].

2.2. Predictive information in CTCs

The most basic information that can be obtained from CTCs is the confirmation of their presence and the evaluation of their numbers [31,32]. Quantification of numbers of CTCs is now commonly used as a prognostic marker in metastatic cancer to evaluate

effectiveness of therapy via correlation of CTC numbers to disease state, with a decrease in CTC count suggesting successful targeting of the tumor [181-183]. Given that CTC numbers have poor correlation with tumor burden and the fact that there is high patient-to-patient variability, the patient's baseline threshold is used as a point of comparison rather than evaluation based on pre-defined threshold [184]. Intact and viable CTCs have been maintained using cell culture to determine proliferative potential and responsiveness to chemotherapeutic drugs [185,186]. More recently, CTC clusters comprising of 2-100s of cells have been identified in circulation and have been found to possess 100-fold higher metastatic potential [187-189]. The presence of even a single CTC cluster in blood liquid biopsies correlates with significantly reduced progression-free survival rates in patients with various types of cancers [189,190]. CTCs can be profiled as a mixture or via single cell profiling to characterize disease in patients, identify CTC heterogeneity and determine distinct subsets of cells which can provide information that can be used to direct patient specific therapy [191,192]. Molecular expression signatures of CTCs also provide important information regarding the patient's status. Proteins contained within cells and cell surface markers including cell-surface receptors can be evaluated using immunofluorescence microscopy or flow cytometry and used to classify disease phenotype.[193,194] Specific mutations and splice variants can be profiled using genetic screening and also used as measures of disease burden to guide effective treatment.[195,196] While there is little doubt regarding the wealth of information regarding the patient's immediate condition, identifying consistent and universal biomarkers has been the major challenge. Reliable and highly sensitive methods to isolate intact CTCs from blood liquid biopsies will hasten progress in identification of new and reliable biomarkers.

2.3. Physical and biochemical characteristics of CTCs

CTCs are a heterogeneous population and their characterization can play a major role in the selection of technique used for their isolation. They range in size from 4-20 μm, stain positive for epithelial cell adhesion molecule (EpCAM) and negative for cluster of differentiation 45 (CD45) [197]. CTCs can also be found in clusters of 2-100 cells and can range in size from 10-100s of micrometers in diameter. To avoid bias associated with EpCAM-mediated cell capture, cancer-type specific biomarkers can be exploited using antibodies or aptamers targeted towards specific markers. When isolated using density gradient centrifugation using a Ficoll or Percoll gradient, CTCs fractionate along with peripheral blood mononuclear cells (PBMCs) with an estimated density ~ 1.064-1.065 g/cm^3.[198]. CTCs are more deformable than WBCs which is an aspect that has been exploited for isolation [199]. CTCs are known to express both epithelial and mesenchymal proteins as a consequence of EMT [200]. More specific markers including different cytokeratins and specialized markers like prostate-specific membrane antigen (PSMA) can allow identification of CTC associated with different organs and metastatic sites [201]. Despite information regarding cancer-type specific labels and biomarkers, it is important to understand that there is no universal biomarker that can be used to classify CTCs and these cells are a heterogeneous population with a percentage of cells expressing a particular marker. Detailed molecular characterization of CTCs at the gene and protein level can provide valuable insights into the biology of the specific type of cancer and potential for metastasis [202]. This information can then be used to classify patients for metastatic risk, select therapeutic options and monitor disease progression and effectiveness of therapy [203].

2.4. Microfluidic devices CTC capture

As previously discussed, CELLSEARCH® is the only FDA approved test for evaluation of CTCs in patients with cancer and is used as a surrogate for imaging to provide additional information as an independent predictor of cancer progression in metastatic cancer and to evaluate response to chemotherapy [168]. Considering the potential for microfluidics to significantly outperform conventional macroscale devices, it is interesting to note that the only FDA approved device is a macroscale device. While microfluidics based approaches have only recently been pursued for cancer monitoring, this is possibly due to the fact that microfluidics-based approaches have yet to demonstrate efficiency and reliability necessary to serve as standalone monitoring tool. Another important factor could be the lengthy nature of the FDA approval process. The complexities associated with CTC detection make reliable isolation of CTCs with conventional macroscale techniques difficult to accomplish and not surprisingly, microfluidics-based approaches have been aggressively explored. Detection and isolation methods exploit physical or biochemical differences between cells to enable discrimination. Microfluidics provides technology to discriminate between cells at the single-cell level thereby enabling separation efficiencies not possible with bulk methods. The CELLSEARCH® system is not a microfluidic system and uses a combination of magnetic nanoparticles to separate target cells and imaging to confirm that the captured cells are indeed CTCs. Critical parameters for evaluation include throughput (mL of blood that can be processed per hour given the low numbers of CTCs), capture efficiency (% of spiked CTCs that can be captured from a known volume of blood) and purity (% of cells captured that are CTCs). The CELLSEARCH® platform can process large volumes of blood (several mL), has a capture efficiency of ~85% but is associated with low purity.

This process utilizes several processes including the labeling and capture steps, that if miniaturized could be significantly improved.

Demonstration of microfluidics-based systems for CTC isolation started with the CTC-chip in 2007 where a microfluidic device with silicon pillars was functionalized with capture antibodies.[204] Following the success of this device in achieving successful identification of CTCs in > 99% of patient samples, several other groups and companies began developing microfluidics-based approaches to capture CTCs. While a majority of these efforts focused on exploiting cell surface markers to enable isolation, others focused on unique physical characteristics (label-free) of CTCs such as size, shape, deformability, and behavior under conditions of microscale flow. Thus far, label-free approaches have yet to demonstrate the efficiencies associated with immuno-affinity based methods but with development of new methods and devices, it appears that label-free technologies may provide not only the sensitivity to compete with immuno-affinity based techniques but provide superior performance in terms of throughput. Overall, while there is significant potential for microfluidics to impact CTC isolation, microfluidics is also associated with some limitations. These limitations primarily relate to throughput and the ability to process sufficient amounts of sample to be able to isolate or detect suitable number of CTCs for subsequent analysis. While parallel processing has been suggested as means to address this issue, it still is a major challenge that will need to be addressed. Other challenges involve non-specific capture of cells and dealing with the heterogeneity within CTC populations. A more detailed discussion on the limitations of microfluidics can be found in the 'Future Directions' section. **Tables 1A and 1B**

summarize microfluidic approaches for immuno-affinity and label-free capture of CTCs respectively and are organized based on capture efficiency.

2.4.1. Microfluidic devices for immuno-affinity capture of CTCs

The first microfluidic device for capture of CTCs was demonstrated in 2007 by Nagrath et al.[204] and consists of a silicon microfabricated platform with 78,000 pillar structures **(Fig. 2A)**. The silicon surface was functionalized with a capture antibody targeted towards EpCAM to enable capture of CTCs of epithelial origin. Preliminary studies focused on demonstration of the ability of this device to capture cancer cell-lines associated with prostate, bladder, lung and breast cancer followed by evaluation of blood samples from cancer patients. This device was able to identify CTCs in 115 out of 116 samples processed demonstrating its utility for detection. Captured CTCs were confirmed using a combination of both positive (DAPI/Cytokeratin) and negative (CD45) immunofluorescence staining. Apart from screening, this platform was also used to monitor patient response to treatment and showed that the CTC numbers of correlated with response to treatment. A follow up study used the same platform to evaluate specific mutations in epidermal growth factor receptor (EGFR) [205]. In terms of performance, this device operated at a flow rate of 1 mL/hour at a capture efficiency of ~ 60% with a purity of ~ 50%.

The basic concept of immuno-affinity capture with silicon post was further enhanced by using design optimization to determine size and organization of the posts and translated into a ‘geometrically enhanced differential immuno-capture’ (GEDI) device [206]. This device was used with different capture antibodies and used to probe prostate

cancer using both cell-lines and patient samples. Optimization of post geometry and arrangement resulted in a capture efficiency of ~ 80% and purity of ~ 68% which is an appreciable advance over the original CTC chip. Murlidhar et al. [207] further optimized post shape to minimize flow separation around the posts and enhance cell interaction with the post surface, unlike commonly used flow through configurations, the sample flows radially outward and can process samples at flow rates up to 10 mL/hour. The reported capture efficiency is between 80-100% with lower efficiency at higher flow rate. However, the purity is increased with increasing flow rates.

Other device designs and modifications were incorporated to enhance throughput, capture efficiency while minimizing non-specific capture. Stott et al. [208] developed a herringbone (HB)-chip which incorporates a staggered double herringbone structure on the roof of the microchannel to induce rotational flow that results in chaotic mixing within microfluidic channels **(Fig. 2B)**. Cells travelling through the channel are forced to interact with the capture surface thereby enhancing interactions between the cells and capture antibodies. The HB-chip when operated at a flow rate of 1.2 mL/hour resulted in an extremely high capture efficiency of ~ 90% at ~ 15% purity. The low purity is presumably due to the low flow rate which is insufficient to dislodge cells that are weakly bound to the capture channel. The concept of the HB chip was combined with the concept of the GEDI chip and resulted in a geometrically enhanced mixing (GEM)-chip [209] which operated at a higher flow rate (3.6 mL/hour) and maintained the capture efficiency. The capture purity was significantly improved to > 80% which can be directly attributed to the higher flow rate which is sufficient to dislodge weak non-specifically bound cells.

Apart from design variations, other modifications have included the use of different types of materials for microfluidic device construction; high-aspect ratio structures fabricated via embossing of polymethylmethacrylate (PMMA) was used to construct a high-throughput microsampling unit (HTMSU) [210,211]. Further complexity was incorporated in the form of sensors for on-chip conductivity measurements which correlates to cell counts. Despite its name, the operating flow rate was low, at ~ 1.2 mL/hour with a capture efficiency of ~ 95%. Yoon et al. [212] combined nanotechnology-based approaches to develop a graphene oxide (GO)-based chip which enhances antibody presentation to the flowing sample. The GO-chip operated at a flow rate of 1 mL/hour is associated with a capture efficiency of ~ 95% with minimal non-specific binding.

CTCs captured within immuno-affinity capture devices are typically stained and evaluated on-chip or lysed to extract proteins and nucleic acids. With the need to isolate intact CTCs for further analysis or cell culture, some groups have focused on developing methods to release CTCs following capture. Using the basic concept of the HB chip, Reategui et al. [213] developed a technique where layer by layer deposition of gelatin and streptavidin were used to immobilize streptavidin coated nanoparticles to ultimately bind biotinylated antibodies for CTC capture. Following capture, the captured cells were released by increasing the temperature to dissolve the gelatin or through acoustic activation. Another group also developed a system based on the HB-chip and developed thermoresponsive polymers that could make immobilized antibodies either available (room temperature) or unavailable (when cooled to below critical solution temperature ~ 4 deg C) [214]. This NanoVelcro system can capture and release cells via targeted temperature changes. Both approaches operate at relatively high flow rates but attain high

efficiency capture (> 90%) at relatively high purities. In another example, Hou et al. [215] demonstrated that capture and release could be accomplished using polymer grafted silicon structures.

With importance being placed on retrieval of captured cells, there have also been efforts to miniaturize conventional immuno-magnetic separation techniques. While every aspect of immuno-magnetic separation including sample-bead mixing and incubation, capture, washing and release can benefit from miniaturization, there are examples of where one or more of these approaches have been exploited for CTC isolation. The VeriFAST system utilizes blood samples mixed with paramagnetic beads conjugated with capture antibodies in a microfluidic device with two unmixable fluids.[216] The labeled cells are manually moved from the blood sample containing well across an oil-pinning well using a hand held magnet. In another example, the CTC-iChip exploits size-based separation to de-bulk the sample of blood cells and then accomplished CTC isolation using immuno-magnetic beads **(Fig. 2C)** [217]. Both these techniques have relatively high throughput (>5 mL/hour), high efficiency (> 90%) and reportedly high purity [218]. More recently, there appears to be a continuing trend to incorporate two or more approaches to accomplish sample pre-processing or debulking followed by more specific immuno-affinity capture. Ahmed et al. used a pillar array to debulk non-target cells followed by imaging, detection and analysis of captured CTCs with a capture efficiency of 92% and a capture purity of 82% [219]. Shields et al. used a three stage process where cells were first aligned using standing acoustic waves (SAW), seprated using antibody-conjugated magnetic beads and isolation of individual CTCs into microwells for single cell analysis [220]. Green et al. used a combination of shear stress and immuno-affinity capture to isolate

phenotypically unique CTCs based on EpCAM expression levels [221]. Finally, optical trapping and photoacoustic detection of nanoparticle labeled CTCs has also been developed to obtain high efficiency CTC capture [222,223].

2.4.2. Microfluidic devices for label-free CTC capture

Label-free approaches for CTC isolation have focused on three specific properties of CTCs: size, deformability, surface energy/charge. Given the heterogeneous nature of CTCs and the wide distribution in the levels of expression of different biomarkers, label-free approaches may provide the means to avoid biomarker 'bias' and potentially isolate larger numbers of cells with diagnostic/prognostic value. However, at the same time, the disadvantage is the lack of specificity which can lead to lower levels of purity of captured cells. Several companies have commercially available products for enrichment focused on size-based discrimination of CTCs from other blood cells. Size-based sorting does not compare in terms of purity associated with antibody-based approaches, however, these approaches provide significantly higher throughput. The use of size also prevents EpCAM induced screening bias and identification of CTCs of non-epithelial origin including mesenchymal CTCs that are common in metastasis. These types of assays are associated with a quick initial enrichment step followed by staining and analysis; Screencell offers a simple 6.5 μm filter for enrichment of fixed CTCs and 5.5 μm filter for unfixed CTCs.[224] Confirmation of CTCs is then accomplished via imaging of the enriched sample. Several other companies including Parsortix (weir-type filter),[225] Creativ Microtech (precision micromachined filters),[226] Ikonisys (size filtration combined with size based isolation) [227] have all developed similar methods where cells are sorted by

size and further evaluated using imaging. Harouaka et al. developed a highly sensitive filter array using flexible springs fabricated using Parylene C.[228] This flexible micro spring array (FMSA) processes whole blood in a very gentle fashion to enable separation of cancer cell lines spiked into whole blood **(Fig. 3A)**. Separation efficiency was ~ 90% at a throughput of 45 mL/hour. The feasibility of this approach was also demonstrated using samples from patients with a variety of cancers and the number of CTCs isolated corresponds well with results from the CELLSEARCH platform [229]. Gogoi et al. exploit both the size and deformability of CTCs to enable trapping and automated staining and screening of CTCs using a microfluidic device reporting 94% sensitivity and 100% specificity [230]. CTC clusters are significantly larger and have been sorted from blood liquid biopsies which contains individual cells in suspension via a process called deterministic lateral displacement (DLD) which causes preferential migration of cells in flow via interaction with obstacles placed at locations along the flow path. Using a two-stage process Au et al. demonstrated separation of small and large clusters of breast cancer cell lines spiked in blood with 99% recovery of large clusters, cell viabilities over 87% and greater than five-log depletion of red blood cells [231].

Cells in flowing fluid can also be fractionated into unique populations based on size differences. In microfluidic channels the balance between inertial lift forces and wall lift forces in high aspect ratio microchannels enables focusing of particles at unique locations close to the wall [232,233]. The larger the particle the closer the focusing location was to the outer wall. This phenomenon has been exploited to separate CTCs or cancer cell lines from red blood cells and white blood cells in a continuous flow fashion at relatively high throughputs. Straight rectangular channels are associated with multiple focusing locations

(2 or 4 depending on the aspect ratio) which can be reduced to one focusing location within curved channels. There have been many examples of rectangular cross-sectional channels organized in a spiral fashion to enable focusing and separation of CTCs [234-236]. Examples of these types of devices include, simple spiral (> 85% efficiency, 3 mL/hour, 3 log depletion) **(Fig. 3B)** [237], 6-loop double spiral (> 85% efficiency, 20 mL/hour, enrichment factor of 19) [238] multiplex spiral [239] cascaded spiral (> 85% efficiency, 33 mL/hour, 98% depletion)[240] and 8-loop slanted spiral where the walls were at different height with the outer wall being taller than the inner wall (> 80% efficiency, 55 mL/hour, 4 log depletion) [241]. While these flow-based technologies for size-based separation offer reasonable efficiency and high throughput, they cannot process whole blood directly and require some prior pre-processing. Even with sample pre-processing, the contamination with non-specific cells is high, for example a 99.9% depletion of red blood cells still amounts to a RBC: CTC ratio of 1×10^6:1 which is a major obstacle to evaluating CTCs.

Other approaches that exploit inertial effects uses a rectangular flow channel with chambers on either side of the microchannel. The fluid within these small chambers is stagnant for the most part and fluid flow in the rectangular channel results in generation of vortices within the chambers. Particles migrating to the walls of the channels interact with the recirculation associated with these vortices and remain trapped in the chamber and are subsequently released from the chambers at higher flow rates. Sollier et al. [242] demonstrated that such a design can be used to capture CTC but the efficiency was ~ 20% and the purity just over 50%. The same technology was used for classification of large captured CTCs [243] and for labeling of CTCs with magnetic beads [244]. Parichehreh et al. [245,246] developed a system that exploits both inertial focusing effects and surface

energy based migration in a technique called ‘inertia enhanced phase partitioning’ **(Fig. 3C)**. Cells are introduced into a microfluidic channel as a thin stream flanked on either side by Dextran. For red blood cells, the energetically favorable location is within the Dextran whereas the CTCs and white blood cells prefer saline and do not migrate towards the Dextran. As red blood cells move to the dextran, inertial focusing effects move the red blood cells towards the outer wall whereas CTCs and white blood cells remained in the middle between the two Dextran streams. Operating at a flow rate of 1.2 mL/hour, a two-pass system using this device resulted in > 99% depletion of red blood cells with 98% recovery of spiked cancer cell line cells.

Acoustic waves in the form of tilted angle standing surface acoustic waves (taSSAW) have been used to influence particle migration within microfluidic channels. Ding et al. [247,248] optimized the power and angle of inclination that could efficiently separate cancer cell-lines spiked in red blood cell depleted blood. At a maximal flow rate of 1.2 mL/hour, this technique achieved 83% purity with 1 log depletion of white blood cells. Dielectrophoresis (DEP) is used in a commercially available device called ApoStream to sort CTCs from other blood cells [249,250]. A combination of acoustic focusing and DEP was used to pre-concentrate target cells using acoustic focusing and trapping of target cells using DEP was used for CTC isolation with 76% recovery of target cells and only 0.12% contamination with non-target cells [251]. With optimized voltage, frequency, buffer and electrode configurations, this device can operate at a maximum flow rate of 1.5 mL/hour with 70% purity and 2-3 log depletion of white blood cells. But the viability of cells was excellent suggesting potential for sub-culturing isolated cells.

Both immuno-affinity and label-free microfluidics approaches have shown great promise for CTC capture. Several factors including throughput, ability to directly process blood samples without significant pre-processing and strategies to deal with the large heterogeneity associated with CTCs need to be addressed prior to widespread clinical adaptation.

3. Tumor Cell Derived Exosomes

3.1. Origins and frequency of occurrence

Exosomes are vesicles that are shed directly from cells via budding of the plasma membrane.[252-254] Exosomes vary in size ~ 25-300 nm and play important roles in transport of signaling molecules to facilitate cell-cell communication [254,255]. Exosome contents include nucleic acids (DNA and RNA), proteins, metabolites, and lipids and facilitate normal physiological processes [256,257]. In disease, exosomes can also mediate pathological signaling [258,259]. Formation of exosomes involves initiation, budding of endocytotic membrane into the cell lumen, formation of multi-vesicular bodies, selection and degradation or secretion of vesicular bodies. Exosomes are secreted in various bodily fluids including blood and are highly stable under physiological conditions and are found at relatively high abundance [254,260]. Typically 1 mL of serum is known to contain between $1 \times 10^9 - 1 \times 10^{12}$ exosomes.[261] While there is evidence to suggest that the exosome cell-surface markers and intra-vesicular contents contained within exosomes change in patients with cancer [262-264], there is also evidence to suggest that the numbers of exosomes in serum increases due to cancer [265,266].

3.2. Predictive information in exosomes

An increase in number of circulating exosomes can be used as a simple but non-specific evaluator of cancer [265,266]. Exosome surface markers provide valuable information that can be used to determine their origin and signaling associated with the cells from which they were secreted. These cell surface markers have been widely used to enable isolation using immuno-affinity capture. Expression of epithelial derived markers like EpCAM can be used to identify tumor cell-derived exosomes [267,268]. Identification of specific organs associated with the tumor can also be identified via examination of specific protein biomarkers to distinguish different types of cancer. Specific protein markers have been identified for breast [269,270], prostate [271,272], pancreatic [273], ovarian [274], and colorectal cancers [275]. The DNA and RNA contained within the exosomes are similar to cell-free DNA and RNA and can be profiled and used as biomarkers for diagnosis and longitudinal disease monitoring [276-279]. A more detailed discussion regarding the predictive information of DNA and RNA is available in sections below.

3.3. Physical and biochemical characteristics of exosomes

Exosomes are variable in size ranging from 25-300 nm and their isolation typically requires ultracentrifugation of serum samples.[280] Exosomes also have well-defined surface markers that have been utilized for immuno-affinity separations. Non-specific capture of exosomes uses common exosome markers CD9, CD63, and CD81[281,282] either immobilized to a surface or coupled to magnetic beads whereas cancer specific exosomes can be isolated using CD24,[267,269] CD37,[283] CD53,[284] CD73,[285] CD82,[262] and EpCAM.[127,128] Exosomes characterization can be accomplished by profiling for specific protein markers based on the endosome biogenesis pathway associated proteins

including annexins [286], flotilin [287], Alix [288], Tsg101 [289], tetraspanins [276,277], heat shock proteins 70 and 90 [290], and EpCAM [127,128].

3.4. Microfluidic approaches for capture and analysis of exosomes

Conventional approaches for isolation of exosomes include ultracentrifugation [268,291], ultrafiltration [262,292] or immuno-magnetic bead based techniques [293-295]. While all three of these approaches successfully isolate exosomes, each is associated with disadvantages which can have a significant impact on targeted isolation of tumor cell associated exosomes which are observed at low frequency in circulation [296]. Ultracentrifugation is a time consuming (4-5 hours), associated with low yield (< 25% recovery), high impurity (all vesicular components), compromised integrity of the vesicle and need for highly skilled personnel [297,298]. Density gradient ultracentrifugation can enhance purity and fractionate vesicular components but the additional processing further complicates an already tedious process. Ultrafiltration using membranes with small pores has also been used to remove large contaminants via size-exclusion. Since this process relies exclusively on size as a basis for separation, protein contamination is a significant issue. Moreover, nanometer sized pores on the filters combined with small open area for fluid transport provides high fluidic resistance and requires large pressure to move fluid across the membrane resulting in limited throughput. Immuno-magnetic bead-based approaches offer a simpler alternative and are increasingly being used for exosome isolation despite issues with capture efficiency and purity. Finally, a simple and easy to use commercially available product Exoquick accomplishes isolation of exosomes via precipitation; despite its scalable nature, the yield of exosomes is low and variable [261]. Microfluidic options for exosome isolation are similar to those available for CTC isolation and either relies on

immuno-affinity mediated capture or label-free approaches. Considering the size of exosomes, exploitation of physical properties to enable separation is limited in comparison to CTCs.

The main advantage of microfluidics based approaches for exosome capture is the adaptability for low abundance exosomes (i.e.) exosomes shed from cancer cells as opposed to exosomes commonly found in circulation. Microfluidic approaches for exosome isolation primarily rely on enhancing immuno-affinity capture via miniaturization and exploiting microarchitectures, high surface-area to volume ratios, and flow phenomena to immobilize a large number of capture probes and enhance and prolong interaction of exosomes with the capture probes. Other label-free microfluidic approaches have also been developed to isolate exosomes using electrophoresis, dielectrophoresis, sieves, physical trapping and optical trapping. **Table 2** summarizes microfluidic approaches for both immuno-affinity and label-free capture of exosomes organized based on capture efficiency.

3.4.1. Immuno-affinity based approaches for exosome isolation

A microfluidic device was developed by Chen et al. as an alternative to conventional ultracentrifugation for isolation of exosomes [299]. To accomplish capture of exosomes, the authors covalently immobilized CD63, an antibody that is specific to exosomal vesicles to the surfaces of a microfluidic channel **(Fig. 4A)**. The channel floor contained a herringbone structure to induce fluidic rotation within the channels and enhanced interaction of the exosomes within the channel with the capture antibodies on the walls.

This technique was rapid, simple and processing of ~ 400 µL of serum samples from non-small cell lung carcinoma patients resulted in isolation of sufficient number of exosomes for isolation and analysis of tumor RNA [299]. Kanwar et al. took this concept further by enabling detection capabilities to quantify captured exosomes via staining with a fluorescent carbocyanine dye (DiO) that specifically labels the exosomes and can be quantified using a standard plate reader [300]. Comparison of serum samples from patients with cancer and healthy controls revealed a nearly 2.5 fold increase in captured exosomes in cancer patients with detectable differences in miRNA profiling. After processing 400 µL of serum they were able to isolate nearly 15-20 µg of protein and 10-15 ng of total RNA [300]. Zhang et al utilized Y-shaped microposts functionalized with CD81 antibody along with a graphene oxide/polydopamine coating to prevent non-specific adhesion and enhance capture of exosomes via an increase in capture surface area and reported a recovery yield of 72% with almost no non-specific binding [301].

Several other groups have combined immuno-affinity capture with different types of detection and quantification techniques. Examples include electrokinetic, force-based, optical, electro-chemical, electro-optical and acoustic-based approaches. One specific example is the nano-plasmonic exosome sensor (nPLEX) where immuno-affinity capture within microfluidic channels is coupled with surface plasmon (SPR) resonance based detection [302]. Rather than focus on a single capture ligand, nPLEX contains an array of up to 36 different proteins to enable phenotyping of captured exosomes. Using this setup, ovarian cancer patients were differentiated from healthy controls via differential phenotyping [302]. While immuno-affinity capture on surfaces has been successful in isolating useful amounts of target exosomes, non-specific binding of contaminating

species is a cause for concern [303,304]. These species can affect detection techniques and are particularly an issue when intra-vesicular contents of the exosomes need to be retrieved [304].

To enhance sorting efficiency and minimize non-target molecules and vesicles, Dudani et al. developed an approach which combines immuno-affinity capture of exosomes on modified polystyrene beads which were then separated from the original sample solution into a buffer via inertial migration in rectangular cross-section microfluidic channels [305]. Using this setup, exosomes were isolated from blood spiked with supernatant from cancer cell cultures. Following red cell lysis and incubation with the immuno-modified beads, a suitable number of exosomes were captured on the surface of the polystyrene beads [305]. While the separation mechanism exploits microfluidic advantages, a four hour incubation period is necessary for binding of the exosomes to the beads limiting the attractiveness of this approach for clinical applications. Several other groups (Shao et al. [306], He et al. [307]and Zhao et al. [274]) have also used immuno-affinity capture using functionalized microbeads to separate exosomes from bodily fluids using magnetic separation within microfluidic devices, however, only Shao et al. [306] reported capture efficiency of > 93%, whereas; others did not evaluate capture efficiency of their devices. Typical samples volumes that can be processed are in the range of 10s to 100s of microliters.

3.4.2. Label-free approaches for exosome isolation

The small size of exosomes limits the use of flow phenomena for focusing, trapping or directed migration within microfluidic channels. Microfluidic adaptation of

ultrafiltration can potentially be used to fractionate exosomes based on size. One group attempted to achieve microfluidic ultrafiltration as a means to separate exosomes from whole blood [308]. Exosomes were transported across a size-exclusion membrane either using pressure or an electrical field (~ 80 ng RNA from 100 µL blood).While reported results seem comparable to conventional macroscale ultrafiltration, there was no significant improvement. While the pressure driven approach was faster, the electric field driven separation resulted in higher purity [308]. However, there appears to be several disadvantages associated with purity, throughput and processing speed. More recently, Woo et al. developed a lab-on-a-disc for exosome isolation called the 'Exodisc' which utilized centrifugal force for transport of fluid across a size-exclusion filter and using urine samples reported removal of > 95% contaminating proteins and > 95% recovery of exosomes in addition to reporting >2 orders of magnitude higher RNA than exosomes isolated using conventional ultracentrifugation [309]. Lee et al. accomplished capture of exosomes from packed red blood cell units via use of acoustic force to enable transport through a filter and demonstrated > 80% recovery [310]. Another approach that exploits the size difference between exosomes and other larger cells, vesicles and molecular species in blood consists of an array of posts containing ciliated structures [311] **(Fig. 4B)**. The ciliated structures are silicon nanowires and serve two purposes. First, they act as a barrier to the entry to larger contaminants. Once a vesicle interacted with the posts, it was trapped within the cilia ensuring capture of the target species. Depending on the spacing between the cilia, specific size vesicles can be targeted [311]. While capture is accomplished within 10s of minutes and imaging of vesicles is relatively straightforward, isolation of intact vesicles requires dissolution of the silicon nanowires and can be complicated. This device was tested with a binary mixture of vesicles of two different sizes [311]. It is difficult

to speculate how this technology will translate to capture of exosomes from serum or blood in terms of throughput and purity. Santana et al. used micro-pillar architectures within microfluidic channels to separate exosomes from cell culture medium based on vesicle size and demonstrated recovery of > 35% of all vesicles [312]. More recently, the use of deterministic lateral displacement (LDL) was used in silicon nanofluidic devices where the precisely machined silicon structures in low Peclet (Pe) number flows enabled particle movement via diffusion and displacement to compete with each other resulting in separation of exosomes and colloids between 20-110 nm [313]. Liu et al. exploited elastic lift forces when samples are suspended in a viscoelastic medium to enable sorting of exosomes from other vesicular bodies and reported a >80% purity and > 90% recovery of exosomes in fetal bovine serum [314].

Microfluidic technologies for exosome isolation are still in early stages of development but results confirm that microfluidics may provide simpler and efficient techniques to conventional filtration and centrifugation based approaches. A better understanding of the utility of exosomes in cancer monitoring and a better understanding of the physical and biochemical markers of target exosomes will enable development of more sophisticated microfluidic approaches.

4. Cell-free tumor cell DNA (ctDNA) and Circulating RNA

4.1. Origins and frequency of occurrence

DNA: Recent high throughput sequencing studies have identified specific genetic mutations that enable survival and expansion of solid tumors. Virtually all cancers carry somatic DNA mutations which are only present in tumor cell DNA. Identifying tumor

DNA provides a highly specific biomarker that can be used to for disease diagnosis and monitoring. While tumor cell DNA is abundant in tumors, their analysis requires invasive biopsies or the capture and analysis of CTCs. Tumor cell associated DNA has been reported in blood samples of patients with malignant and non-malignant cancer [315]. Presence of tumor DNA in blood is a consequence of tumor cells undergoing apoptosis or necrosis causing nucleosomes to be released into blood, circulating freely in plasma [316,317]. Necrosis results in larger fragments of up to 10,000 base pairs (bp) and apoptosis leads to DNA fragmentation resulting in fragments as small as ~ 100 bp. The half-life of cell free ctDNA is very short and is cleared from circulation within a couple of hours. In aggressive cancers, the increased tumor burden results in higher levels of necrosis leading to large amounts of cell free ctDNA [318].

RNA: Tumor cell associated RNAs have been reported in blood liquid biopsies of patients with different types of solid tumors [319]. Considering the role of messenger RNAs in cellular function, RNA from apoptotic or necrotic cancer cells in circulation could potentially provide valuable information regarding intracellular tumor cell phenotype and function. There are several types of circulating RNA including coding RNA or messenger RNA (mRNA), and non-coding RNAs like micro RNA (miRNA), long non-coding RNA (lncRNA), and small interfering RNA (siRNA). The abundance of mRNA in circulation is low as it is unstable and subject to degradation. In contrast, non-coding RNAs are stable and usually found at detectable levels within circulation [320].

4.2. Predictive information in ctDNA and circulating RNA

The identification and relative amount of ctDNA in circulation correlates with tumor burden. Screening for ctDNA within blood can provide a monitoring tool for early diagnosis and monitoring of response to treatment. The size of ctDNA fragments can provide information regarding the mechanism of cell death which can be used to understand tumor regression or remodeling. The most promising utilization of ctDNA may in the identification of specific mutations that are predictive of acquired resistance to chemotherapy via selection of resistant tumor cells during drug treatment. The tumor genome also plays a critical role in how patients respond to chemotherapeutic drugs. Genome sequencing has resulted in identification of somatic genetic mutations and genomic, transcriptomic and epigenetic changes in various tumors have being mapped. This information can be used to develop chemotherapeutic drugs that have the best chance for clinical benefit in cancer patients.

The presence of circulating mRNA in cancer patients has been known for over two decades. Evaluation of circulating mRNA can potentially provide information regarding key intracellular processes in tumor cells and serve as biomarkers for diagnosis and monitoring. Their increased presence in serum or blood has been previously found to be predictive of clinical outcome and disease prognosis [321,322]. Of the non-coding RNAs, miRNA is the most promising target and is actively being evaluated as a cancer biomarker. miRNAs are highly conserved short strands of non-coding RNA and is known to play a role in repressing or activating translation of proteins. miRNAs are known to be dysregulated in cancer enabling crucial processes like proliferation, metastasis, apoptosis and angiogenesis. Profiling and quantification of miRNAs in circulation can provide

important information for diagnosis, longitudinal patient monitoring and development of therapeutics [323-325]. Other non-coding RNAs like small interfering (siRNAs) and long non-coding RNA (lncRNAs) are attractive targets, however, there is not much information regarding how they might influence onset and progression cancer.

4.3. Microfluidic approaches for capture and analysis of ctDNA and circulating RNA

The use of microfluidic approaches for DNA and RNA isolation in the context of cancer has not been extensively explored. This can be attributed to the fact that there is limited information available in terms of circulating DNA or RNA in blood or serum samples and their relevance to cancer. While microRNAs are stable and commonly found in circulation, other nucleic acids like DNA and mRNA are usually found within intact cells or exosomes where they are protected from degradation and clearance. In cancer, rapid turnover of cells via either apoptosis or necrosis results in detectable amounts of cell-free ctDNA and mRNA in circulation with the amounts directly correlating to stage of cancer and the size of the tumor [316,317]. While tumor cell DNA and mRNA can provide valuable insights into specific mutations and transcriptional activity, the use of this information for evaluation of cancer requires more extensive investigation.

Microfluidic approaches for isolation of nucleic acids present both in low and high abundance have been widely explored for several non-cancer based applications. These techniques are broadly applicable to any disease where nucleic acids need to be isolated from fluids that contain other molecular and cellular contaminants. Therefore, in this section we will review promising microfluidic-based approaches for nucleic acid

isolation from blood or plasma samples that can be readily adapted for cancer diagnostics. Microfluidic approaches for nucleic acid isolation are typically preferred if the sample volume is small and if either the target nucleic acids occur at low frequencies. Microfluidics also offers rapid and high-efficiency separations with the potential to integrate pre- and post- isolation process into a seamless fashion to create point-of-care (POC) technologies that can be deployed in resource limited settings or in the clinic. Microfluidic devices for isolation of nucleic acids can be broadly classified as either solid phase isolation or liquid phase isolation. Solid phase isolation techniques rely on the use of a charged surface or immobilized probes to bind and capture nucleic acids. Liquid phase isolation techniques rely on the mobility of nucleic acids via charge/polarizability or solution chemistry for separation. A summary of possible microfluidic approaches that can be adapted for capture of ctDNA and circulating RNA are listed in **Table 3** and organized based on reported sensitivity of the approach.

4.3.1. Microfluidic Solid Phase Extraction

The microfluidics field has heavily borrowed techniques and processes from the semiconductor fabrication industry and it is not surprising that a majority of early generation microfluidic devices used silicon as the primary substrate for device fabrication. Silica is negatively charged and when treated with high concentrations of a chaotropic agent like guanidinium or sodium iodide, a salt bridge forms between the negatively charged silica and the negatively charged nucleic acid backbone to enable non-specific binding [326]. To capture cell-free nucleic acids, it is important to debulk the sample of cells and vesicles to ensure that cellular or vesicular nucleic acids are not captured as chaotropic agents can potentially cause lysis and release of intra-cellular or

intra-vesicular contents. Captured nucleic acids can be extracted by washing with organic solvents like ethanol or isopropyl alcohol. The most basic version of this device is a rectangular cross-section microfluidic channel which still has significantly larger surface area to volume ratio than available with any macroscale approach. Silica beads packed within microfluidic channels have also been used for capture of nucleic acids to further increase the capture surface area [327-329]. Beads are packed into narrow microfluidic channels or capillaries using a weir structure that enables packing of beads within the channel. Packed silica beads have been successfully used to capture both DNA and RNA which have either been eluted for further processing or subsequent processing including amplification and detection performed on-chip [330]. A major disadvantage of this approach is the extremely high fluidic resistance resulting in high back pressure. An improvement over packed silica bead capillaries is embedding of silica beads in hydrogels [331]. Silica beads were directly incorporated into the hydrogel solution prior to gelation resulting in free standing structures or channels filled with silica bead containing hydrogel. Due to the high porosity of the hydrogel, the back pressure necessary to feed sample through is diminished. Successful DNA isolation has been demonstrated using this approach. Hydrogels have been incorporated into both glass and polymer microfluidic devices with the polymer devices providing cheaper alternatives. Variations of the same approach have been accomplished using construction of silicon microstructures using surface micromachining or bulk micromachining approaches with the goal of increasing surface area available for a given volume for nucleic acid capture [332-336]. Precisely defined microstructures greatly minimize variability typically seen with packed beads or beads in hydrogel but the cost of manufacturing these structures is high. Silicon microstructures have been used for DNA isolation and integrated within micro total analysis systems

(μTAS) for seamless integrated processing. There are also several other examples including silica membranes [337], porous silica-based structures [338], etched silica structures [339] which have all been used for nucleic acid isolation The major drawback of silica or silicon based capture is the use of the harsh chaotropic agent which can interfere with downstream processing [330].

An alternative to immobilized beads is the use of paramagnetic beads to enable either immobilization or extraction of captured nucleic acids to minimize the amounts of non-specific contaminants [340-343]. Paramagnetic beads have large surface area to volume ratio, can be temporarily immobilized to interact with sample and then extracted during washing steps from the microfluidic device or moved to another chamber within the microfluidic device for subsequent processing. Other tunable features that can be adjusted depending on the application are: the charge on the surface of the beads, surface chemistry, and immobilization of specific capture moieties. Beads can be introduced in suspension within the sample and efficient mixing can enhance interaction of the magnetic beads with targets thereby minimizing incubation times. Examples of paramagnetic bead-based approaches include silica coated beads that possess the ability to bind nucleic acids non-specifically in the presence of a chaotropic agent. The most common approach using silica coated paramagnetic beads involves immobilization of beads within a microfluidic channel using an external magnetic field with sample solutions and washing buffers flowing over the beads. Once the capture and washing steps are complete, the magnetic field is removed to allow elution of the beads in an elution buffer [341]. In other examples the solution is maintained stationary and the beads directed through the solution via application of a magnetic field. The beads are then

exchanged from the sample solution into buffer solutions [344,345]. There are also examples of silica coated paramagnetic bead-based isolation techniques integrated within μTAS [342]. Alternatives to silica coating include the use of electrical charge to selectively capture negatively charged nucleic acids. This is accomplished by coating the beads with a multivalent cationic polymer like polyethyleneimine which is positively charged at low pH. The sample is introduced into the microfluidic device where beads are immobilized in a low pH solution for capture, following capture, the solution is washed and then a higher pH elution buffer is used to collect the captured nucleic acids [346,347]. This approach has been shown to be highly effective for low abundance nucleic acids and has been integrated within μTAS [343]. Finally, isolation of mRNA can also be accomplished using non-specific probes such as oligo-dT which binds to the polyadenosine tail. This technique provides a degree of specificity in isolating only mRNA sequences and the combination of this approach with paramagnetic beads can be scaled up as the beads are not saturated with non-specific nucleic acids [348,349]. This approach can potentially be of great value when probing cell-free mRNA released from tumor cells into circulation. If the target nucleic acid sequence is known, then specific oligonucleotide sequences can be generated and functionalized into paramagnetic beads to enable capture of desired targets [340,350,351]. The only drawback of this approach is the fact that there needs to be prior knowledge regarding the target sequences.

Microfluidic devices with functionalized surfaces have also been used for capture of nucleic acids. Depending on the type of material used to construct the microfluidic device, these approaches can vary. Silicon and glass have been commonly used for fabrication of microfluidic devices but are expensive. Cheaper alternatives include

various polymeric materials that have already been shown to be effective for nucleic acid isolation including polycarbonate (PC) [352], (poly) dimethyl siloxane (PDMS) and polymethylmethacrylate (PMMA). Surface modifications can either be accomplished via simple adsorption, covalent cross-linking or deposition. Examples of coatings used for nucleic acid capture include oligonucleotides [353-355], chitosan [356,357], aluminum oxide [358,359], activated polycarbonate [360,361] and amines [362].

4.3.2. Microfluidic Liquid Phase Extraction

Liquid phase extraction refers to techniques that do not utilize probes to capture nucleic acids, rather, nucleic acids are selectively trapped or migrated based on their response to an applied electric field or specific solution chemistry. Both electrophoresis (EP) and dielectrophoresis (DEP) have been used to selectively migrate or trap negatively charged nucleic acids to separate them from positively charged contaminants. DEP is primarily used for trapping and has been used with the commercially available Nanogen platform that exploits the polarizability of nucleic acids to trap chromatin from lysed cells using an alternating field and then using a direct current field to remove contaminants [363,364]. Gel electrophoresis within microfluidic channels has been used to separate nucleic acids based on their differences in length [365]. Nucleic acids fractionated using this approach can be extracted as it exits the gel using buffer solutions. Another approach that exploits charge is isotachophoresis where a two buffer system containing a leading and trailing electrolyte with electrophoretic mobility higher and lower than the nucleic acids respectively. When an electric field is applied, the nucleic acids migrate to the interface where the field gradient exists away from the impurities. Microfluidic adaptation of this approach has been successfully validated for isolation of DNA from lysed blood samples

[366-369]. While charge based approaches are effective and can result in highly pure nucleic acid samples, they are more complex in terms of both device fabrication and device operation. The throughput may also be limited and their integration with μTAS may be more complicated.

Liquid phase extraction using organic solvents like phenol-chloroform extraction is a commonly used macroscale approach to exploit aqueous and organic phases to enable partitioning of biomolecules into energetically favorable locations. Following cellular lysis, biomolecules including cellular debris and proteins fractionate into the organic phase leaving nucleic acids in the organic phase. This approach has been adapted within a microfluidic platform which allows automated metering and collection of the two phases which can then be processed on-chip for subsequent amplification and detection [353,370]. The purity of nucleic acids attainable using this approach is very high but there are also issues involving the use of hazardous solvents which make operation and disposal a problem.

Given that circulating cell-free DNA and RNA are not aggressively being pursued as markers to monitor cancer, there have not been many efforts to develop microfluidic devices to isolate and evaluate circulating cell-free nucleic acids. However, recent literature suggests that both cell-free DNA and RNA may contain important prognostic and diagnostic information that can be harnessed to monitor, stage and treat cancer. This section summarizes microfluidic approaches for capture of nucleic acids and any of these approaches can be adopted and modified to process blood liquid biopsies. There may be some sample pre-processing that needs to be accomplished prior to nucleic acid

isolation. We also refer you to recent reviews by Ansari et al. [371] and Bruijins et al. [372] that provide greater detail on microfluidic approaches for isolation and analysis of nucleic acids.

5. Future Directions

Miniaturization offers advantages over conventional approaches and can enable completely new separation methods not possible using macroscale techniques. Despite these obvious advantages, adoption of microfluidics based approaches for clinical or commercial applications has not been widespread. This can be attributed to the complexities associated with translating laboratory prototypes to pre-clinical or clinical devices and the reluctance of users to adopt new and unfamiliar technologies. Prior to pursuing a microfluidics option, it is important to ask the following questions **(1)** Is there a critical or unmet clinical need? **(2)** Will this problem benefit significantly from miniaturization? **(3)** Can this process be performed reliably and consistently in the clinical setting? **(4)** Can the miniaturized protocol be automated with minimal user intervention? As long as the answer to the first two questions is 'yes' and the answer to the third and fourth questions are not 'no', it is worth the time and effort to develop microfluidic options to address the particular problem.

For cancer diagnostics, the answer to the first two questions is 'yes' and recent progress in CTC and exosome isolation suggest that the answer to both questions three and four is 'highly probable'. Isolation of CTCs for example has been likened to 'finding a needle in a haystack' where the need is to develop technologies to find 1-10 cells in 10 mL of blood, 1 in 1 X 10^9 RBCs or 1 in 1 X 10^7 WBCs. This is a problem that

conventional macroscale approaches cannot address in a reliable fashion with consistently high levels of purity and efficiency. Another critical issue is the biomarkers used to classify and isolate CTCs and exosomes. CTCs and exosomes are highly heterogeneous populations and expression of various cell surface and intracellular markers are reflective of various factors including the physiology of the individual, organ/tissue of origin, interaction with the local microenvironment, location within the primary tumor, stage of the tumor, mechanisms that enabled release into circulation, their interaction with other cellular and biomolecular components in blood. Therefore it is important to understand that biomarker selection is critical and can dictate the success of the type of separation process in demonstrating clinical benefit. Microfluidic approaches have shown clear superiority where miniaturization and unique flow phenomena have been exploited to isolate CTCs in numbers not possible using conventional methods. This high sensitivity in terms of being able to probe low-abundance targets comes at the cost of throughput and purity. Most CTC platforms have high efficiency (ratio of captured target cells to target cells in the sample) but there is also an increase in non-specific binding of leukocytes. Profiling of cells contained in small volumes adversely affects throughput and this can be a major issue with CTC profiling as sometimes ~ 50 mL of blood needs to be processed to obtain a significant number of cancer cells for analysis. To address the issue of throughput, integrating multiple smaller devices in a massively parallel fashion has been proposed. This however is a challenge and care needs to be taken to ensure that there is a high-level of consistency between devices integrated in parallel. Other options include sample pre-processing to de-bulk the initial sample of contaminating cells. Any technique seeking to address CTC isolation must understand and provide solutions that can address issues with processing of 10s of mLs of sample in

a relatively quick time. Techniques like density gradient centrifugation or even inertial focusing have been used to separate out red blood cells from the samples to provide highly de-bulked samples that contain CTCs at higher concentrations and are easier to process. The disadvantages include the time and effort to de-bulk the samples and additional opportunities to lose already rare CTCs during processing. The issue of non-specific binding can be partially addressed by using appropriate blocking strategies with surface functionalization using proteins (albumin) or cell repulsive compounds like (polyethylene glycol or pluoronic). Important parameters to be considered include functionalization density and anchorage mechanism which can greatly affect their function and utility. Addressing or overcoming issues related to purity and throughput and increasing numbers of captured intact CTCs is the key to addressing important gaps in knowledge. Given the multitude of uses of intact CTCs in early diagnosis, longitudinal monitoring of patients, drug testing and developing patient specific therapeutics, there are a large number of companies developing CTC isolation kits. A majority of these companies have adopted microfluidics-based approaches [36,40,43,44,78-81] and are faced with the challenge of addressing concerns with throughput and purity.

Microfluidic isolation of exosomes faces similar challenges to those associated with CTC isolation, however, the number of exosomes is significantly larger than CTCs and issues concerning throughput are minimal. Given the success of conventional macroscale approaches in isolating intact exosomes, microfluidic approaches may need to focus on isolation and quantification of cancer specific exosomes which are available at lower frequencies and where microfluidic advantages associated with interrogation of samples in small volumes is a significant advantage. While microfluidics may not have significant

benefit over conventional approaches when it comes to unbiased evaluation of exosomes in serum, microfluidics certainly has an advantage when it comes to identification cancer cell-associated exosomes with specific surface markers. Microfluidic approaches can be used to accomplish rapid and highly efficient identification with opportunities to integrate further analytical complexity downstream including lysis and extraction of nucleic acids, proteins, metabolites and lipids. An area that needs to be addressed is the sample pre-processing to rapidly remove cellular components and abundant proteins from plasma without loss of exosomes. Currently, the use of exosomes for cancer diagnostics is still in the early stages and significant work needs to be done prior to use of exosomes or exosomal contents for diagnosis or patient monitoring. As a result, there are not many efforts to commercialize platforms for exosome isolation for cancer. Examples discussed in this review clearly demonstrate that there is great potential for microfluidic approaches and with advances in our understanding of exosome cancer biology and advancements in microfluidic separations, it is only a matter of time before commercially available exosome based cancer screening assays become available.

A variety of microfluidic techniques for capture and isolation of nucleic acids were discussed in this review and clearly establish that microfluidic adaptation can accomplish both specific and non-specific capture of target nucleic acids in a highly efficient and rapid fashion. Microfluidics provide two unique advantages: **(1)** integration of nucleic acid capture within μTAS to accomplish cell capture, lysis, nucleic acid isolation, amplification, quantification, and detection all on a single platform for point-of-care applications, and **(2)** The ability to isolate low-abundance nucleic acids found in circulation or in a single cell at high efficiency. While there are several examples of

integrated devices, the integration of different components is not always seamless and operation of these devices may also be complicated. Regardless, with advancements in technologies to design and fabricate microfluidic devices will provide unique tools to probe low-abundance nucleic acids efficiently and rapidly. As with exosomes, there is limited knowledge regarding cell-free DNA and RNA and how they can be exploited for cancer diagnostics and monitoring. There are already a handful of companies offering tests to probe cell-free tumor cell DNA and it appears that with new knowledge regarding the relevance of these markers, that the number of applications will expand rapidly and microfluidics-based approaches will become essential for point-of-care translation.

As mentioned earlier, a major concern with microfluidics-based approaches is the poor rate of translation of promising technologies to the research or clinical setting and ultimately commercialization. Particularly in the area of cellular and biomolecular separations, it is rather surprising that microfluidics-based approaches have not supplanted conventional approaches given the advantages of microfluidics-based technologies. In reviewing literature, there appears to be a large disparity between the numbers of new microfluidics technologies being developed versus those actually undergoing commercialization or clinical translation. To achieve commercialization, it may be beneficial to learn prior shortcomings. Shields et al. [373] present a comprehensive review detailing the challenges with translation of microfluidics-based approaches for cell sorting including **(a)** Changing from a mindset where we develop technologies and then search for an application to a mindset where we design new approaches based on a critical unmet need, **(b)** creating user-friendly interfaces that can enable ease of operation of complex microfluidic devices, minimizing the need for initial setup for smooth

translation as a commercial product, **(c)** developing modular solutions and standardized manufacturing to address the cost and volume issues necessary for successful commercialization, and **(d)** adopting aggressive strategies to protect intellectual property and efficient marketing new technologies. For other applications, conventional technologies may provide a comparable solution; but in the case of cancer monitoring, the low abundance of target species necessitates successful translation of microfluidics based approaches to accomplish better treatment options and disease management. Therefore, it is critical that these issues be carefully considered prior to development of new technologies to enable smooth and rapid translation to the research and clinical setting.

7. Acknowledgements

Our research program is supported by an NSF CAREER award, grant # 1149059 and an NIH R21 grant # EB020282.

FIGURE LEGENDS.

Figure 1: Schematic highlighting progression of cancer and presence of cancer cells and cell-derived products in blood circulation and the use of microfluidics-based approaches to process liquid biopsies from patient's blood and enable isolation of specific targets which can then be used for a wide array f processes that can impact screening, diagnostics, prognostics and treatment of patients.

Figure 2: Examples of microfluidic devices for immuno-affinity based capture of CTCs. **(A)** CTC chip: the first example of a microfluidic device for isolation of CTCs from blood [204]. **(A1)** Complete setup for delivery of blood samples to the CTC chip, **(A2)** Pressure source which drives fluid flow, **(A3)** CTC chip with blood perfusing the chip, and **(A4)** Picture of micromachined posts with captured CTC. **(B)** Herringbone Chip: Demonstration of how efficient mixing can enhance interaction of CTCs with capture surfaces [208]. **(B1)** Herringbone chip perfused with blood, **(B2)** Design and placement of herringbone structures within the microfluidic channel, **(B3)** Schematic demonstrating rotational fluid flow within the microfluidic channels, and **(B4)** Simulation of fluid flow within the channels. **(C)** CTC-iChip: Example of how multiple separation mechanisms can be integrated together on a single platform to de-bulk samples and enable efficient separation [217].

Figure 3: Examples of microfluidic devices for label-free capture of CTCs. **(A)** Filtration: Exploiting size differences to ensure separation of CTCs based on differences in size and deformability [228]. **(A1)** Microscopic images of flexible spring microarrays that are used for exosome capture, and **(A2)** Actual setup including a schematic of the various

components of the capture system. **(B)** Spiral Devices: Demonstration of the use of inertial focusing within microfluidic channels to enable size based separation of cancer cell lines from other blood cells [237]. **(B1)** Design and mechanism of separation of cells and particles using spiral microchannels, and **(B2)** Actual devices and workflow for processing of samples for CTC isolation. **(C)** Surface Energy: Using differences in cell surface energy to enable initial phase partitioning and the initial separation is enhanced via inertial forces [245,246]. **(C1)** Schematic of the device for inertia enhanced phase partitioning, **(C2)** Actual fabricated device and **(C3)** Setup for operation of the device.

Figure 4: Examples of microfluidic devices for isolation of exosomes: **(A)** Herringbone Chip: The herringbone chip was the first demonstration of microfluidics to isolate exosomes. Capture was accomplished using affinity of exosomes to specific antibodies immobilized within the device [299]. **(B)** Ciliated Structures: Ciliated structures exploit size difference between exosomes and cells in blood to enable selective trapping of exosomes for subsequent isolation [311]. **(B1)** Schematic demonstrating the process of size exclusion and capture using ciliated structures, and **(B2)** High magnification images of the posts with ciliated structures including and image of exosomes captured on the structures.

Table Legends:

Table1: Summary of **(A)** microfluidic immuno-affinity based and **(B)** label-free approaches for isolation of circulating tumor cells (CTCs). **Note:** Table is organized based on reported capture efficiency.

Table 2: Summary of microfluidic techniques for isolation of exosomes for diagnosis and evaluation of cancer. **Note:** Table is organized based on reported capture efficiency.

Table 3: Summary of microfluidic approaches for isolation of nucleic acids. **Note:** Table is organized based on reported sensitivity of the approach.

Figure 1:

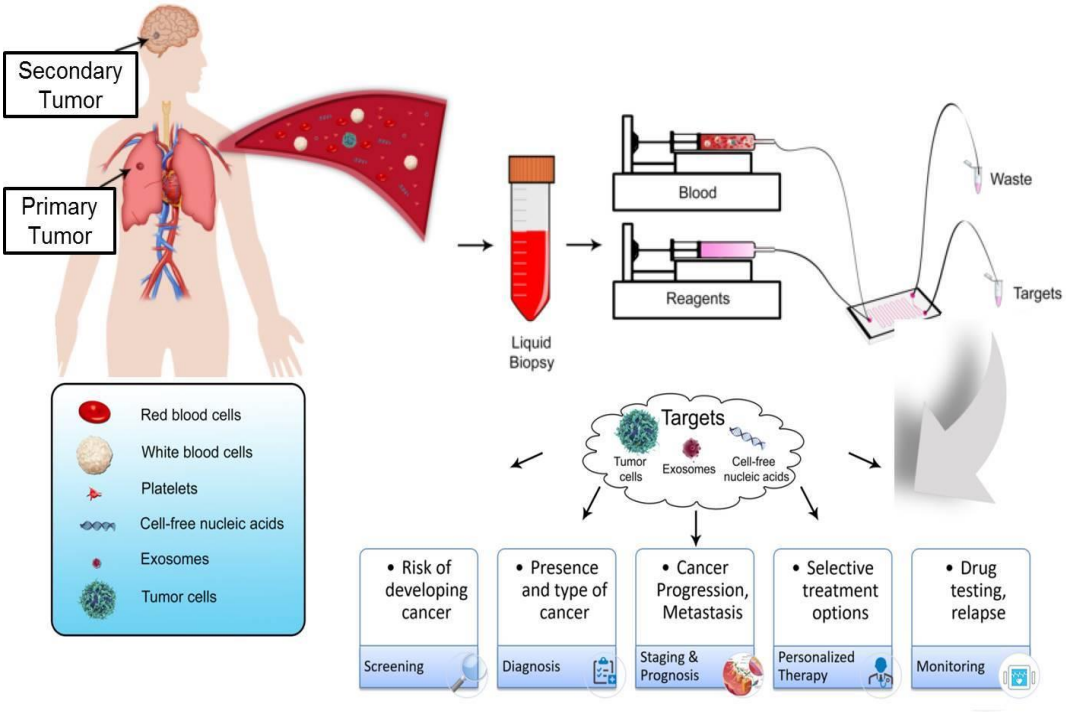
Secondary Tumor
Primary Tumor
Red blood cells
White blood cells
Platelets
Cell-free nucleic acids
Exosomes
Tumor cells
Liquid Biopsy
Blood
Reagents
Waste
Targets
Targets
Tumor cells
Exosomes
Cell-free nucleic acids
• Risk of developing cancer
Screening
• Presence and type of cancer
Diagnosis
• Cancer Progression, Metastasis
Staging & Prognosis
• Selective treatment options
Personalized Therapy
• Drug testing, relapse
Monitoring

Figure 2:

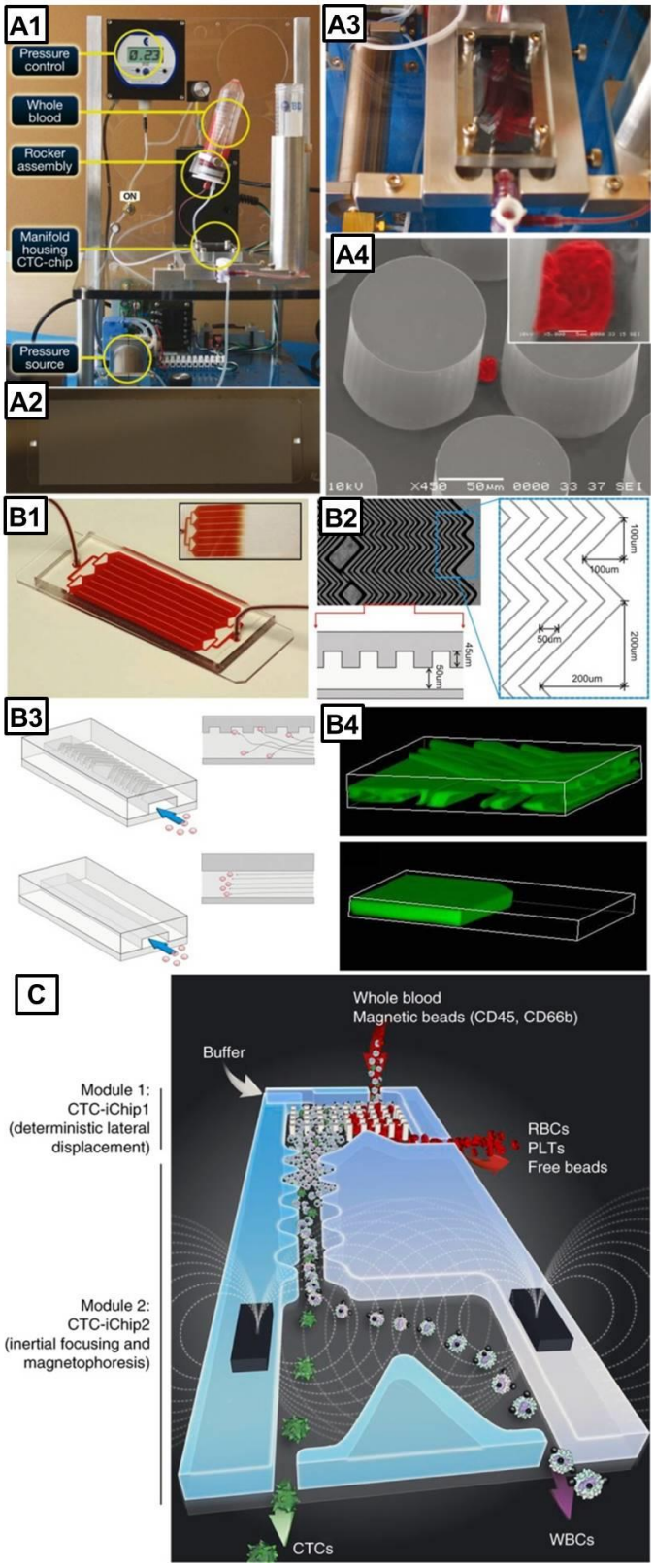
A1
Pressure control
Whole blood
Rocker assembly
Manifold housing CTC-chip
Pressure source
A2
A3
A4
B1
B2
100um
100um
50um
200um
200um
45um
50um
B3
B4
C
Whole blood
Magnetic beads (CD45, CD66b)
Buffer
Module 1: CTC-iChip1 (deterministic lateral displacement)
RBCs
PLTs
Free beads
Module 2: CTC-iChip2 (inertial focusing and magnetophoresis)
CTCs
WBCs

Figure 3:

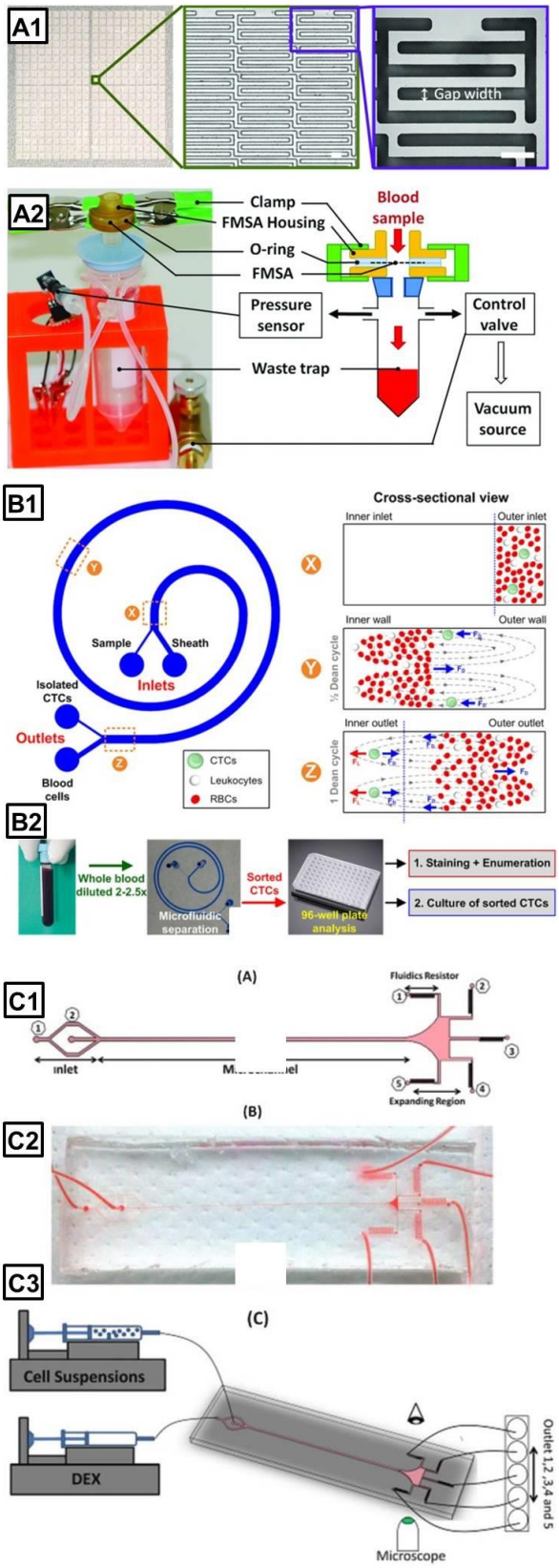
A1
Gap width
A2
Clamp
FMSA Housing
O-ring
FMSA
Blood sample
Pressure sensor
Control valve
Waste trap
Vacuum source
B1
Cross-sectional view
Inner inlet
Outer inlet
Inner wall
Outer wall
Inner outlet
Outer outlet
½ Dean cycle
1 Dean cycle
Sample
Sheath
Inlets
Isolated CTCs
Outlets
Blood cells
CTCs
Leukocytes
RBCs
B2
Whole blood diluted 2-2.5x
Microfluidic separation
Sorted CTCs
96-well plate analysis
1. Staining + Enumeration
2. Culture of sorted CTCs
C1
(A)
Fluidics Resistor
Inlet
Expanding Region
(B)
C2
C3
(C)
Cell Suspensions
DEX
Outlet 1,2 ,3,4 and 5
Microscope

Figure 4:

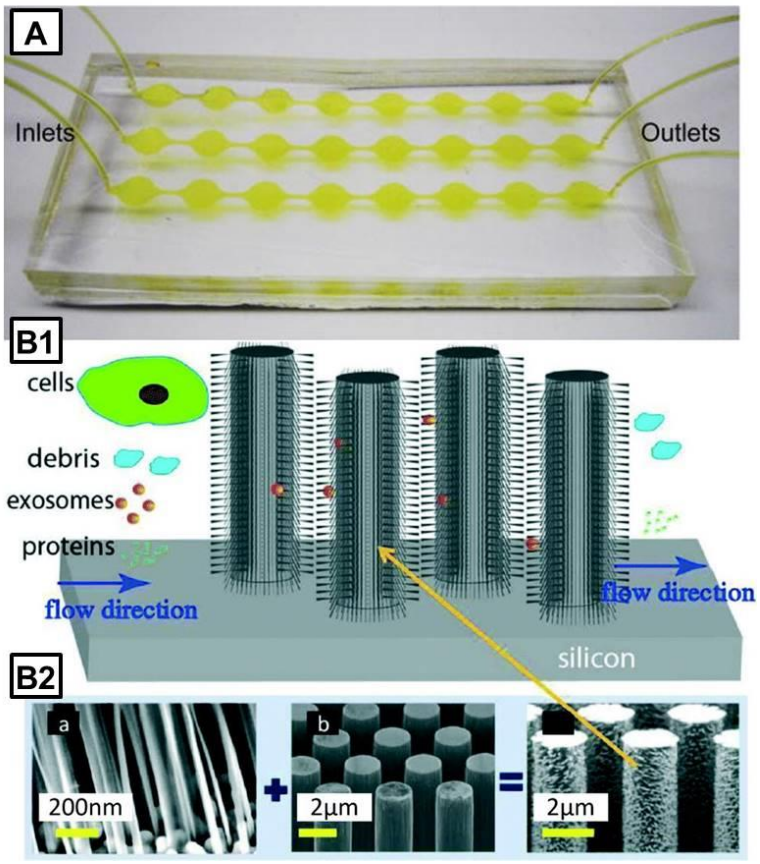
A
Inlets
Outlets
B1
cells
debris
exosomes
proteins
flow direction
flow direction
silicon
B2
a
200nm
b
2µm
2µm

Table 1 (A-B)

Circulating Tumor Cells (Antibody based approaches)

Authors	Description of Method	Sensitivity	Purity	Downstream Clinical Application
Nagrath et al. [204]	EpCam antibody and microposts rocking chip	99%	50%	Epithelially derived cancer detection, diagnosis, and monitoring
Adams et al. [211]	High throughput microsampling unit and EpCAM antigen	97%	>99%	Epithelially derived cancer detection, diagnosis, and monitoring
Stott et al. [208]	Herringbone-Chip microfluidic mixing and EpCAM antigen	93%	14%	Epithelially derived cancer detection, diagnosis, and monitoring
Reátegui et al. [213]	Gelatine nanocoating, microfluidic mixing, EpCam, EGFR, and HER2 antigens	93%	80%	CTC detection, diagnosis, and monitoring
Murlidhar et al. [207]	Radial flow mixing with bean-shaped microposts and EpCAM antigen	93%	-	Epithelially derived cancer detection, diagnosis, and monitoring
Sheng et al. [209]	GEM microfluidic mixing and EpCAM antigen	90%	80%	Epithelially derived cancer detection, diagnosis, and monitoring
Ozkumur et al. [218]	CTC-iChip system. Inertial focusing, antigen coated magnetic bead sorting, cell size sorting	90%	98%	CTC enrichment and quantification
Gleghorn et al. [206]	GEDI chip: Microfluidic mixing and prostate-specific membrane antigen	85%	68%	Diagnosis and monitoring prostate cancer progressiong
Allard et al. [374]	CELLSEARCH: ferrofluid antibody enrichement	85%	Low	Outcome diagnostic for epithelial derived cancers
Yoon et al. [212]	Graphene oxide nanosheets and EpCAM antigen	73%	-	Epithelially derived cancer detection, diagnosis, and monitoring
Ke et al. [214]	Microfluidic and thermoresponsive anti-EpCAM adhesion	70%	35%	Epithelially derived cancer detection, diagnosis, and monitoring

Circulating Tumor Cells (Antibody free approaches)

Authors	Description of Method	Sensitivity	Purity	Downstream Clinical Application
Warkiani et al. [241]	Centrifugal throughput, Dean's drag, and inertial lift	100%	80%	CTC detection and analysis
Sollier et al. [242]	Micro-scale vortices and inertial focusing	100%	57-94%	CTC detection and analysis
Ding et al. [247]	Acoustic wave focusing	99%	83%	CTC enrichment and quantification
Gupta et al. [249]	Dielectrophoretic field-flow fractionation	99%	73%	CTC detection and analysis

Parichehreh et al. [246]	Inertial focusing	>95%	>99%	CTC enumeration
Hou et al. [237]	Centrifugal throughput, Dean's drag, and inertial lift	93%	85%	CTC detection and analysis
Ozkumur et al. [218]	CTC-iChip system. Inertial focusing, antigen coated magnetic bead sorting, cell size sorting	90%	98%	CTC enrichment and quantification
Harouaka et al. [228]	Micro spring array	90%	10^4 enrichment	CTC enrichment and quantification
Sun et al. [238]	Dean's drag and inertial lift	89%	-	CTC quantification

Table 2:

Exosomes

Authors	Description of Method	Sensitivity	Purity	Sample
Shao et al. [306]	Immunomagnetic beads (Exo chip)	90%	-	Exosome isolation from plasma sample
Liang et al. [375]	Filtration	81%	90%	Exosome isolation from urine sample and cell culture medium
Liu et al. [314]	Viscoelastic flow	>80%	>90%	Exosome isolation from cell culture medium
Lee et al. [310]	acoustic force	>80%	-	Exosome isolation from cell culture medium
Chen et al. [299]	Immunoaffinity	42-94%	-	Exosome isolation from serum sample
Zhao et al. [274]	Immunomagnetic beads	42-97%	-	Exosome isolation from plasma sample
Wang et al. [311]	filtration through nanowires	45-60%	-	Liposome isolation from water/PBS
Santana et al. [312]	filtration through microarrays based on the principle of deterministic lateral displacement	39%	99%	Exosome isolation from cell culture medium
He et al. [307]	immunomagnetic beads	-	-	Exosome isolation from plasma sample
Kanwar et al. [300]	Immunoaffinity	-	-	Exosome isolation from serum sample
Dudani et al. [305]	Immunobead combined with inertial force	-	-	Exosome isolation from cell culture medium

Table 3:

Cell-free nucleic acids

Authors	Description of Method	Sensitivity	Purity	Sample
Wu et al. [352]	Photoactivated polycarbonate surface	98%	-	DNA extraction from E.coli
Cao et al. [357]	pH mediated Chitosan-coated beads	75%	-	DNA extraction from lysed whole blood
Wu et al.[339]	Monolithic tetramethyl orthosilicate-based sol-gels	~70%	-	DNA extraction from lysed whole blood
Wen et al. [338]	Capillary-based photopolymerized monolith.	69%	-	DNA extraction from whole blood
Duarte et al. [341]	Magnetic silica beads in polyester microfluidic device	>65%	-	Nucleic acid extraction from lysed whole blood
Günal et al. [329]	Monodisperse-porous silica microspheres	50%	-	DNA extracted from lysed whole blood
Nakagawa et al.[362]	Amine-coated surface based on the electrostatic interaction between surface amine groups and DNA.	27-40%	-	DNA extraction from lysed whole blood
Sonnenberg et al. [368]	Dielectrophoresis.	550ng/ml from 25ul	-	Cancer related DNA isolated from whold blood directly
Zhang et al. [370]	Phenol-chloroform extraction of nucleic acid from low copy/single bacteria	10 fold higher	-	DNA isolation from P.aeruginosa
Yang et al. [369]	Electrophoretic	-	-	DNA extracted directly from blood plasma
Persat et al. [367]	Isotachnophoresis	-	-	Nucleic acid extraction from lysed whole blood
Root et al. [355]	Oligonucleotide capture matrix	-	-	RNA extraction from 10% serum sample

REFERENCES

(1) Fritsche, A.; Haring, H.; Stumvoll, M. *Dtsch Med Wochenschr* **2004**, *129*, 244-248.

(2) Erlinger, T. P.; Muntner, P.; Helzlsouer, K. J. *Cancer Epidemiol Biomarkers Prev* **2004**, *13*, 1052-1056.

(3) He, J.; Le, D. S.; Xu, X.; Scalise, M.; Ferrante, A. W.; Krakoff, J. *Eur J Endocrinol* **2010**, *162*, 275-280.

(4) Curbelo, J.; Luquero Bueno, S.; Galvan-Roman, J. M.; Ortega-Gomez, M.; Rajas, O.; Fernandez-Jimenez, G.; Vega-Piris, L.; Rodriguez-Salvanes, F.; Arnalich, B.; Diaz, A.; Costa, R.; de la Fuente, H.; Lancho, A.; Suarez, C.; Ancochea, J.; Aspa, J. *PloS one* **2017**, *12*, e0173947.

(5) Koga, H.; Miyahara, N.; Fuchimoto, Y.; Ikeda, G.; Waseda, K.; Ono, K.; Tanimoto, Y.; Kataoka, M.; Gelfand, E. W.; Tanimoto, M.; Kanehiro, A. *Respir Res* **2013**, *14*, 8.

(6) Le, N. P.; Channabasappa, S.; Hossain, M.; Liu, L.; Singh, B. *Am J Physiol Lung Cell Mol Physiol* **2015**, *309*, L995-1008.

(7) Suratannon, N.; Yeetong, P.; Srichomthong, C.; Amarinthnukrowh, P.; Chatchatee, P.; Sosothikul, D.; van Hagen, P. M.; van der Burg, M.; Wentink, M.; Driessen, G. J.; Suphapeetiporn, K.; Shotelersuk, V. *Pediatr Allergy Immunol* **2016**, *27*, 214-217.

(8) Peters, T.; Bloch, W.; Pabst, O.; Wickenhauser, C.; Uthoff-Hachenberg, C.; Schmidt, S. V.; Varga, G.; Grabbe, S.; Kess, D.; Oreshkova, T.; Sindrilaru, A.; Addicks, K.; Forster, R.; Muller, W.; Scharffetter-Kochanek, K. *Clin Dev Immunol* **2012**, *2012*, 450738.

(9) Fei, C.; Pemberton, J. G.; Lillico, D. M.; Zwozdesky, M. A.; Stafford, J. L. *Biology (Basel)* **2016**, *5*.

(10) Hajishengallis, G.; Krauss, J. L.; Jotwani, R.; Lambris, J. D. *Mol Oral Microbiol* **2017**, *32*, 154-165.

(11) Ovsyannikova, I. G.; Vierkant, R. A.; Pankratz, V. S.; Jacobson, R. M.; Poland, G. A. *J Infect Dis* **2011**, *203*, 1546-1555.

(12) Chertov, O.; Yang, D.; Howard, O. M.; Oppenheim, J. J. *Immunol Rev* **2000**, *177*, 68-78.

(13) Lobo, P. I.; Bajwa, A.; Schlegel, K. H.; Vengal, J.; Lee, S. J.; Huang, L.; Ye, H.; Deshmukh, U.; Wang, T.; Pei, H.; Okusa, M. D. *J Immunol* **2012**, *188*, 1675-1685.

(14) Michaud, D. S. *Urol Oncol* **2007**, *25*, 260-268.

(15) Shacter, E.; Weitzman, S. A. *Oncology (Williston Park)* **2002**, *16*, 217-226, 229; discussion 230-212.

(16) Manabe, I. *Circ J* **2011**, *75*, 2739-2748.

(17) Lopez-Candales, A.; Hernandez Burgos, P. M.; Hernandez-Suarez, D. F.; Harris, D. *J Nat Sci* **2017**, *3*.

(18) de Rooij, S. R.; Nijpels, G.; Nilsson, P. M.; Nolan, J. J.; Gabriel, R.; Bobbioni-Harsch, E.; Mingrone, G.; Dekker, J. M.; Relationship Between Insulin, S.; Cardiovascular Disease, I. *Diabetes Care* **2009**, *32*, 1295-1301.

(19) von Hundelshausen, P.; Weber, C. *Dtsch Med Wochenschr* **2013**, *138*, 1839-1844.

(20) van Wolfswinkel, M. E.; Langenberg, M. C. C.; Wammes, L. J.; Sauerwein, R. W.; Koelewijn, R.; Hermsen, C. C.; van Hellemond, J. J.; van Genderen, P. J. *Malar J* **2017**, *16*, 457.

(21) Jacobsen, J.; Grankvist, K.; Rasmuson, T.; Ljungberg, B. *Eur J Cancer Prev* **2002**, *11*, 245-252.

(22) Getz, G. S. *J Lipid Res* **2005**, *46*, 619-622.

(23) Barger, A. M. *Vet Clin North Am Small Anim Pract* **2003**, *33*, 1207-1222.

(24) Allan, G. M.; Young, J. *Can Fam Physician* **2017**, *63*, 772.

(25) An, X.; Chen, L. *Methods Mol Biol* **2018**, *1698*, 153-174.

(26) Galbraith, D. *Methods* **2012**, *57*, 249-250.

(27) Tzur, A.; Moore, J. K.; Jorgensen, P.; Shapiro, H. M.; Kirschner, M. W. *PloS one* **2011**, *6*, e16053.

(28) O'Connell, G. C.; Treadway, M. B.; Tennant, C. S.; Lucke-Wold, N.; Chantler, P. D.; Barr, T. L. *Translational stroke research* **2018**.

(29) Akhtar, N.; Adil, M. M.; Ahmed, W.; Habib ur, R.; Shahs, M. A. *J Pak Med Assoc* **2011**, *61*, 51-54.

(30) Jamsa, J.; Huotari, V.; Savolainen, E. R.; Syrjala, H.; Ala-Kokko, T. *J Clin Lab Anal* **2011**, *25*, 118-125.

(31) Reinhardt, M.; Bader, A.; Giri, S. *Expert review of medical devices* **2015**, *12*, 353-364.

(32) Behzad-Behbahani, A.; Yaghobi, R.; Sabahi, F.; Rostaei, M. H.; Alborzi, A. *Exp Clin Transplant* **2005**, *3*, 316-319.

(33) Zeya, H. I.; Spitznagel, J. K. *Lab Invest* **1971**, *24*, 237-245.

(34) Ellis, W. D.; Mulvaney, B. D.; Saathoff, D. J. *Prep Biochem* **1975**, *5*, 179-187.

(35) Kalmar, J. R.; Arnold, R. R.; Warbington, M. L.; Gardner, M. K. *Journal of immunological methods* **1988**, *110*, 275-281.

(36) Pelak, O.; Kuzilkova, D.; Thurner, D.; Kiene, M. L.; Stanar, K.; Stuchly, J.; Vaskova, M.; Stary, J.; Hrusak, O.; Stadler, H.; Kalina, T. *Cytometry. Part A : the journal of the International Society for Analytical Cytology* **2016**.

(37) Kuta, A. E.; Reynolds, C. R.; Henkart, P. A. *J Immunol* **1989**, *142*, 4378-4384.

(38) Takiguchi, T. *Saishin Igaku* **1972**, *27*, 598-606.

(39) Naranbhai, V.; Bartman, P.; Ndlovu, D.; Ramkalawon, P.; Ndung'u, T.; Wilson, D.; Altfeld, M.; Carr, W. H. *Journal of immunological methods* **2011**, *366*, 28-35.

(40) Zhou, L.; Somasundaram, R.; Nederhof, R. F.; Dijkstra, G.; Faber, K. N.; Peppelenbosch, M. P.; Fuhler, G. M. *Clinical and vaccine immunology : CVI* **2012**, *19*, 1065-1074.

(41) Runkel, S.; Hitzler, W. E.; Hellstern, P. *Transfusion* **2015**, *55*, 796-804.

(42) Yip, L.; Fuhlbrigge, R.; Atkinson, M. A.; Fathman, C. G. *BMC Genomics* **2017**, *18*, 636.

(43) Chernyshev, A. V.; Tarasov, P. A.; Semianov, K. A.; Nekrasov, V. M.; Hoekstra, A. G.; Maltsev, V. P. *Journal of theoretical biology* **2008**, *251*, 93-107.

(44) Cheng, X.; Gupta, A.; Chen, C.; Tompkins, R. G.; Rodriguez, W.; Toner, M. *Lab on a chip* **2009**, *9*, 1357-1364.

(45) Felix, J. S.; Doherty, R. A. *Clin Genet* **1979**, *15*, 215-220.

(46) Nieto, J. C.; Canto, E.; Zamora, C.; Ortiz, M. A.; Juarez, C.; Vidal, S. *PloS one* **2012**, *7*, e31297.

(47) Carter, C. S.; Leitman, S. F.; Cullis, H.; Muul, L. M.; Nason-Burchenal, K.; Rosenberg, S. A.; Klein, H. G. *Transfusion* **1987**, *27*, 362-365.

(48) Ferrero, D.; Tarella, C.; Cherasco, C.; Bondesan, P.; Omede, P.; Ravaglia, R.; Caracciolo, D.; Castellino, C.; Pileri, A. *Bone Marrow Transplant* **1998**, *21*, 409-413.

(49) Sethu, P.; Anahtar, M.; Moldawer, L. L.; Tompkins, R. G.; Toner, M. *Analytical chemistry* **2004**, *76*, 6247-6253.

(50) Pelegri, C.; Rodriguez-Palmero, M.; Morante, M. P.; Comas, J.; Castell, M.; Franch, A. *Journal of immunological methods* **1995**, *187*, 265-271.

(51) McCarthy, D. A.; Macey, M. G.; Cahill, M. R.; Newland, A. C. *Cytometry* **1994**, *17*, 39-49.

(52) Du, G.; Fang, Q.; den Toonder, J. M. *Analytica chimica acta* **2016**, *903*, 36-50.

(53) Shields, C. W. t.; Reyes, C. D.; Lopez, G. P. *Lab on a chip* **2015**, *15*, 1230-1249.

(54) Gazzaniga, P.; Gradilone, A.; de Berardinis, E.; Busetto, G. M.; Raimondi, C.; Gandini, O.; Nicolazzo, C.; Petracca, A.; Vincenzi, B.; Farcomeni, A.; Gentile, V.; Cortesi, E.; Frati, L. *Ann Oncol* **2012**, *23*, 2352-2356.

(55) Chen, Y.; Li, P.; Huang, P. H.; Xie, Y.; Mai, J. D.; Wang, L.; Nguyen, N. T.; Huang, T. J. *Lab on a chip* **2014**, *14*, 626-645.

(56) Gou, Y.; Jia, Y.; Wang, P.; Sun, C. *Sensors (Basel)* **2018**, *18*.

(57) Bayat, P.; Rezai, P. *Soft Matter* **2018**.

(58) Zhao, C.; Cheng, X. *Biomicrofluidics* **2011**, *5*, 32004-3200410.

(59) Chen, X.; Cui, D.; Liu, C.; Li, H.; Chen, J. *Analytica chimica acta* **2007**, *584*, 237-243.

(60) Williamson, J. D.; Sadofsky, L. R.; Crooks, M. G.; Greenman, J.; Hart, S. P. *Exp Lung Res* **2016**, *42*, 397-407.

(61) Murdoch, C.; Tazzyman, S.; Webster, S.; Lewis, C. E. *J Immunol* **2007**, *178*, 7405-7411.

(62) Campbell, J. J.; Haraldsen, G.; Pan, J.; Rottman, J.; Qin, S.; Ponath, P.; Andrew, D. P.; Warnke, R.; Ruffing, N.; Kassam, N.; Wu, L.; Butcher, E. C. *Nature* **1999**, *400*, 776-780.

(63) Kim, E.; Schueller, O.; Sweetnam, P. M. *Lab on a chip* **2012**, *12*, 2255-2264.

(64) Ley, K.; Laudanna, C.; Cybulsky, M. I.; Nourshargh, S. *Nat Rev Immunol* **2007**, *7*, 678-689.

(65) Zaslavsky, B. Y.; Uversky, V. N.; Chait, A. *Biochim Biophys Acta* **2016**, *1864*, 622-644.

(66) Soares, R. R.; Azevedo, A. M.; Van Alstine, J. M.; Aires-Barros, M. R. *Biotechnology journal* **2015**, *10*, 1158-1169.

(67) Cabral, J. M. *Adv Biochem Eng Biotechnol* **2007**, *106*, 151-171.

(68) Hatti-Kaul, R. *Mol Biotechnol* **2001**, *19*, 269-277.

(69) Bras, E. J. S.; Soares, R. R. G.; Azevedo, A. M.; Fernandes, P.; Arevalo-Rodriguez, M.; Chu, V.; Conde, J. P.; Aires-Barros, M. R. *J Chromatogr A* **2017**, *1515*, 252-259.

(70) Vazquez-Villegas, P.; Ouellet, E.; Gonzalez, C.; Ruiz-Ruiz, F.; Rito-Palomares, M.; Haynes, C. A.; Aguilar, O. *Lab on a chip* **2016**, *16*, 2662-2672.

(71) Byeon, Y.; Ki, C. S.; Han, K. H. *Biomedical microdevices* **2015**, *17*, 118.

(72) Aghazarian, A.; Stancik, I.; Huf, W.; Pfluger, H. *Urology* **2015**, *86*, 52-56.

(73) Schafer, D.; Dressen, P.; Brettner, S.; Rath, N. F.; Molderings, G. J.; Jensen, K.; Ziemann, C. *Journal of translational medicine* **2014**, *12*, 213.

(74) Wojcik, M.; Zieleniak, A.; Zurawska-Klis, M.; Cypryk, K.; Wozniak, L. A. *Experimental biology and medicine (Maywood, N.J.)* **2016**, *241*, 457-465.

(75) Hashemian, A. M.; Ahmadi, K.; Zamani Moghaddam, H.; Zakeri, H.; Davoodi Navakh, S. A.; Sharifi, M. D.; Bahrami, A. *Iranian Red Crescent medical journal* **2015**, *17*, e21341.

(76) Wang, H.; Xu, L.; Lu, L. *Journal of fish diseases* **2016**, *39*, 155-162.

(77) Mariucci, S.; Rovati, B.; Manzoni, M.; Della Porta, M. G.; Comolli, G.; Delfanti, S.; Danova, M. *Clinical and experimental medicine* **2011**, *11*, 199-210.

(78) Mitroulis, I.; Alexaki, V. I.; Kourtzelis, I.; Ziogas, A.; Hajishengallis, G.; Chavakis, T. *Pharmacology & therapeutics* **2015**, *147*, 123-135.

(79) Brosseron, F.; Marcus, K.; May, C. *Methods in molecular biology (Clifton, N.J.)* **2015**, *1295*, 33-42.

(80) Newton, R. A.; Thiel, M.; Hogg, N. *Journal of leukocyte biology* **1997**, *61*, 422-426.

(81) Bhuvanendran Nair Gourikutty, S.; Chang, C. P.; Puiu, P. D. *Journal of chromatography. B, Analytical technologies in the biomedical and life sciences* **2016**, *1011*, 77-88.

(82) Chen, G. D.; Fachin, F.; Colombini, E.; Wardle, B. L.; Toner, M. *Lab on a chip* **2012**, *12*, 3159-3167.

(83) Chen, W.; Huang, N. T.; Oh, B.; Lam, R. H.; Fan, R.; Cornell, T. T.; Shanley, T. P.; Kurabayashi, K.; Fu, J. *Advanced healthcare materials* **2013**, *2*, 965-975.

(84) Li, X.; Chen, W.; Liu, G.; Lu, W.; Fu, J. *Lab on a chip* **2014**, *14*, 2565-2575.

(85) Xiang, N.; Ni, Z. *Biomedical microdevices* **2015**, *17*, 110.

(86) Darabi, J.; Guo, C. *Biomedical microdevices* **2016**, *18*, 77.

(87) Ding, X.; Peng, Z.; Lin, S. C.; Geri, M.; Li, S.; Li, P.; Chen, Y.; Dao, M.; Suresh, S.; Huang, T. J. *Proceedings of the National Academy of Sciences of the United States of America* **2014**, *111*, 12992-12997.

(88) Grenvall, C.; Magnusson, C.; Lilja, H.; Laurell, T. *Analytical chemistry* **2015**, *87*, 5596-5604.

(89) Zhu, H.; Lin, X.; Su, Y.; Dong, H.; Wu, J. *Biosensors & bioelectronics* **2015**, *63*, 371-378.

(90) Al-Faqheri, W.; Thio, T. H. G.; Qasaimeh, M. A.; Dietzel, A.; Madou, M. *Microfluidics and Nanofluidics* **2017**, *21*, 102.

(91) Balter, M. L.; Chen, A. I.; Colinco, C. A.; Gorshkov, A.; Bixon, B.; Martin, V.; Fromholtz, A.; Maguire, T. J.; Yarmush, M. L. *Analytical methods : advancing methods and applications* **2016**, *8*, 8272-8279.

(92) Yu, Z. T. F.; Joseph, J. G.; Liu, S. X.; Cheung, M. K.; Haffey, P. J.; Kurabayashi, K.; Fu, J. *Sensors and Actuators B: Chemical* **2017**, *245*, 1050-1061.

(93) Ramachandraiah, H.; Amasia, M.; Cole, J.; Sheard, P.; Pickhaver, S.; Walker, C.; Wirta, V.; Lexow, P.; Lione, R.; Russom, A. *Lab on a chip* **2013**, *13*, 1578-1585.

(94) Walsh III, D. I.; Sommer, G. J.; Schaff, U. Y.; Hahn, P. S.; Jaffe, G. J.; Murthy, S. K. *Lab on a chip* **2014**, *14*, 2673-2680.

(95) Schaff, U. Y.; Sommer, G. J. *Clinical chemistry* **2011**, *57*, 753-761.

(96) Zhang, J.; Guo, Q.; Liu, M.; Yang, J. *Journal of micromechanics and microengineering* **2008**, *18*, 125025.

(97) Kinahan, D. J.; Kearney, S. M.; Glynn, M. T.; Ducrée, J. *Sensors and Actuators A: Physical* **2014**, *215*, 71-76.

(98) Kinahan, D. J.; Kearney, S. M.; Kilcawley, N. A.; Early, P. L.; Glynn, M. T.; Ducrée, J. *PloS one* **2016**, *11*, e0155545.

(99) Moen, S. T.; Hatcher, C. L.; Singh, A. K. *PloS one* **2016**, *11*, e0153137.

(100) Ukita, Y.; Oguro, T.; Takamura, Y. *Biomedical microdevices* **2017**, *19*, 24.

(101) Patibandla, P. K.; Rogers, A. J.; Giridharan, G. A.; Pallero, M. A.; Murphy-Ullrich, J. E.; Sethu, P. *Analytical chemistry* **2014**, *86*, 10948-10954.

(102) Arras, M.; Ito, W. D.; Scholz, D.; Winkler, B.; Schaper, J.; Schaper, W. *J Clin Invest* **1998**, *101*, 40-50.

(103) Hersh, E. M.; Butler, W. T.; Rossen, R. D.; Morgan, R. O.; Suki, W. *J Immunol* **1971**, *107*, 571-578.

(104) Mellembakken, J. R.; Aukrust, P.; Olafsen, M. K.; Ueland, T.; Hestdal, K.; Videm, V. *Hypertension* **2002**, *39*, 155-160.

(105) Feezor, R. J.; Baker, H. V.; Mindrinos, M.; Hayden, D.; Tannahill, C. L.; Brownstein, B. H.; Fay, A.; MacMillan, S.; Laramie, J.; Xiao, W.; Moldawer, L. L.; Cobb, J. P.; Laudanski, K.; Miller-Graziano, C. L.; Maier, R. V.; Schoenfeld, D.; Davis, R. W.; Tompkins, R. G.; Inflammation; Host Response to Injury, L.-S. C. R. P. *Physiol Genomics* **2004**, *19*, 247-254.

(106) Fukuda, S.; Yasu, T.; Predescu, D. N.; Schmid-Schonbein, G. W. *Circ Res* **2000**, *86*, E13-18.

(107) Gibson, G. *Nat Rev Genet* **2008**, *9*, 575-581.

(108) Frank, R. S. *Blood* **1990**, *76*, 2606-2612.

(109) Jude, B.; Agraou, B.; McFadden, E. P.; Susen, S.; Bauters, C.; Lepelley, P.; Vanhaesbroucke, C.; Devos, P.; Cosson, A.; Asseman, P. *Circulation* **1994**, *90*, 1662-1668.

(110) Krutmann, J.; Kirnbauer, R.; Kock, A.; Schwarz, T.; Schopf, E.; May, L. T.; Sehgal, P. B.; Luger, T. A. *J Immunol* **1990**, *145*, 1337-1342.

(111) von Bonin, A.; Huhn, J.; Fleischer, B. *Immunol Rev* **1998**, *161*, 43-53.

(112) Dubois, N. C.; Craft, A. M.; Sharma, P.; Elliott, D. A.; Stanley, E. G.; Elefanty, A. G.; Gramolini, A.; Keller, G. *Nat Biotechnol* **2011**, *29*, 1011-1018.

(113) Hofland, L. J.; van Koetsveld, P. M.; Verleun, T. M.; Lamberts, S. W. *Acta Endocrinol (Copenh)* **1989**, *121*, 270-278.

(114) Li, S. H.; Liao, X.; Zhou, T. E.; Xiao, L. L.; Chen, Y. W.; Wu, F.; Wang, J. R.; Cheng, B.; Song, J. X.; Liu, H. W. *Ann Plast Surg* **2017**, *78*, 83-90.

(115) English, D.; Andersen, B. R. *J Immunol Methods* **1974**, *5*, 249-252.

(116) Helms, C. C.; Marvel, M.; Zhao, W.; Stahle, M.; Vest, R.; Kato, G. J.; Lee, J. S.; Christ, G.; Gladwin, M. T.; Hantgan, R. R.; Kim-Shapiro, D. B. *J Thromb Haemost* **2013**, *11*, 2148-2154.

(117) Weber, C.; Erl, W.; Weber, P. C. *Biochem Biophys Res Commun* **1995**, *206*, 621-628.

(118) Sethu, P.; Moldawer, L. L.; Mindrinos, M. N.; Scumpia, P. O.; Tannahill, C. L.; Wilhelmy, J.; Efron, P. A.; Brownstein, B. H.; Tompkins, R. G.; Toner, M. *Anal Chem* **2006**, *78*, 5453-5461.

(119) Sun, Y.; Sethu, P. *Bioengineering (Basel)* **2017**, *4*.

(120) Kinahan, D. J.; Kearney, S. M.; Kilcawley, N. A.; Early, P. L.; Glynn, M. T.; Ducree, J. *PloS one* **2016**, *11*, e0155545.

(121) Parichehreh, V.; Estrada, R.; Kumar, S. S.; Bhavanam, K. K.; Raj, V.; Raj, A.; Sethu, P. *Biomedical microdevices* **2011**, *13*, 453-462.

(122) Parichehreh, V.; Medepallai, K.; Babbarwal, K.; Sethu, P. *Lab on a chip* **2013**, *13*, 892-900.

(123) Parichehreh, V.; Sethu, P. *Lab on a chip* **2012**, *12*, 1296-1301.

(124) Amasia, M.; Madou, M. *Bioanalysis* **2010**, *2*, 1701-1710.

(125) Burger, R.; Ducree, J. *Expert Rev Mol Diagn* **2012**, *12*, 407-421.

(126) Siegel, R. L.; Miller, K. D.; Jemal, A. *CA Cancer J Clin* **2017**, *67*, 7-30.

(127) Miller, K. D.; Siegel, R. L.; Lin, C. C.; Mariotto, A. B.; Kramer, J. L.; Rowland, J. H.; Stein, K. D.; Alteri, R.; Jemal, A. *CA Cancer J Clin* **2016**, *66*, 271-289.

(128) Pantel, K.; Alix-Panabières, C. *Cancer research* **2013**, *73*, 6384-6388.

(129) Crowley, E.; Di Nicolantonio, F.; Loupakis, F.; Bardelli, A. *Nature reviews Clinical oncology* **2013**, *10*, 472-484.

(130) Chen, W.; Yanming, L.; Xiangdong, F. *Yi Chuan* **2017**, *39*, 220-231.

(131) Siravegna, G.; Marsoni, S.; Siena, S.; Bardelli, A. *Nat Rev Clin Oncol* **2017**.

(132) Alix-Panabières, C.; Pantel, K. *Clinical chemistry* **2013**, *59*, 110-118.

(133) Alix-Panabières, C.; Pantel, K. *Cancer discovery* **2016**, *6*, 479-491.

(134) Berghuis, A. M.; Koffijberg, H.; Prakash, J.; Terstappen, L. W.; MJ, I. J. *Int J Mol Sci* **2017**, *18*.

(135) Birkenkamp-Demtröder, K.; Nordentoft, I.; Christensen, E.; Høyer, S.; Reinert, T.; Vang, S.; Borre, M.; Agerbæk, M.; Jensen, J. B.; Ørntoft, T. F. *European urology* **2016**, *70*, 75-82.

(136) Nagata, M.; Muto, S.; Horie, S. *Dis Markers* **2016**, *2016*, 8205836.

(137) Alberice, J. V.; Amaral, A. F.; Armitage, E. G.; Lorente, J. A.; Algaba, F.; Carrilho, E.; Márquez, M.; García, A.; Malats, N.; Barbas, C. *Journal of Chromatography A* **2013**, *1318*, 163-170.

(138) Imperiale, T. F.; Ransohoff, D. F.; Itzkowitz, S. H.; Levin, T. R.; Lavin, P.; Lidgard, G. P.; Ahlquist, D. A.; Berger, B. M. *New England Journal of Medicine* **2014**, *370*, 1287-1297.

(139) Huth, L.; Jakel, J.; Dahl, E. *Microarrays (Basel)* **2014**, *3*, 168-179.

(140) Hu, S.; Arellano, M.; Boontheung, P.; Wang, J.; Zhou, H.; Jiang, J.; Elashoff, D.; Wei, R.; Loo, J. A.; Wong, D. T. *Clinical Cancer Research* **2008**, *14*, 6246-6252.

(141) Rapado-Gonzalez, O.; Majem, B.; Muinelo-Romay, L.; Lopez-Lopez, R.; Suarez-Cunqueiro, M. M. *Int J Mol Sci* **2016**, *17*.

(142) Schmidt, H.; Kulasinghe, A.; Perry, C.; Nelson, C.; Punyadeera, C. *Expert review of molecular diagnostics* **2016**, *16*, 165-172.

(143) Baraniskin, A.; Kuhnhenn, J.; Schlegel, U.; Chan, A.; Deckert, M.; Gold, R.; Maghnouj, A.; Zöllner, H.; Reinacher-Schick, A.; Schmiegel, W. *Blood* **2011**, *117*, 3140-3146.

(144) Touat, M.; Duran-Pena, A.; Alentorn, A.; Lacroix, L.; Massard, C.; Idbaih, A. *Expert Rev Mol Diagn* **2015**, *15*, 1311-1323.

(145) Pan, W.; Gu, W.; Nagpal, S.; Gephart, M. H.; Quake, S. R. *Clinical chemistry* **2015**, *61*, 514-522.

(146) Siegel, R. L.; Miller, K. D.; Jemal, A. *CA: a cancer journal for clinicians* **2015**, *65*, 5-29.

(147) Taketo, M. M. *Cancer Prev Res (Phila)* **2011**, *4*, 324-328.

(148) Mehlen, P.; Puisieux, A. *Nat Rev Cancer* **2006**, *6*, 449-458.

(149) Fulda, S. *International journal of cancer* **2009**, *124*, 511-515.

(150) Igney, F. H.; Krammer, P. H. *Nat Rev Cancer* **2002**, *2*, 277-288.

(151) Akakura, N.; Kobayashi, M.; Horiuchi, I.; Suzuki, A.; Wang, J.; Chen, J.; Niizeki, H.; Kawamura, K.-i.; Hosokawa, M.; Asaka, M. *Cancer research* **2001**, *61*, 6548-6554.

(152) Yu, M.; Stott, S.; Toner, M.; Maheswaran, S.; Haber, D. A. *The Journal of cell biology* **2011**, *192*, 373-382.

(153) Kleiner, D. E.; Stetler-Stevenson, W. G. *Cancer chemotherapy and pharmacology* **1999**, *43*, S42-S51.

(154) Gupta, G. P.; Massague, J. *Cell* **2006**, *127*, 679-695.

(155) Lu, P.; Weaver, V. M.; Werb, Z. *J Cell Biol* **2012**, *196*, 395-406.

(156) Chambers, A. F.; Groom, A. C.; MacDonald, I. C. *Nature Reviews Cancer* **2002**, *2*, 563-572.

(157) Faraji, F.; Eissenberg, J. C. *Mo Med* **2013**, *110*, 302-308.

(158) Hart, I. R.; Fidler, I. J. *Q Rev Biol* **1980**, *55*, 121-142.

(159) Rolfo, C.; Castiglia, M.; Hong, D.; Alessandro, R.; Mertens, I.; Baggerman, G.; Zwaenepoel, K.; Gil-Bazo, I.; Passiglia, F.; Carreca, A. P. *Biochimica et Biophysica Acta (BBA)-Reviews on Cancer* **2014**, *1846*, 539-546.

(160) Bhagat, A. A. S.; Bow, H.; Hou, H. W.; Tan, S. J.; Han, J.; Lim, C. T. *Medical and Biological Engineering and Computing* **2010**, *48*, 999-1014.

(161) Radisic, M.; Iyer, R. K.; Murthy, S. K. *International journal of nanomedicine* **2006**, *1*, 3.

(162) Patabadige, D. E.; Jia, S.; Sibbitts, J.; Sadeghi, J.; Sellens, K.; Culbertson, C. T. *Analytical chemistry* **2016**, *88*, 320-338.

(163) Sibbitts, J.; Sellens, K. A.; Jia, S.; Klasner, S. A.; Culbertson, C. T. *Analytical chemistry* **2017**.

(164) Dharmasiri, U.; Witek, M. A.; Adams, A. A.; Soper, S. A. *Annual review of analytical chemistry* **2010**, *3*, 409-431.

(165) Yan, S.; Zhang, J.; Yuan, D.; Li, W. *Electrophoresis* **2017**, *38*, 238-249.

(166) Chen, J.; Li, J.; Sun, Y. *Lab on a Chip* **2012**, *12*, 1753-1767.

(167) Khamenehfar, A.; Li, P. C. *Current pharmaceutical biotechnology* **2016**, *17*, 810-821.

(168) Riethdorf, S.; Fritsche, H.; Muller, V.; Rau, T.; Schindlbeck, C.; Rack, B.; Janni, W.; Coith, C.; Beck, K.; Janicke, F.; Jackson, S.; Gornet, T.; Cristofanilli, M.; Pantel, K. *Clin Cancer Res* **2007**, *13*, 920-928.

(169) Miller, M. C.; Doyle, G. V.; Terstappen, L. W. *J Oncol* **2010**, *2010*, 617421.

(170) Sandri, M. T.; Zorzino, L.; Cassatella, M. C.; Bassi, F.; Luini, A.; Casadio, C.; Botteri, E.; Rotmensz, N.; Adamoli, L.; Nole, F. *Ann Surg Oncol* **2010**, *17*, 1539-1545.

(171) Ashworth, T. *Aust Med J.* **1869**, *14*, 146.

(172) Maheswaran, S.; Haber, D. A. *Current opinion in genetics & development* **2010**, *20*, 96-99.

(173) Chang, J.; Erler, J. In *Tumor Microenvironment and Cellular Stress*; Springer, 2014, pp 55-81.

(174) Liu, Y.; Cao, X. *Cancer Cell* **2016**, *30*, 668-681.

(175) Thiery, J. P.; Lim, C. T. *Cancer cell* **2013**, *23*, 272-273.

(176) Mohme, M.; Riethdorf, S.; Pantel, K. *Nature Reviews Clinical Oncology* **2017**, *14*, 155-167.

(177) THORSTEINSSON, M.; SÖLETORMOS, G.; JESS, P. *Anticancer Research* **2011**, *31*, 613-617.

(178) Plaks, V.; Koopman, C. D.; Werb, Z. *Science* **2013**, *341*, 1186-1188.

(179) Attard, G.; de Bono, J. S. *Current opinion in genetics & development* **2011**, *21*, 50-58.

(180) Hiltermann, T.; Pore, M.; Van den Berg, A.; Timens, W.; Boezen, H.; Liesker, J.; Schouwink, J.; Wijnands, W.; Kerner, G.; Kruyt, F. *Annals of oncology* **2012**, *23*, 2937-2942.

(181) Cristofanilli, M.; Budd, G. T.; Ellis, M. J.; Stopeck, A.; Matera, J.; Miller, M. C.; Reuben, J. M.; Doyle, G. V.; Allard, W. J.; Terstappen, L. W. *N Engl J Med* **2004**, *2004*, 781-791.

(182) De Bono, J. S.; Scher, H. I.; Montgomery, R. B.; Parker, C.; Miller, M. C.; Tissing, H.; Doyle, G. V.; Terstappen, L. W.; Pienta, K. J.; Raghavan, D. *Clinical cancer research* **2008**, *14*, 6302-6309.

(183) Cohen, S. J.; Punt, C. J.; Iannotti, N.; Saidman, B. H.; Sabbath, K. D.; Gabrail, N. Y.; Picus, J.; Morse, M.; Mitchell, E.; Miller, M. C. *Journal of clinical oncology* **2008**, *26*, 3213-3221.

(184) Scher, H. I.; Jia, X.; de Bono, J. S.; Fleisher, M.; Pienta, K. J.; Raghavan, D.; Heller, G. *The lancet oncology* **2009**, *10*, 233-239.

(185) Yu, M.; Bardia, A.; Aceto, N.; Bersani, F.; Madden, M. W.; Donaldson, M. C.; Desai, R.; Zhu, H.; Comaills, V.; Zheng, Z. *Science* **2014**, *345*, 216-220.

(186) Crystal, A. S.; Shaw, A. T.; Sequist, L. V.; Friboulet, L.; Niederst, M. J.; Lockerman, E. L.; Frias, R. L.; Gainor, J. F.; Amzallag, A.; Greninger, P. *Science* **2014**, *346*, 1480-1486.

(187) Cheung, K. J.; Padmanaban, V.; Silvestri, V.; Schipper, K.; Cohen, J. D.; Fairchild, A. N.; Gorin, M. A.; Verdone, J. E.; Pienta, K. J.; Bader, J. S.; Ewald, A. J. *Proceedings of the National Academy of Sciences* **2016**, *113*, E854-E863.

(188) Au, S. H.; Storey, B. D.; Moore, J. C.; Tang, Q.; Chen, Y.-L.; Javaid, S.; Sarioglu, A. F.; Sullivan, R.; Madden, M. W.; O'Keefe, R.; Haber, D. A.; Maheswaran, S.; Langenau, D. M.; Stott, S. L.; Toner, M. *Proceedings of the National Academy of Sciences* **2016**, *113*, 4947-4952.

(189) Aceto, N.; Bardia, A.; Miyamoto, D. T.; Donaldson, M. C.; Wittner, B. S.; Spencer, J. A.; Yu, M.; Pely, A.; Engstrom, A.; Zhu, H.; Brannigan, B. W.; Kapur, R.; Stott, S. L.; Shioda, T.; Ramaswamy, S.; Ting, D. T.; Lin, C. P.; Toner, M.; Haber, D. A.; Maheswaran, S. *Cell* **2014**, *158*, 1110-1122.

(190) Hou, J. M.; Krebs, M. G.; Lancashire, L.; Sloane, R.; Backen, A.; Swain, R. K.; Priest, L. J.; Greystoke, A.; Zhou, C.; Morris, K.; Ward, T.; Blackhall, F. H.; Dive, C. *J Clin Oncol* **2012**, *30*, 525-532.

(191) Kelloff, G. J.; Sigman, C. C. *Nature reviews Drug discovery* **2012**, *11*, 201-214.

(192) Gradilone, A.; Naso, G.; Raimondi, C.; Cortesi, E.; Gandini, O.; Vincenzi, B.; Saltarelli, R.; Chiapparino, E.; Spremberg, F.; Cristofanilli, M. *Annals of Oncology* **2010**, *22*, 86-92.

(193) Smirnov, D. A.; Zweitzig, D. R.; Foulk, B. W.; Miller, M. C.; Doyle, G. V.; Pienta, K. J.; Meropol, N. J.; Weiner, L. M.; Cohen, S. J.; Moreno, J. G. *Cancer research* **2005**, *65*, 4993-4997.

(194) Gervasoni, A.; Munoz, R. M. M.; Wengler, G. S.; Rizzi, A.; Zaniboni, A.; Parolini, O. *Cancer letters* **2008**, *263*, 267-279.

(195) Jiang, Y.; Palma, J. F.; Agus, D. B.; Wang, Y.; Gross, M. E. *Clinical chemistry* **2010**, *56*, 1492-1495.

(196) Tesoriero, A.; Wong, E.; Jenkins, M.; Hopper, J.; Brown, M.; Chenevix-Trench, G.; Spurdle, A.; Southey, M. *Human mutation* **2005**, *26*, 495-495.

(197) Miller, M. C.; Doyle, G. V.; Terstappen, L. W. *Journal of oncology* **2009**, *2010*.

(198) Werner, S. L.; Graf, R. P.; Landers, M.; Valenta, D. T.; Schroeder, M.; Greene, S. B.; Bales, N.; Dittamore, R.; Marrinucci, D. *Journal of Circulating Biomarkers* **2015**, *4*, 3.

(199) Kuo, J. S.; Zhao, Y.; Schiro, P. G.; Ng, L.; Lim, D. S.; Shelby, J. P.; Chiu, D. T. *Lab on a Chip* **2010**, *10*, 837-842.

(200) Armstrong, A. J.; Marengo, M. S.; Oltean, S.; Kemeny, G.; Bitting, R.; Turnbull, J.; Herold, C. I.; Marcom, P. K.; George, D.; Garcia-Blanco, M. *Molecular cancer research* **2011**, molcanres. 0490.2010.

(201) Alix-Panabières, C.; Vendrell, J.-P.; Pellé, O.; Rebillard, X.; Riethdorf, S.; Müller, V.; Fabbro, M.; Pantel, K. *Clinical chemistry* **2007**, *53*, 537-539.

(202) Schwartz, M. *Genetic Engineering & Biotechnology News* **2013**, *33*.

(203) Lianidou, E. S.; Markou, A.; Strati, A. *Cancer and Metastasis Reviews* **2012**, 1-9.

(204) Nagrath, S.; Sequist, L. V.; Maheswaran, S.; Bell, D. W.; Irimia, D.; Ulkus, L.; Smith, M. R.; Kwak, E. L.; Digumarthy, S.; Muzikansky, A. *Nature* **2007**, *450*, 1235-1239.

(205) Maheswaran, S.; Sequist, L. V.; Nagrath, S.; Ulkus, L.; Brannigan, B.; Collura, C. V.; Inserra, E.; Diederichs, S.; Iafrate, A. J.; Bell, D. W. *New England Journal of Medicine* **2008**, *359*, 366-377.

(206) Gleghorn, J. P.; Pratt, E. D.; Denning, D.; Liu, H.; Bander, N. H.; Tagawa, S. T.; Nanus, D. M.; Giannakakou, P. A.; Kirby, B. J. *Lab on a chip* **2010**, *10*, 27-29.

(207) Murlidhar, V.; Zeinali, M.; Grabauskiene, S.; Ghannad-Rezaie, M.; Wicha, M. S.; Simeone, D. M.; Ramnath, N.; Reddy, R. M.; Nagrath, S. *Small* **2014**, *10*, 4895-4904.

(208) Stott, S. L.; Hsu, C.-H.; Tsukrov, D. I.; Yu, M.; Miyamoto, D. T.; Waltman, B. A.; Rothenberg, S. M.; Shah, A. M.; Smas, M. E.; Korir, G. K. *Proceedings of the National Academy of Sciences* **2010**, *107*, 18392-18397.

(209) Sheng, W.; Ogunwobi, O. O.; Chen, T.; Zhang, J.; George, T. J.; Liu, C.; Fan, Z. H. *Lab on a Chip* **2014**, *14*, 89-98.

(210) Dharmasiri, U.; Balamurugan, S.; Adams, A. A.; Okagbare, P. I.; Obubuafo, A.; Soper, S. A. *Electrophoresis* **2009**, *30*, 3289-3300.

(211) Adams, A. A.; Okagbare, P. I.; Feng, J.; Hupert, M. L.; Patterson, D.; Göttert, J.; McCarley, R. L.; Nikitopoulos, D.; Murphy, M. C.; Soper, S. A. *Journal of the American Chemical Society* **2008**, *130*, 8633-8641.

(212) Yoon, H. J.; Shanker, A.; Wang, Y.; Kozminsky, M.; Jin, Q.; Palanisamy, N.; Burness, M. L.; Azizi, E.; Simeone, D. M.; Wicha, M. S. *Advanced materials* **2016**, *28*, 4891-4897.

(213) Reátegui, E.; Aceto, N.; Lim, E. J.; Sullivan, J. P.; Jensen, A. E.; Zeinali, M.; Martel, J. M.; Aranyosi, A. J.; Li, W.; Castleberry, S. *Advanced Materials* **2015**, *27*, 1593-1599.

(214) Ke, Z.; Lin, M.; Chen, J.-F.; Choi, J.-s.; Zhang, Y.; Fong, A.; Liang, A.-J.; Chen, S.-F.; Li, Q.; Fang, W. *ACS nano* **2014**, *9*, 62-70.

(215) Hou, S.; Zhao, H.; Zhao, L.; Shen, Q.; Wei, K. S.; Suh, D. Y.; Nakao, A.; Garcia, M. A.; Song, M.; Lee, T. *Advanced materials* **2013**, *25*, 1547-1551.

(216) Casavant, B. P.; Strotman, L. N.; Tokar, J. J.; Thiede, S. M.; Traynor, A. M.; Ferguson, J. S.; Lang, J. M.; Beebe, D. J. *Lab on a chip* **2014**, *14*, 99-105.

(217) Karabacak, N. M.; Spuhler, P. S.; Fachin, F.; Lim, E. J.; Pai, V.; Ozkumur, E.; Martel, J. M.; Kojic, N.; Smith, K.; Chen, P. I.; Yang, J.; Hwang, H.; Morgan, B.; Trautwein, J.; Barber, T. A.; Stott, S. L.; Maheswaran, S.; Kapur, R.; Haber, D. A.; Toner, M. *Nature protocols* **2014**, *9*, 694-710.

(218) Ozkumur, E.; Shah, A. M.; Ciciliano, J. C.; Emmink, B. L.; Miyamoto, D. T.; Brachtel, E.; Yu, M.; Chen, P.-i.; Morgan, B.; Trautwein, J. *Science translational medicine* **2013**, *5*, 179ra147-179ra147.

(219) Ahmed, M. G.; Abate, M. F.; Song, Y.; Zhu, Z.; Yan, F.; Xu, Y.; Wang, X.; Li, Q.; Yang, C. *Angew Chem Int Ed Engl* **2017**, *56*, 10681-10685.

(220) Shields Iv, C. W.; Wang, J. L.; Ohiri, K. A.; Essoyan, E. D.; Yellen, B. B.; Armstrong, A. J.; Lopez, G. P. *Lab on a Chip* **2016**, *16*, 3833-3844.

(221) Green, B. J.; Kermanshah, L.; Labib, M.; Ahmed, S. U.; Silva, P. N.; Mahmoudian, L.; Chang, I. H.; Mohamadi, R. M.; Rocheleau, J. V.; Kelley, S. O. *ACS Appl Mater Interfaces* **2017**, *9*, 20435-20443.

(222) Hu, X.; Wei, C. W.; Xia, J.; Pelivanov, I.; O'Donnell, M.; Gao, X. *Small* **2013**, *9*, 2046-2052, 2045.

(223) Wei, C. W.; Xia, J.; Pelivanov, I.; Jia, C.; Huang, S. W.; Hu, X.; Gao, X.; O'Donnell, M. *J Biophotonics* **2013**, *6*, 513-522.

(224) Awe, J. A.; Saranchuk, J.; Drachenberg, D.; Mai, S. *Urologic Oncology: Seminars and Original Investigations* **2017**, *35*, 300-309.

(225) Hvichia, G.; Google Patents, 2011.

(226) Adams, D. L.; Martin, S. S.; Alpaugh, R. K.; Charpentier, M.; Tsai, S.; Bergan, R. C.; Ogden, I. M.; Catalona, W.; Chumsri, S.; Tang, C.-M. *Proceedings of the National Academy of Sciences* **2014**, *111*, 3514-3519.

(227) Tsipouras, P.; Tafas, T.; Google Patents, 2004.

(228) Harouaka, R. A.; Zhou, M.-D.; Yeh, Y.-T.; Khan, W. J.; Das, A.; Liu, X.; Christ, C. C.; Dicker, D. T.; Baney, T. S.; Kaifi, J. T. *Clinical chemistry* **2014**, *60*, 323-333.

(229) Gallant, J.-N.; Matthew, E. M.; Harouaka, R.; Lamparella, N.; Kunkel, M.; Yang, Z.; Cream, L. V.; Kumar, S. M.; Robertson, G. P.; Zheng, S. *Cell Cycle* **2013**, *12*, 2132-2143.

(230) Gogoi, P.; Sepehri, S.; Zhou, Y.; Gorin, M. A.; Paolillo, C.; Capoluongo, E.; Gleason, K.; Payne, A.; Boniface, B.; Cristofanilli, M.; Morgan, T. M.; Fortina, P.; Pienta, K. J.; Handique, K.; Wang, Y. *PLoS One* **2016**, *11*, e0147400.

(231) Au, S. H.; Edd, J.; Stoddard, A. E.; Wong, K. H. K.; Fachin, F.; Maheswaran, S.; Haber, D. A.; Stott, S. L.; Kapur, R.; Toner, M. *Sci Rep* **2017**, *7*, 2433.

(232) Di Carlo, D.; Irimia, D.; Tompkins, R. G.; Toner, M. *Proceedings of the National Academy of Sciences* **2007**, *104*, 18892-18897.

(233) Zhou, J.; Papautsky, I. *Lab on a Chip* **2013**, *13*, 1121-1132.

(234) Martel, J. M.; Toner, M. *Physics of Fluids* **2012**, *24*, 032001.

(235) Ramachandraiah, H.; Svahn, H. A.; Russom, A. *RSC Advances* **2017**, *7*, 29505-29514.

(236) Bhagat, A. A. S.; Kuntaegowdanahalli, S. S.; Papautsky, I. *Lab on a Chip* **2008**, *8*, 1906-1914.

(237) Hou, H. W.; Warkiani, M. E.; Khoo, B. L.; Li, Z. R.; Soo, R. A.; Tan, D. S.-W.; Lim, W.-T.; Han, J.; Bhagat, A. A. S.; Lim, C. T. *Scientific reports* **2013**, *3*.

(238) Sun, J.; Li, M.; Liu, C.; Zhang, Y.; Liu, D.; Liu, W.; Hu, G.; Jiang, X. *Lab on a chip* **2012**, *12*, 3952-3960.

(239) Khoo, B. L.; Warkiani, M. E.; Tan, D. S.-W.; Bhagat, A. A. S.; Irwin, D.; Lau, D. P.; Lim, A. S.; Lim, K. H.; Krisna, S. S.; Lim, W.-T. *PloS one* **2014**, *9*, e99409.

(240) Kim, T. H.; Yoon, H. J.; Stella, P.; Nagrath, S. *Biomicrofluidics* **2014**, *8*, 064117.

(241) Warkiani, M. E.; Guan, G.; Luan, K. B.; Lee, W. C.; Bhagat, A. A. S.; Chaudhuri, P. K.; Tan, D. S.-W.; Lim, W. T.; Lee, S. C.; Chen, P. C. *Lab on a Chip* **2014**, *14*, 128-137.

(242) Sollier, E.; Go, D. E.; Che, J.; Gossett, D. R.; O'Byrne, S.; Weaver, W. M.; Kummer, N.; Rettig, M.; Goldman, J.; Nickols, N. *Lab on a Chip* **2014**, *14*, 63-77.

(243) Che, J.; Yu, V.; Dhar, M.; Renier, C.; Matsumoto, M.; Heirich, K.; Garon, E. B.; Goldman, J.; Rao, J.; Sledge, G. W. *Oncotarget* **2016**, *7*, 12748.

(244) Lin, M. X.; Hyun, K.-A.; Moon, H.-S.; Sim, T. S.; Lee, J.-G.; Park, J. C.; Lee, S. S.; Jung, H.-I. *Biosensors and Bioelectronics* **2013**, *40*, 63-67.

(245) Parichehreh, V.; Sethu, P. *Lab on a chip* **2012**, *12*, 1296-1301.

(246) Parichehreh, V.; Medepallai, K.; Babbarwal, K.; Sethu, P. *Lab on a Chip* **2013**, *13*, 892-900.

(247) Ding, X.; Peng, Z.; Lin, S.-C. S.; Geri, M.; Li, S.; Li, P.; Chen, Y.; Dao, M.; Suresh, S.; Huang, T. J. *Proceedings of the National Academy of Sciences* **2014**, *111*, 12992-12997.

(248) Li, P.; Mao, Z.; Peng, Z.; Zhou, L.; Chen, Y.; Huang, P.-H.; Truica, C. I.; Drabick, J. J.; El-Deiry, W. S.; Dao, M. *Proceedings of the National Academy of Sciences* **2015**, *112*, 4970-4975.

(249) Gupta, V.; Jafferji, I.; Garza, M.; Melnikova, V. O.; Hasegawa, D.; Davis, D. W.; AACR, 2012.

(250) Gupta, V.; Jafferji, I.; Garza, M.; Melnikova, V. O.; Hasegawa, D. K.; Pethig, R.; Davis, D. W. *Biomicrofluidics* **2012**, *6*, 024133.

(251) Antfolk, M.; Kim, S. H.; Koizumi, S.; Fujii, T.; Laurell, T. *Sci Rep* **2017**, *7*, 46507.

(252) Tkach, M.; Thery, C. *Cell* **2016**, *164*, 1226-1232.

(253) Théry, C.; Zitvogel, L.; Amigorena, S. *Nature Reviews Immunology* **2002**, *2*, 569-579.

(254) Keller, S.; Sanderson, M. P.; Stoeck, A.; Altevogt, P. *Immunology letters* **2006**, *107*, 102-108.

(255) Raposo, G.; Stoorvogel, W. *J Cell Biol* **2013**, *200*, 373-383.

(256) Andaloussi, S. E.; Mäger, I.; Breakefield, X. O.; Wood, M. J. *Nature reviews Drug discovery* **2013**, *12*, 347-357.

(257) De Toro, J.; Herschlik, L.; Waldner, C.; Mongini, C. *Frontiers in immunology* **2015**, *6*.

(258) Meckes, D. G. *Journal of virology* **2015**, *89*, 5200-5203.

(259) Kucharzewska, P.; Belting, M. *Journal of extracellular vesicles* **2013**, *2*, 20304.

(260) Kowal, J.; Tkach, M.; Théry, C. *Current opinion in cell biology* **2014**, *29*, 116-125.

(261) Caradec, J.; Kharmate, G.; Hosseini-Beheshti, E.; Adomat, H.; Gleave, M.; Guns, E. *Clinical biochemistry* **2014**, *47*, 1286-1292.

(262) Taylor, D. D.; Gercel-Taylor, C. *Gynecologic oncology* **2008**, *110*, 13-21.

(263) Abusamra, A. J.; Zhong, Z.; Zheng, X.; Li, M.; Ichim, T. E.; Chin, J. L.; Min, W.-P. *Blood Cells, Molecules, and Diseases* **2005**, *35*, 169-173.

(264) Mathivanan, S.; Simpson, R. J. *Proteomics* **2009**, *9*, 4997-5000.

(265) King, H. W.; Michael, M. Z.; Gleadle, J. M. *BMC cancer* **2012**, *12*, 421.

(266) Logozzi, M.; De Milito, A.; Lugini, L.; Borghi, M.; Calabro, L.; Spada, M.; Perdicchio, M.; Marino, M. L.; Federici, C.; Iessi, E. *PloS one* **2009**, *4*, e5219.

(267) Runz, S.; Keller, S.; Rupp, C.; Stoeck, A.; Issa, Y.; Koensgen, D.; Mustea, A.; Sehouli, J.; Kristiansen, G.; Altevogt, P. *Gynecologic oncology* **2007**, *107*, 563-571.

(268) Taylor, D. D.; Zacharias, W.; Gercel-Taylor, C. *Serum/Plasma Proteomics: Methods and Protocols* **2011**, 235-246.

(269) Rupp, A.-K.; Rupp, C.; Keller, S.; Brase, J. C.; Ehehalt, R.; Fogel, M.; Moldenhauer, G.; Marmé, F.; Sültmann, H.; Altevogt, P. *Gynecologic oncology* **2011**, *122*, 437-446.

(270) Moon, P.-G.; Lee, J.-E.; Cho, Y.-E.; Lee, S. J.; Jung, J. H.; Chae, Y. S.; Bae, H.-I.; Kim, Y.-B.; Kim, I.-S.; Park, H. Y. *Clinical Cancer Research* **2016**, *22*, 1757-1766.

(271) Nilsson, J.; Skog, J.; Nordstrand, A.; Baranov, V.; Mincheva-Nilsson, L.; Breakefield, X.; Widmark, A. *British journal of cancer* **2009**, *100*, 1603-1607.

(272) Khan, S.; Jutzy, J. M.; Valenzuela, M. M. A.; Turay, D.; Aspe, J. R.; Ashok, A.; Mirshahidi, S.; Mercola, D.; Lilly, M. B.; Wall, N. R. *PloS one* **2012**, *7*, e46737.

(273) Melo, S. A.; Luecke, L. B.; Kahlert, C.; Fernandez, A. F.; Gammon, S. T.; Kaye, J.; LeBleu, V. S.; Mittendorf, E. A.; Weitz, J.; Rahbari, N. *Nature* **2015**, *523*, 177-182.

(274) Zhao, Z.; Yang, Y.; Zeng, Y.; He, M. *Lab on a Chip* **2016**, *16*, 489-496.

(275) Smalley, D. M.; Sheman, N. E.; Nelson, K.; Theodorescu, D. *Journal of proteome research* **2008**, *7*, 2088-2096.

(276) Valadi, H.; Ekström, K.; Bossios, A.; Sjöstrand, M.; Lee, J. J.; Lötvall, J. O. *Nature cell biology* **2007**, *9*, 654-659.

(277) Ratajczak, J.; Wysoczynski, M.; Hayek, F.; Janowska-Wieczorek, A.; Ratajczak, M. *Leukemia* **2006**, *20*, 1487-1495.

(278) Kahlert, C.; Melo, S. A.; Protopopov, A.; Tang, J.; Seth, S.; Koch, M.; Zhang, J.; Weitz, J.; Chin, L.; Futreal, A. *Journal of Biological Chemistry* **2014**, *289*, 3869-3875.

(279) Balaj, L.; Lessard, R.; Dai, L.; Cho, Y.-J.; Pomeroy, S. L.; Breakefield, X. O.; Skog, J. *Nature communications* **2011**, *2*, 180.

(280) Théry, C.; Amigorena, S.; Raposo, G.; Clayton, A. *Current protocols in cell biology* **2006**, 3.22. 21-23.22. 29.

(281) Caby, M.-P.; Lankar, D.; Vincendeau-Scherrer, C.; Raposo, G.; Bonnerot, C. *International immunology* **2005**, *17*, 879-887.

(282) Andre, F.; Schartz, N.; Chaput, N.; Flament, C.; Raposo, G.; Amigorena, S.; Angevin, E.; Zitvogel, L. *Vaccine* **2002**, *20*, A28-A31.

(283) Lee, T. H.; D'Asti, E.; Magnus, N.; Al-Nedawi, K.; Meehan, B.; Rak, J. In *Seminars in immunopathology*; Springer, 2011, pp 455-467.

(284) Beach, A.; Zhang, H.-G.; Ratajczak, M. Z.; Kakar, S. S. *Journal of ovarian research* **2014**, *7*, 14.

(285) Clayton, A.; Al-Taei, S.; Webber, J.; Mason, M. D.; Tabi, Z. *The Journal of Immunology* **2011**, *187*, 676-683.

(286) Schostak, M.; Schwall, G. P.; Poznanović, S.; Groebe, K.; Müller, M.; Messinger, D.; Miller, K.; Krause, H.; Pelzer, A.; Horninger, W. *The Journal of urology* **2009**, *181*, 343-353.

(287) Silva, J.; Garcia, V.; Rodriguez, M.; Compte, M.; Cisneros, E.; Veguillas, P.; Garcia, J.; Dominguez, G.; Campos-Martin, Y.; Cuevas, J. *Genes, Chromosomes and Cancer* **2012**, *51*, 409-418.

(288) Tauro, B. J.; Greening, D. W.; Mathias, R. A.; Ji, H.; Mathivanan, S.; Scott, A. M.; Simpson, R. J. *Methods* **2012**, *56*, 293-304.

(289) Février, B.; Raposo, G. *Current opinion in cell biology* **2004**, *16*, 415-421.

(290) Khan, S.; Jutzy, J. M.; Aspe, J. R.; McGregor, D. W.; Neidigh, J. W.; Wall, N. R. *Apoptosis* **2011**, *16*, 1-12.

(291) Kalra, H.; Adda, C. G.; Liem, M.; Ang, C. S.; Mechler, A.; Simpson, R. J.; Hulett, M. D.; Mathivanan, S. *Proteomics* **2013**, *13*, 3354-3364.

(292) Muller, L.; Hong, C.-S.; Stolz, D. B.; Watkins, S. C.; Whiteside, T. L. *Journal of immunological methods* **2014**, *411*, 55-65.

(293) Xu, R.; Greening, D. W.; Zhu, H.-J.; Takahashi, N.; Simpson, R. J. *The Journal of clinical investigation* **2016**, *126*, 1152-1162.

(294) Sandvig, K.; Llorente, A. *Molecular & Cellular Proteomics* **2012**, *11*, M111. 012914.

(295) Hyun, K.-A.; Kim, J.; Gwak, H.; Jung, H.-I. *Analyst* **2016**, *141*, 382-392.

(296) Petersen, K. E.; Manangon, E.; Hood, J. L.; Wickline, S. A.; Fernandez, D. P.; Johnson, W. P.; Gale, B. K. *Analytical and bioanalytical chemistry* **2014**, *406*, 7855.

(297) Lamparski, H. G.; Metha-Damani, A.; Yao, J.-Y.; Patel, S.; Hsu, D.-H.; Ruegg, C.; Le Pecq, J.-B. *Journal of immunological methods* **2002**, *270*, 211-226.

(298) Momen-Heravi, F.; Balaj, L.; Alian, S.; Mantel, P.-Y.; Halleck, A. E.; Trachtenberg, A. J.; Soria, C. E.; Oquin, S.; Bonebreak, C. M.; Saracoglu, E. *Biological chemistry* **2013**, *394*, 1253-1262.

(299) Chen, C.; Skog, J.; Hsu, C.-H.; Lessard, R. T.; Balaj, L.; Wurdinger, T.; Carter, B. S.; Breakefield, X. O.; Toner, M.; Irimia, D. *Lab on a chip* **2010**, *10*, 505-511.

(300) Kanwar, S. S.; Dunlay, C. J.; Simeone, D. M.; Nagrath, S. *Lab on a Chip* **2014**, *14*, 1891-1900.

(301) Zhang, P.; He, M.; Zeng, Y. *Lab on a chip* **2016**, *16*, 3033-3042.

(302) Im, H.; Shao, H.; Park, Y. I.; Peterson, V. M.; Castro, C. M.; Weissleder, R.; Lee, H. *Nature biotechnology* **2014**, *32*, 490-495.

(303) Vaidyanathan, R.; Naghibosadat, M.; Rauf, S.; Korbie, D.; Carrascosa, L. G.; Shiddiky, M. J.; Trau, M. *Analytical chemistry* **2014**, *86*, 11125-11132.

(304) Witwer, K. W.; Buzas, E. I.; Bemis, L. T.; Bora, A.; Lässer, C.; Lötvall, J.; Nolte-'t Hoen, E. N.; Piper, M. G.; Sivaraman, S.; Skog, J. *Journal of extracellular vesicles* **2013**, *2*, 20360.

(305) Dudani, J. S.; Gossett, D. R.; Tse, H. T.; Lamm, R. J.; Kulkarni, R. P.; Carlo, D. D. *Biomicrofluidics* **2015**, *9*, 014112.

(306) Shao, H.; Chung, J.; Lee, K.; Balaj, L.; Min, C.; Carter, B. S.; Hochberg, F. H.; Breakefield, X. O.; Lee, H.; Weissleder, R. *Nature communications* **2015**, *6*, 6999.

(307) He, M.; Crow, J.; Roth, M.; Zeng, Y.; Godwin, A. K. *Lab Chip* **2014**, *14*, 3773-3780.

(308) Davies, R. T.; Kim, J.; Jang, S. C.; Choi, E.-J.; Gho, Y. S.; Park, J. *Lab on a chip* **2012**, *12*, 5202-5210.

(309) Woo, H. K.; Sunkara, V.; Park, J.; Kim, T. H.; Han, J. R.; Kim, C. J.; Choi, H. I.; Kim, Y. K.; Cho, Y. K. *ACS nano* **2017**, *11*, 1360-1370.

(310) Lee, K.; Shao, H.; Weissleder, R.; Lee, H. *ACS Nano* **2015**, *9*, 2321-2327.

(311) Wang, Z.; Wu, H.-j.; Fine, D.; Schmulen, J.; Hu, Y.; Godin, B.; Zhang, J. X.; Liu, X. *Lab on a Chip* **2013**, *13*, 2879-2882.

(312) Santana, S. M.; Antonyak, M. A.; Cerione, R. A.; Kirby, B. J. *Biomed Microdevices* **2014**, *16*, 869-877.

(313) Wunsch, B. H.; Smith, J. T.; Gifford, S. M.; Wang, C.; Brink, M.; Bruce, R. L.; Austin, R. H.; Stolovitzky, G.; Astier, Y. *Nat Nanotechnol* **2016**, *11*, 936-940.

(314) Liu, C.; Guo, J.; Tian, F.; Yang, N.; Yan, F.; Ding, Y.; Wei, J.; Hu, G.; Nie, G.; Sun, J. *ACS nano* **2017**, *11*, 6968-6976.

(315) Bettegowda, C.; Sausen, M.; Leary, R. J.; Kinde, I.; Wang, Y.; Agrawal, N.; Bartlett, B. R.; Wang, H.; Luber, B.; Alani, R. M. *Science translational medicine* **2014**, *6*, 224ra224-224ra224.

(316) Jahr, S.; Hentze, H.; Englisch, S.; Hardt, D.; Fackelmayer, F. O.; Hesch, R.-D.; Knippers, R. *Cancer research* **2001**, *61*, 1659-1665.

(317) Stroun, M.; Lyautey, J.; Lederrey, C.; Olson-Sand, A.; Anker, P. *Clinica chimica acta* **2001**, *313*, 139-142.

(318) Diehl, F.; Schmidt, K.; Choti, M. A.; Romans, K.; Goodman, S.; Li, M.; Thornton, K.; Agrawal, N.; Sokoll, L.; Szabo, S. A. *Nature medicine* **2008**, *14*, 985-990.

(319) Cuk, K.; Zucknick, M.; Heil, J.; Madhavan, D.; Schott, S.; Turchinovich, A.; Arlt, D.; Rath, M.; Sohn, C.; Benner, A. *International journal of cancer* **2013**, *132*, 1602-1612.

(320) Kosaka, N.; Iguchi, H.; Ochiya, T. *Cancer science* **2010**, *101*, 2087-2092.

(321) Ma, Y.; Zhang, P.; Wang, F.; Zhang, H.; Yang, J.; Peng, J.; Liu, W.; Qin, H. *Gut* **2011**, gutjnl-2011-301122.

(322) Moussay, E.; Wang, K.; Cho, J.-H.; van Moer, K.; Pierson, S.; Paggetti, J.; Nazarov, P. V.; Palissot, V.; Hood, L. E.; Berchem, G. *Proceedings of the National Academy of Sciences* **2011**, *108*, 6573-6578.

(323) Zhao, H.; Shen, J.; Medico, L.; Wang, D.; Ambrosone, C. B.; Liu, S. *PloS one* **2010**, *5*, e13735.

(324) Weber, J. A.; Baxter, D. H.; Zhang, S.; Huang, D. Y.; Huang, K. H.; Lee, M. J.; Galas, D. J.; Wang, K. *Clinical chemistry* **2010**, *56*, 1733-1741.

(325) Park, N. J.; Zhou, H.; Elashoff, D.; Henson, B. S.; Kastratovic, D. A.; Abemayor, E.; Wong, D. T. *Clinical Cancer Research* **2009**, *15*, 5473-5477.

(326) Breadmore, M. C.; Wolfe, K. A.; Arcibal, I. G.; Leung, W. K.; Dickson, D.; Giordano, B. C.; Power, M. E.; Ferrance, J. P.; Feldman, S. H.; Norris, P. M. *Analytical chemistry* **2003**, *75*, 1880-1886.

(327) Easley, C. J.; Karlinsey, J. M.; Bienvenue, J. M.; Legendre, L. A.; Roper, M. G.; Feldman, S. H.; Hughes, M. A.; Hewlett, E. L.; Merkel, T. J.; Ferrance, J. P.; Landers, J. P. *Proc Natl Acad Sci U S A* **2006**, *103*, 19272-19277.

(328) Hagan, K. A.; Bienvenue, J. M.; Moskaluk, C. A.; Landers, J. P. *Analytical chemistry* **2008**, *80*, 8453-8460.

(329) Gunal, G.; Kip, C.; Ogut, S. E.; Usta, D. D.; Senlik, E.; Kibar, G.; Tuncel, A. *Mater Sci Eng C Mater Biol Appl* **2017**, *74*, 10-20.

(330) Bienvenue, J. M.; Legendre, L. A.; Ferrance, J. P.; Landers, J. P. *Forensic science international: genetics* **2010**, *4*, 178-186.

(331) Legendre, L. A.; Bienvenue, J. M.; Roper, M. G.; Ferrance, J. P.; Landers, J. P. *Analytical chemistry* **2006**, *78*, 1444-1451.

(332) Huang, S.; Do, J.; Mahalanabis, M.; Fan, A.; Zhao, L.; Jepeal, L.; Singh, S. K.; Klapperich, C. M. *PLoS One* **2013**, *8*, e60059.

(333) Kulinski, M. D.; Mahalanabis, M.; Gillers, S.; Zhang, J. Y.; Singh, S.; Klapperich, C. M. *Biomed Microdevices* **2009**, *11*, 671-678.

(334) Mahalanabis, M.; Al-Muayad, H.; Kulinski, M. D.; Altman, D.; Klapperich, C. M. *Lab Chip* **2009**, *9*, 2811-2817.

(335) Bhattacharyya, A.; Klapperich, C. M. *Sensors and Actuators B: Chemical* **2008**, *129*, 693-698.

(336) Cao, Q.; Mahalanabis, M.; Chang, J.; Carey, B.; Hsieh, C.; Stanley, A.; Odell, C. A.; Mitchell, P.; Feldman, J.; Pollock, N. R. *PLoS One* **2012**, *7*, e33176.

(337) Chen, D.; Mauk, M.; Qiu, X.; Liu, C.; Kim, J.; Ramprasad, S.; Ongagna, S.; Abrams, W. R.; Malamud, D.; Corstjens, P. L. *Biomedical microdevices* **2010**, *12*, 705-719.

CONCLUSION

In summary, it is essential that techniques that can accomplish rapid and activation-free isolation of WBC sub-populations be developed to harness the enormous and valuable information contained within WBCs for diagnostics, patient monitoring and determination of accurate management of patients.

In my thesis, I developed unique technologies to enable centrifugal microfluidics based cell separation techniques. I first developed a platform where conventional density gradient centrifugation can be enabled by ensuring laminar flow and minimizing secondary Deans flow. Proof of concept studies were accomplished using binary bead mixtures. I then demonstrated the potential for centrifugal microfluidics to rapidly isolate WBC subpopulations in a manner that results in minimal activation. Finally, I have also used centrifugal microfluidics to demonstrate that conventional phase partitioning can be miniaturized and potentially used for sorting of cells.

REFERENCES

(1) O'Connell, G. C.; Treadway, M. B.; Tennant, C. S.; Lucke-Wold, N.; Chantler, P. D.; Barr, T. L. *Translational stroke research* **2018**.

(2) Gou, Y.; Jia, Y.; Wang, P.; Sun, C. *Sensors (Basel)* **2018**, *18*.

(3) Bayat, P.; Rezai, P. *Soft Matter* **2018**.

(4) An, X.; Chen, L. *Methods Mol Biol* **2018**, *1698*, 153-174.

(5) Yip, L.; Fuhlbrigge, R.; Atkinson, M. A.; Fathman, C. G. *BMC Genomics* **2017**, *18*, 636.

(6) van Wolfswinkel, M. E.; Langenberg, M. C. C.; Wammes, L. J.; Sauerwein, R. W.; Koelewijn, R.; Hermsen, C. C.; van Hellemond, J. J.; van Genderen, P. J. *Malar J* **2017**, *16*, 457.

(7) Nadar, S. S.; Pawar, R. G.; Rathod, V. K. *Int J Biol Macromol* **2017**, *101*, 931-957.

(8) Lopez-Candales, A.; Hernandez Burgos, P. M.; Hernandez-Suarez, D. F.; Harris, D. *J Nat Sci* **2017**, *3*.

(9) Hoornaert, C. J.; Le Blon, D.; Quarta, A.; Daans, J.; Goossens, H.; Berneman, Z.; Ponsaerts, P. *Stem Cells Transl Med* **2017**, *6*, 1434-1441.

(10) Hajishengallis, G.; Krauss, J. L.; Jotwani, R.; Lambris, J. D. *Mol Oral Microbiol* **2017**, *32*, 154-165.

(11) Curbelo, J.; Luquero Bueno, S.; Galvan-Roman, J. M.; Ortega-Gomez, M.; Rajas, O.; Fernandez-Jimenez, G.; Vega-Piris, L.; Rodriguez-Salvanes, F.; Arnalich, B.; Diaz, A.; Costa, R.; de la Fuente, H.; Lancho, A.; Suarez, C.; Ancochea, J.; Aspa, J. *PloS one* **2017**, *12*, e0173947.

(12) Bras, E. J. S.; Soares, R. R. G.; Azevedo, A. M.; Fernandes, P.; Arevalo-Rodriguez, M.; Chu, V.; Conde, J. P.; Aires-Barros, M. R. *J Chromatogr A* **2017**, *1515*, 252-259.

(13) Allan, G. M.; Young, J. *Can Fam Physician* **2017**, *63*, 772.

(14) Zaslavsky, B. Y.; Uversky, V. N.; Chait, A. *Biochim Biophys Acta* **2016**, *1864*, 622-644.

(15) Xavier, M.; Oreffo, R. O. C.; Morgan, H. *Biotechnol Adv* **2016**, *34*, 908-923.

(16) Williamson, J. D.; Sadofsky, L. R.; Crooks, M. G.; Greenman, J.; Hart, S. P. *Exp Lung Res* **2016**, *42*, 397-407.

(17) Wang, H.; Xu, L.; Lu, L. *Journal of fish diseases* **2016**, *39*, 155-162.

(18) Vazquez-Villegas, P.; Ouellet, E.; Gonzalez, C.; Ruiz-Ruiz, F.; Rito-Palomares, M.; Haynes, C. A.; Aguilar, O. *Lab on a chip* **2016**, *16*, 2662-2672.

(19) Suratannon, N.; Yeetong, P.; Srichomthong, C.; Amarinthnukrowh, P.; Chatchatee, P.; Sosothikul, D.; van Hagen, P. M.; van der Burg, M.; Wentink, M.; Driessen, G. J.; Suphapeetiporn, K.; Shotelersuk, V. *Pediatr Allergy Immunol* **2016**, *27*, 214-217.

(20) Pelak, O.; Kuzilkova, D.; Thurner, D.; Kiene, M. L.; Stanar, K.; Stuchly, J.; Vaskova, M.; Stary, J.; Hrusak, O.; Stadler, H.; Kalina, T. *Cytometry. Part A : the journal of the International Society for Analytical Cytology* **2016**.

(21) Pappas, D. *The Analyst* **2016**, *141*, 525-535.

(22) Liesz, A.; Kleinschnitz, C. *Translational stroke research* **2016**, *7*, 313-321.

(23) Kinahan, D. J.; Kearney, S. M.; Kilcawley, N. A.; Early, P. L.; Glynn, M. T.; Ducree, J. *PloS one* **2016**, *11*, e0155545.

(24) Fei, C.; Pemberton, J. G.; Lillico, D. M.; Zwozdesky, M. A.; Stafford, J. L. *Biology (Basel)* **2016**, *5*.

(25) Du, G.; Fang, Q.; den Toonder, J. M. *Analytica chimica acta* **2016**, *903*, 36-50.

(26) Darabi, J.; Guo, C. *Biomedical microdevices* **2016**, *18*, 77.

(27) Bhuvanendran Nair Gourikutty, S.; Chang, C. P.; Puiu, P. D. *Journal of chromatography. B, Analytical technologies in the biomedical and life sciences* **2016**, *1011*, 77-88.

(28) Zhu, H.; Lin, X.; Su, Y.; Dong, H.; Wu, J. *Biosensors & bioelectronics* **2015**, *63*, 371-378.

(29) Xiang, N.; Ni, Z. *Biomedical microdevices* **2015**, *17*, 110.

(30) Warkiani, M. E.; Wu, L.; Tay, A. K.; Han, J. *Annual review of biomedical engineering* **2015**, *17*, 1-34.

(31) Wang, G.; Crawford, K.; Turbyfield, C.; Lam, W.; Alexeev, A.; Sulchek, T. *Lab on a chip* **2015**, *15*, 532-540.

(32) Soares, R. R.; Azevedo, A. M.; Van Alstine, J. M.; Aires-Barros, M. R. *Biotechnology journal* **2015**, *10*, 1158-1169.

(33) Shields, C. W. t.; Reyes, C. D.; Lopez, G. P. *Lab on a chip* **2015**, *15*, 1230-1249.

(34) Runkel, S.; Hitzler, W. E.; Hellstern, P. *Transfusion* **2015**, *55*, 796-804.

(35) Reinhardt, M.; Bader, A.; Giri, S. *Expert review of medical devices* **2015**, *12*, 353-364.

(36) Le, N. P.; Channabasappa, S.; Hossain, M.; Liu, L.; Singh, B. *Am J Physiol Lung Cell Mol Physiol* **2015**, *309*, L995-1008.

(37) King, P. T. *Clin Transl Med* **2015**, *4*, 68.

(38) Hashemian, A. M.; Ahmadi, K.; Zamani Moghaddam, H.; Zakeri, H.; Davoodi Navakh, S. A.; Sharifi, M. D.; Bahrami, A. *Iranian Red Crescent medical journal* **2015**, *17*, e21341.

(39) Grenvall, C.; Magnusson, C.; Lilja, H.; Laurell, T. *Analytical chemistry* **2015**, *87*, 5596-5604.

(40) Byeon, Y.; Ki, C. S.; Han, K. H. *Biomedical microdevices* **2015**, *17*, 118.

(41) Shen, S.; Ma, C.; Zhao, L.; Wang, Y.; Wang, J. C.; Xu, J.; Li, T.; Pang, L.; Wang, J. *Lab on a chip* **2014**, *14*, 2525-2538.

(42) Schafer, D.; Dressen, P.; Brettner, S.; Rath, N. F.; Molderings, G. J.; Jensen, K.; Ziemann, C. *Journal of translational medicine* **2014**, *12*, 213.

(43) Plouffe, B. D.; Murthy, S. K. *Analytical chemistry* **2014**, *86*, 11481-11488.

(44) Li, X.; Chen, W.; Liu, G.; Lu, W.; Fu, J. *Lab on a chip* **2014**, *14*, 2565-2575.

(45) Lee, A.; Park, J.; Lim, M.; Sunkara, V.; Kim, S. Y.; Kim, G. H.; Kim, M. H.; Cho, Y. K. *Analytical chemistry* **2014**, *86*, 11349-11356.

(46) Hulspas, R.; Villa-Komaroff, L.; Koksal, E.; Etienne, K.; Rogers, P.; Tuttle, M.; Korsgren, O.; Sharpe, J. C.; Berglund, D. *Cytotherapy* **2014**, *16*, 1384-1389.

(47) Ding, X.; Peng, Z.; Lin, S. C.; Geri, M.; Li, S.; Li, P.; Chen, Y.; Dao, M.; Suresh, S.; Huang, T. J. *Proceedings of the National Academy of Sciences of the United States of America* **2014**, *111*, 12992-12997.

(48) Chen, Y.; Li, P.; Huang, P. H.; Xie, Y.; Mai, J. D.; Wang, L.; Nguyen, N. T.; Huang, T. J. *Lab on a chip* **2014**, *14*, 626-645.

(49) von Hundelshausen, P.; Weber, C. *Dtsch Med Wochenschr* **2013**, *138*, 1839-1844.

(50) Tan, S. J.; Kee, M. Z.; Mathuru, A. S.; Burkholder, W. F.; Jesuthasan, S. J. *PloS one* **2013**, *8*, e78261.

(51) Muller, W. A. *Vet Pathol* **2013**, *50*, 7-22.

(52) Koga, H.; Miyahara, N.; Fuchimoto, Y.; Ikeda, G.; Waseda, K.; Ono, K.; Tanimoto, Y.; Kataoka, M.; Gelfand, E. W.; Tanimoto, M.; Kanehiro, A. *Respir Res* **2013**, *14*, 8.

(53) Chen, W.; Huang, N. T.; Oh, B.; Lam, R. H.; Fan, R.; Cornell, T. T.; Shanley, T. P.; Kurabayashi, K.; Fu, J. *Advanced healthcare materials* **2013**, *2*, 965-975.

(54) Bruchet, A.; Taniga, V.; Descroix, S.; Malaquin, L.; Goutelard, F.; Mariet, C. *Talanta* **2013**, *116*, 488-494.

(55) Zhou, L.; Somasundaram, R.; Nederhof, R. F.; Dijkstra, G.; Faber, K. N.; Peppelenbosch, M. P.; Fuhler, G. M. *Clinical and vaccine immunology : CVI* **2012**, *19*, 1065-1074.

(56) Posel, C.; Moller, K.; Frohlich, W.; Schulz, I.; Boltze, J.; Wagner, D. C. *PloS one* **2012**, *7*, e50293.

(57) Peters, T.; Bloch, W.; Pabst, O.; Wickenhauser, C.; Uthoff-Hachenberg, C.; Schmidt, S. V.; Varga, G.; Grabbe, S.; Kess, D.; Oreshkova, T.; Sindrilaru, A.; Addicks, K.; Forster, R.; Muller, W.; Scharffetter-Kochanek, K. *Clin Dev Immunol* **2012**, *2012*, 450738.

(58) Nieto, J. C.; Canto, E.; Zamora, C.; Ortiz, M. A.; Juarez, C.; Vidal, S. *PloS one* **2012**, *7*, e31297.

(59) Lobo, P. I.; Bajwa, A.; Schlegel, K. H.; Vengal, J.; Lee, S. J.; Huang, L.; Ye, H.; Deshmukh, U.; Wang, T.; Pei, H.; Okusa, M. D. *J Immunol* **2012**, *188*, 1675-1685.

(60) Kim, E.; Schueller, O.; Sweetnam, P. M. *Lab on a chip* **2012**, *12*, 2255-2264.

(61) Gazzaniga, P.; Gradilone, A.; de Berardinis, E.; Busetto, G. M.; Raimondi, C.; Gandini, O.; Nicolazzo, C.; Petracca, A.; Vincenzi, B.; Farcomeni, A.; Gentile, V.; Cortesi, E.; Frati, L. *Ann Oncol* **2012**, *23*, 2352-2356.

(62) Galbraith, D. *Methods* **2012**, *57*, 249-250.

(63) Chen, G. D.; Fachin, F.; Colombini, E.; Wardle, B. L.; Toner, M. *Lab on a chip* **2012**, *12*, 3159-3167.

(64) Arimilli, S.; Damratoski, B. E.; Chen, P.; Jones, B. A.; Prasad, G. L. *Cryo Letters* **2012**, *33*, 376-384.

(65) Zhao, C.; Cheng, X. *Biomicrofluidics* **2011**, *5*, 32004-3200410.

(66) Tzur, A.; Moore, J. K.; Jorgensen, P.; Shapiro, H. M.; Kirschner, M. W. *PloS one* **2011**, *6*, e16053.

(67) Ovsyannikova, I. G.; Vierkant, R. A.; Pankratz, V. S.; Jacobson, R. M.; Poland, G. A. *J Infect Dis* **2011**, *203*, 1546-1555.

(68) Naranbhai, V.; Bartman, P.; Ndlovu, D.; Ramkalawon, P.; Ndung'u, T.; Wilson, D.; Altfeld, M.; Carr, W. H. *Journal of immunological methods* **2011**, *366*, 28-35.

(69) Mariucci, S.; Rovati, B.; Manzoni, M.; Della Porta, M. G.; Comolli, G.; Delfanti, S.; Danova, M. *Clinical and experimental medicine* **2011**, *11*, 199-210.

(70) Manabe, I. *Circ J* **2011**, *75*, 2739-2748.

(71) Jamsa, J.; Huotari, V.; Savolainen, E. R.; Syrjala, H.; Ala-Kokko, T. *J Clin Lab Anal* **2011**, *25*, 118-125.

(72) Akhtar, N.; Adil, M. M.; Ahmed, W.; Habib ur, R.; Shahs, M. A. *J Pak Med Assoc* **2011**, *61*, 51-54.

(73) de Rooij, S. R.; Nijpels, G.; Nilsson, P. M.; Nolan, J. J.; Gabriel, R.; Bobbioni-Harsch, E.; Mingrone, G.; Dekker, J. M.; Relationship Between Insulin, S.; Cardiovascular Disease, I. *Diabetes Care* **2009**, *32*, 1295-1301.

(74) Cheng, X.; Gupta, A.; Chen, C.; Tompkins, R. G.; Rodriguez, W.; Toner, M. *Lab on a chip* **2009**, *9*, 1357-1364.

(75) Andel, M.; Polak, J.; Kraml, P.; Dlouhy, P.; Stich, V. *Vnitr Lek* **2009**, *55*, 659-665.

(76) Chernyshev, A. V.; Tarasov, P. A.; Semianov, K. A.; Nekrasov, V. M.; Hoekstra, A. G.; Maltsev, V. P. *Journal of theoretical biology* **2008**, *251*, 93-107.

(77) Murdoch, C.; Tazzyman, S.; Webster, S.; Lewis, C. E. *J Immunol* **2007**, *178*, 7405-7411.

(78) Michaud, D. S. *Urol Oncol* **2007**, *25*, 260-268.

(79) Ley, K.; Laudanna, C.; Cybulsky, M. I.; Nourshargh, S. *Nat Rev Immunol* **2007**, *7*, 678-689.

(80) Chen, X.; Cui, D.; Liu, C.; Li, H.; Chen, J. *Analytica chimica acta* **2007**, *584*, 237-243.

(81) Cabral, J. M. *Adv Biochem Eng Biotechnol* **2007**, *106*, 151-171.

(82) Getz, G. S. *J Lipid Res* **2005**, *46*, 619-622.

(83) Behzad-Behbahani, A.; Yaghobi, R.; Sabahi, F.; Rostaei, M. H.; Alborzi, A. *Exp Clin Transplant* **2005**, *3*, 316-319.

(84) Sethu, P.; Anahtar, M.; Moldawer, L. L.; Tompkins, R. G.; Toner, M. *Analytical chemistry* **2004**, *76*, 6247-6253.

(85) Barger, A. M. *Vet Clin North Am Small Anim Pract* **2003**, *33*, 1207-1222.

(86) Shacter, E.; Weitzman, S. A. *Oncology (Williston Park)* **2002**, *16*, 217-226, 229; discussion 230-212.

(87) Jacobsen, J.; Grankvist, K.; Rasmuson, T.; Ljungberg, B. *Eur J Cancer Prev* **2002**, *11*, 245-252.

(88) Hatti-Kaul, R. *Mol Biotechnol* **2001**, *19*, 269-277.

(89) Chertov, O.; Yang, D.; Howard, O. M.; Oppenheim, J. J. *Immunol Rev* **2000**, *177*, 68-78.

(90) Campbell, J. J.; Haraldsen, G.; Pan, J.; Rottman, J.; Qin, S.; Ponath, P.; Andrew, D. P.; Warnke, R.; Ruffing, N.; Kassam, N.; Wu, L.; Butcher, E. C. *Nature* **1999**, *400*, 776-780.

(91) Ferrero, D.; Tarella, C.; Cherasco, C.; Bondesan, P.; Omede, P.; Ravaglia, R.; Caracciolo, D.; Castellino, C.; Pileri, A. *Bone Marrow Transplant* **1998**, *21*, 409-413.

(92) Newton, R. A.; Thiel, M.; Hogg, N. *Journal of leukocyte biology* **1997**, *61*, 422-426.

(93) Pelegri, C.; Rodriguez-Palmero, M.; Morante, M. P.; Comas, J.; Castell, M.; Franch, A. *Journal of immunological methods* **1995**, *187*, 265-271.

(94) McCarthy, D. A.; Macey, M. G.; Cahill, M. R.; Newland, A. C. *Cytometry* **1994**, *17*, 39-49.

(95) Alzona, M.; Jack, H. M.; Fisher, R. I.; Ellis, T. M. *J Immunol* **1994**, *153*, 2861-2867.

(96) Kuta, A. E.; Reynolds, C. R.; Henkart, P. A. *J Immunol* **1989**, *142*, 4378-4384.

(97) Kalmar, J. R.; Arnold, R. R.; Warbington, M. L.; Gardner, M. K. *Journal of immunological methods* **1988**, *110*, 275-281.

(98) Carter, C. S.; Leitman, S. F.; Cullis, H.; Muul, L. M.; Nason-Burchenal, K.; Rosenberg, S. A.; Klein, H. G. *Transfusion* **1987**, *27*, 362-365.

(99) Cott, M. E.; Oh, J. H.; Vroon, D. H. *Transfusion* **1986**, *26*, 272-273.

(100) Felix, J. S.; Doherty, R. A. *Clin Genet* **1979**, *15*, 215-220.

(101) Ellis, W. D.; Mulvaney, B. D.; Saathoff, D. J. *Prep Biochem* **1975**, *5*, 179-187.

(102) Takiguchi, T. *Saishin Igaku* **1972**, *27*, 598-606.

(103) Zeya, H. I.; Spitznagel, J. K. *Lab Invest* **1971**, *24*, 237-245.